STIC-ILL NPL

From: Canella, Karen
Sent: Friday, October 24, 2003 7:40 PM
To: STIC-ILL
Subject: ill order 09/854,204

Art Unit 1642 Location 8E12(mail)

Telephone Number 308-8362

Application Number 09/854,204

1. Cell, 1984, Vol. 39, No. 3, part 2, pp. 499-509

2. Journal of Biological Chemistry, 2001, 276(8):5836-5840

3. Pharmaceutical Research, 1996, 13 (11): 1615-1623

4. Journal of Peptide Research, 1998, 51(3): 235-243

5. Neuroscience Letters 1998, 255 (1): 41-44

6. EMBO, 1990, 9 (3): 815-819

7. Journal of Organic Chemistry, 1997, 62 (5): 1356-1362

8. CAPLUS COPYRIGHT 2003 ACS on STN
ACCESSION NUMBER: 1981:454710 CAPLUS
DOCUMENT NUMBER: 95:54710
TITLE: Natural peptide lactones as ion carriers in membranes
AUTHOR(S): Oberbaeumer, Ilse; Feigl, Peter; Ruf, Horst; Grell, Ernst
CORPORATE SOURCE: Max-Planck-Inst. Biophys., Frankfurt, D-6000/71, Fed. Rep. Ger.
SOURCE: Struct. Act. Nat. Pept., Proc. Fall Meet. Ges. Biol. Chem. (1981), Meeting Date 1979, 523-38. Editor(s): Voelter, Wolfgang; Weitzel, Guenther. de Gruyter: Berlin, Fed. Rep. Ger.
CODEN: 45VYAS
DOCUMENT TYPE: Conference
LANGUAGE: English

9. CAPLUS COPYRIGHT 2003 ACS on STN
ACCESSION NUMBER: 1998:72644 CAPLUS
DOCUMENT NUMBER: 128:141012
TITLE: Rational design of peptides with enhanced membrane permeability
AUTHOR(S): Borchardt, Ronald T.
CORPORATE SOURCE: Department of Pharmaceutical Chemistry, The University of Kansas, Lawrence, KS, 66045, USA
SOURCE: Medicinal Chemistry: Today and Tomorrow, Proceedings of the AFMC International Medicinal Chemistry Symposium, Tokyo, Sept. 3-8, 1995 (1997), Meeting Date 1995, 191-196. Editor(s): Yamazaki, Mikio. Blackwell: Oxford, UK.
CODEN: 65ONAG
DOCUMENT TYPE: Conference
LANGUAGE: English

MECHANISM OF REACTION OF RECOIL HYDROGEN IN THE GAS PHASE

BY MOSTAFA AMR EL-SAYED, PEDER J. ESTRUP AND RICHARD WOLFGANG

Contribution No. 1476 Sterling Chemistry Laboratory, Yale University, New Haven, Conn.

Received April 3, 1958

The interaction of high energy tritium (H^3), formed by nuclear recoil, with gaseous methane and ethane, has been investigated under a wide variety of conditions. In the case of methane, a number of labeled products, chiefly HT and CH_3T, together with smaller amounts of higher tritium labeled hydrocarbons are formed. If a radical scavenger, such as I_2, is present, the yield of CH_3T is little changed, but the amount of HT is halved and the higher hydrocarbons eliminated. These results are not consistent with present theories of the mechanism of the primary step of hot-atom reaction. An alternative hypothesis that reactions of gas phase hot "atoms" are really due to ions does not appear tenable in the case of recoil tritium. A mechanism involving a high energy one-step displacement reaction as the primary reaction of the hot atom is suggested. Some of the labeled products of this primary reaction reach thermal energies as radicals which will then undergo further secondary reaction. Unlike the primary hot reactions, these thermal secondary processes are sensitive to the addition of radical scavengers. Evidence for this mechanism is obtained from a consideration of the detailed product distributions and their changes when certain experimental conditions, such as radiation intensity, are varied. Particularly significant are the consequences of the addition of a large excess of He^4 to moderate the hot atoms. A review of earlier data makes it appear probable that the primary hot replacement mechanism thus indicated for the gas phase reaction of recoil tritium is also operative in the condensed phase. The further extension of this mechanism to hot atom reactions in general is briefly discussed.

Introduction

This paper reports investigations on reactions in the gas-phase systems $H + CH_4$ and $H + C_2H_6$, in which high-energy tritium recoiling from nuclear reaction is the source of hydrogen.[2,3] The nuclear reactions $Li^6(n,\alpha)H^3$ and $He^3(n,p)H^3$ served to provide 2.7 and 0.18 Mev. tritons, respectively. As in our earlier studies of recoil tritium "labeling" reactions,[4-6] mixtures of the tritium source and the chemical reactant (CH_4 or C_2H_6 in this case) were neutron irradiated and then analyzed by separating and counting the various tritiated species produced.

The reacting systems $H + CH_4$ and $H + C_2H_6$ have previously been extensively studied.[7] Gorin, Kauzmann, Walter and Eyring[8] have constructed energy surfaces for possible reactions of $H + CH_4$ using Eyring's semi-empirical method. Many experimental data on the reactions of thermal hydrogen atoms also has been obtained and indicates that in this energy range the hydrogen reacts by abstraction $H + RH \rightarrow R + H_2$.[9] Our work extends these studies to higher energies where new reactions are observed to appear.

The systems described here are perhaps the simplest of the many "hot atom" reactions, induced as a result of nuclear transformation, that have been studied. On the basis of the hypotheses suggested by the large (but incompletely understood) body of work on hot atom reactions in more complex systems, our results appear anomalous and, if valid, suggest a re-evaluation of some of the concepts in this field.

The theories of hot atom chemistry suggest[10] that reaction proceeds in two steps. First, the hot atom produces radicals by collision, and then, presumably after deactivation by further collisions, it combines with one of these radicals. So that this reaction may proceed efficiently, it is necessary to provide a "cage" of surrounding molecules to keep the hot atom and the radicals it has produced together until they combine. Since such a cage cannot exist in the gas phase, what are normally considered to be hot atom reactions should occur efficiently only in condensed media. However, Willard and co-investigators[11] have shown that reactions such as that of recoil iodine with methane to form methyl iodide do occur with high yield in the gas phase. In most of these cases, however, evidence is cited which may make it plausible that the reaction is not due to a hot atom but rather to an ion. Hamill and Williams[12] have observed earlier that recoil Br^{80} forms HBr with gaseous ethyl bromide and have shown that this is consistent with a hot atom mechanism. Here again, however, more recent suggestions hold that a Br ion rather than atom may be the reacting species (see Appendix).

In the case of recoil tritium, however, there should be, as mentioned in an earlier paper[4] little doubt that the species reacting to give labeled molecules is a hot atom and not an ion. (Willard in presenting some parallel results has favored an alternative view.[8,11] The rather fundamental problem of whether T^+ or T^0 is involved is discussed, from the point of view of the slowing of fast particles, in the Appendix.) Our preliminary finding that recoil tritium reacts in the gas phase, before reaching thermal energies, therefore led us to propose[2] that the primary chemical interaction of the hot tritium atom must be by an efficient one-step hot atom displacement reaction. This paper presents ex-

(1) Article No. IV in the series "Studies of the Recoil Tritium-labeling Reaction." This work was supported by the U. S. Atomic Energy Commission under contract No. AT(30-1)-1957. Results on similar systems communicated earlier (see ref. 2) were obtained at Brookhaven National Laboratory.

(2) M. Amr El-Sayed and R. Wolfgang, *J. Am. Chem. Soc.*, 79, 3286 (1957).

(3) A. Gordus, M. Sauer and J. Willard, *ibid.*, 79, 3284 (1957).

(4) F. S. Rowland, C. N. Turton and R. Wolfgang, *ibid.*, 78, 2354 (1956).

(5) R. Wolfgang, J. Rigner and F. S. Rowland, THIS JOURNAL, 60, 1137 (1956).

(6) F. S. Rowland and R. Wolfgang, *Nucleonics*, 14, no. 8, 58 (1956).

(7) E. W. R. Steacie, "Atomic and Free Radical Reaction," 2nd ed., Reinhold Publ. Corp., New York, N. Y., 1954, pp. 449 *et seq.*

(8) Gorin, Kauzmann, Walter and H. Eyring, *J. Chem. Phys.*, 7, 633 (1939).

(9) M. R. Berlie and D. J. Le Roy, *Can. J. Chem.*, 32, 650 (1954); *Disc. Faraday Soc.*, 14, 50 (1953).

(10) Reviews of hot atom chemistry are given by J. Willard, *Ann. Rev. Nuc. Sci.*, 3, 193 (1953); *Ann. Rev. Phys. Chem.*, 6, 141 (1955). For more recent references, see the other papers in this symposium.

(11) J. E. Willard, *et al.*, *J. Chem. Phys.*, 20, 1556 (1952); 25, 904 (1956); *J. Am. Chem. Soc.*, 75, 6100 (1953); 79, 4609 (1957).

(12) R. R. Williams and W. H. Hamill, *J. Chem. Phys.*, 18, 783 (1950).

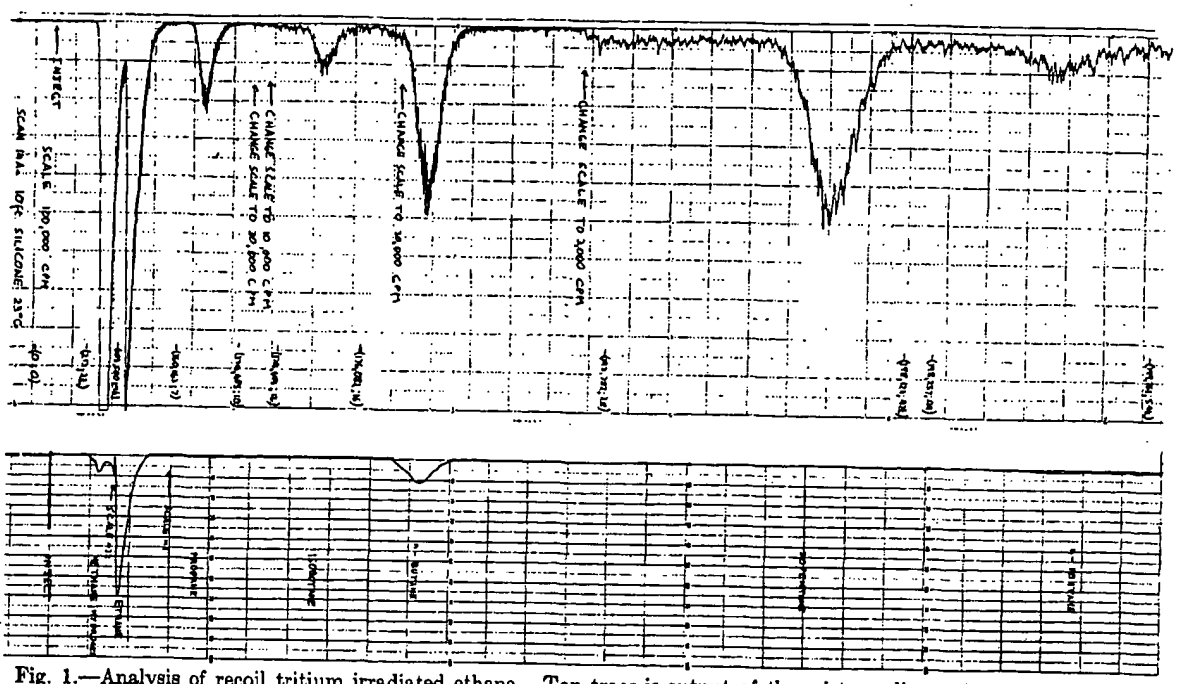

Fig. 1.—Analysis of recoil tritium irradiated ethane. Top trace is output of thermistor cell, synchronized lower trace that of count rate meter. Note scale changes: ×32 means 320 millivolts full scale, ×1 means 10 millivolts; CPM refers to counts per minute, full scale. Radioactivity not in peaks is natural background.

perimental evidence supporting the detailed mechanism proposed and discusses some general aspects of this view of hot atom reactions.

Experimental

Irradiations.—Samples of methane or ethane at 1–70 cm. pressure were irradiated in 7–11 ml. quartz ampoules. In most of the runs 1–3 mm. pressure of He^3 was added to provide the recoil tritium and in those runs where Li^6 was the tritium source, the walls of the ampoule were coated with a film of normal $LiNO_3$. The hydrocarbons were purified by repeated low temperature distillations and fractionations. Any tritium contamination in He^3 was removed by passage over hot copper oxide. A small amount of solid iodine was added to some of the tubes to provide a low pressure of I_2 vapor as a radical scavenger. A measured excess of He^4 (to serve as moderator) was present in some experiments.

Most irradiations were carried out for periods of 1–20 min. at a flux of 5×10^{12} n./cm.^{2} sec. in the Brookhaven reactor. The effective temperature for these runs was 40–60°. Other runs, lasting 1–4 days, were made at a flux of 2×10^9 n./cm.^{2} sec. in the "tunnel" under the reactor. In the high temperature runs the samples were heated by a standard infrared heating lamp.

Separation and Counting.—After irradiation the sample tubes were opened and components separated. In some cases carriers (hydrogen, ethane, propane, etc.) were added and the mixture separated by low temperature distillation. The various fractions obtained were counted in a silver-walled glass proportional counter. This technique has been described earlier.[5]

In other runs, separation was made by gas chromatography. The apparatus used has been described in detail in a separate publication.[13] An aliquot of the sample was injected into a stream of He passing through the chromatograph column. After separation, the gas stream passed through a thermal conductivity cell which detected and recorded any macroscopic amounts of material. The He was then converted into a counter gas by continuous injection of methane and flowed through an internal flow proportional counter of special design. The radioactivity detected was fed into an integrating scale and a recording rate-meter. A silica-gel column was used to separate HT, CH_3T and C_2H_5T, and silicone on fire brick was used to separate the higher hydrocarbons and the iodides from each other and from the hydrogen and methane. The columns were operated at a constant temperature (usually 22°). Relative retention volumes of the various fractions were measured by injections of small amounts of the unlabeled gases mixed with *n*-butane as an internal standard.

Figure 1 shows the first part of an analysis on a silicone column of recoil-T irradiated ethane. The trace at the top shows the response of the thermal conductivity cell and the synchronized trace of the bottom that of the count-rate meter. The expected positions of the various fractions and the integrated counts at certain times are marked.

In this particular run, measurable masses of butane produced by radiation decomposition of the ethane were observed. They amount to 1–2% of the original ethane. This represents the upper limit for radiation damage observed in these experiments. In most runs this decomposition was well under 1%.

In some runs the sum of the activities in each peak was compared to the total gaseous activity obtained by passing a portion of the sample through the counter without separation. This showed that substantially all of the gaseous yield was detected. From the decreasing activity in successively larger hydrocarbons it is believed that, with the exception of TI, no significant amount of non-gaseous activity was produced.

Since the amount of gas in the ampules was, in general, small compared to the range of the recoil tritium, a major and indeterminate fraction of the activity did not react in the gas phase but recoiled into the walls. By heating used, empty ampules it was found that some of the tritium would diffuse back out of the walls at higher temperature to appear in the gas phase as HT. (Even in the presence of CH_4 this diffusion tritium appears only in the form of molecular hydrogen.) This nuisance effect was most apparent in the experiments on the effect of heat on the hot-atom reaction. As will be discussed below, suitable correction was made in this case by reference to control runs at lower temperature. Experience on varying the time delay between irradiation and analysis indicates that the diffusion effect is negligible at about 25°, the temperature at which the low flux runs were made. However it appears that at ~60°, the temperature of most of the irradiations, the contribution to the total activity of diffusion HT is not quite negligible. Thus the two 60-minute runs yielded about 3–5% more HT than the average of the many runs made for 20 minutes or less. Diffusion HT also appears to be a significant spurious

(13) R. Wolfgang and F. S. Rowland, *Anal. Chem.*, 30, 903 (1958).

TABLE I

REACTION OF RECOIL T WITH CH_4 (I_2 ABSENT)

Run and method[a]	Source of T	Flux, n./cm.² sec.	Time of irrad., min.	Pressure, cm.	% of obsd. activity in H_2	CH_4	C_2H_6	C_3H_8	C_4H_{10}	Higher hydrocarbons
D2	Li^6NO_3	$\sim 5 \times 10^{12}$	10	7	49.0	30.5	11.2		9.3	
D10	He^3	$\sim 5 \times 10^{12}$	10	11	49.6	31.5	9.0		9.7	
D7	He^3	$\sim 5 \times 10^{12}$	10	44	51.8	31.3	6.4		10.5	
D9	He^3	$\sim 5 \times 10^{12}$	10	44	51.9	30.3	6.4		11.4	
C12	He^3	$\sim 4 \times 10^{12}$	60	20	55.3[b]	29.4	5.7	3.6	2.3	3.6
C16	He^3	$\sim 4 \times 10^{12}$	20	25	48.6	32.7	9.2	4.2	2.8	2.3
C9	He^3	$\sim 4 \times 10^{12}$	20	30	52.6	31.1	4.5	7.7	4.3	..
C22	He^3	$\sim 5 \times 10^{12}$	20	48	46.5	35.4	7.5	3.7	2.8	4.1
D46	He^3	$\sim 2 \times 10^9$	48 hr.	15	61.0	30.6	2.5		5.9	
D42	He^3	$\sim 2 \times 10^9$	96 hr.	38	62.8	27.6	3.3		6.3	
D47	He^3	$\sim 2 \times 10^9$	48 hr.	15	61.2	31.2	2.1		5.5	
Av. at flux $\sim 5 \times 10^{12}$ n./cm.² sec. ($\sim 50°$)					50.0	31.8	7.7		10.4	
Av. at flux $\sim 2 \times 10^9$ n./cm.² sec. ($\sim 30°$)					61.7	29.8	2.6		5.4	

[a] Prefix C indicates analysis by chromatography. Prefix D indicates analysis by distillation. [b] Probably includes several per cent. of HT from diffusion out of quartz walls. Not included in average.

source of activity in He^4 moderated runs at 50–60°. Because of the low stopping power of He^4 only a small fraction of the T is stopped in the gas phase, and consequently the diffusion may be relatively more important. Present studies on He^4 moderation are thus being made at low temperatures.

The best measure of the over-all accuracy of the results is given by their reproducibility and consistency. This is very satisfactory, especially for methane, where entirely different techniques in both irradiation and analysis gave essentially identical results.

Results

Tables I and IV show the products produced by the interaction of recoil T with pure methane. It is observed that about half of the tritium has reacted to form labeled hydrocarbons, chiefly CH_3T, under quite a wide variety of experimental conditions. The source of the tritium whether from Li^6 coating the walls, or from homogeneously distributed He^3 appears to have no effect. The activity distribution is also independent of the pressure of methane.

TABLE II

EFFECT OF HEAT DURING IRRADIATION AT LOW FLUX

Fraction	Run #D46 (~22°) Total activity in fraction (c.p.m.) × 10^{-3}	% of total gaseous activity	Run #D47 (~200°) Total activity in fraction (c.p.m.) × 10^{-3}	% of total gaseous activity	% of total gaseous activity cor. for HT from walls
H_2	3.86	61.0	6.16	71.5	61.2
CH_4	1.94	30.6	1.97	22.9	31.2
C_2H_6	0.16	2.5	0.13	1.5	2.1
C_3H_8, C_4H_{10}	0.38	5.9	0.35	4.1	5.5

A drastic lowering of the neutron flux and hence of the radiation density does, however, seem to have a measurable effect. If the labeled hydrocarbons had been formed by reaction of thermal T with radiation produced radicals a sharp drop in their yields would have been expected. A drop in the yields of C_2H_5T and higher tritiated species with a corresponding rise of HT is indeed observed but the yield of CH_3T seems little affected.

The effect of temperature change under low flux conditions has been studied. As shown in Table II, a considerable increase in the amount of HT was observed when a tube being irradiated at 2×10^9 n./cm.² sec. was heated to ~200°. This excess HT is, however, due to a temperature dependent diffusion of T from the quartz walls, as discussed in the Experimental section. On correcting for the diffusion HT by reference to an identical run at lower temperature, it is seen (Table II) that the distribution of activity at the higher temperature is not different outside the limit of experimental error. It has unfortunately not been practical to raise the temperature of the runs at 2×10^{12} n./cm.² sec. However, preliminary results on high flux runs made at approximately −50° do show some temperature dependence, at least under high radiation density conditions.

The addition of I_2 (or Br_2) as a radical scavenger has the profound effect noted in Table III. The production of higher labeled hydrocarbons is virtually eliminated and the yield of HT is halved. However, the yield of CH_3T is reduced only slightly. This highly specific effect of I_2 is unaffected by variation of pressure and neutron flux.

It should be noted that the percentage yields in the I_2 runs are not based on the total observed activity as is the case in the iodine-free runs. Instead, these yields were computed on the basis of the total observed activity in identical control runs in which no I_2 was present. This was done because in the presence of I_2, labeled iodides, especially TI, which would not pass our separation system would be expected. This appears to be the case since the addition of I_2 to a run consistently reduced the total observed activity (including CH_2TI and C_2H_4TI) to 60% (Table III) of what it would otherwise have been. The deficit in activity is almost certainly due to formation of TI. Unfortunately we have not observed this species directly.

It is of interest to compare these results with data on similar systems reported by Gordus, Sauer and Willard[3] at the time that preliminary publication of our work[2] was made. The distribution of activity found by these workers for pure CH_4 irradiated with T from He^3 is in fair agreement with our results. But their results on the per cent. of total T in each product when I_2 was present during irradiation differ sharply from our findings. This

TABLE III

REACTION OF RECOIL T WITH CH_4 (I_2 PRESENT, ~30–50°)

Run and method[a]	Source of T	Flux n./cm.² sec.	Time of irrad., min.	Pressure, cm.	% of total tritium reacting in methane in: H_2	CH_4	C_2H_6	Hydrocarbons $>C_2H_6$	CH_3I	C_2H_5I	Total detected
D44	He^3	2×10^9	96 hr.	37	29.7	26.0	0.1		7.3		63.1
C11	He^3	4×10^{12}	20	29	27.2	27.8	.2	0.0	4.9	0	60.1
C18	He^3	4×10^{12}	20	25	28.4	26.6	.2	0.4	4.1	0.1	59.8
C23	He^3	5×10^{12}	20	48	25.4	26.5	.0	0.7	3.7	0.5	56.8
C24[a]	He^3	4×10^{12}	20	48	30.1	30.4	.1	(1.9)	(6.4)[b]	(0.5)[b]	69.4[b]
Av. (excluding C24)					28.2	27.5	.1	0.4	4.3	~0	60.5

[a] Prefixes C and D denote separation by chromatography and distillation, respectively. [b] Br_2 instead of I_2 used.

TABLE IV

REACTION OF RECOIL T WITH C_2H_6(~30°)

Run[a] and method	Source of T	Flux, n./cm.² sec. × 10^{-12}	Time of irrad., min.	Pressure, cm.	% of obsd. activity in: H_2	CH_4	C_2H_6	C_3H_8	C_4H_{10}	Higher hydrocarbons	CH_3I	C_2H_5I
D12	He^3	5	10	C_2H_6, 61	41.7	5.0	29.4	11.0	13.4		..	...
D13	He^3	5	10	C_2H_6, 65	38.0	3.0	29.0	11.5	18.5		..	...
C14	He^3	4	60	C_2H_6, 82	50.3[b]	3.7	25.8	7.3	9.1	3.9	..	...
C19	He^3	4	20	C_2H_6, 49	44.9	3.3	26.2	8.7	11.5	5.4	..	...
C21	He^3	4	20	C_2H_6, 17	48.8	3.9	25.3	7.7	8.9	5.2	..	...
Av. of above runs					43.4	3.8	27.5	9.7	10.2	5.1		
C20	He^3	4	20	C_2H_6, 48; I_2, 0.2	40.0	3.6	22.3	~0.8	~1.3	~2.5	5.5	~1.9
C15	He^3	4	60	C_2H_6, 1; He^4, 56	58.8	2.8	11.8	7.8	11.1	7.4	..	....

[a] Prefixes C and D denote separation by chromatography and distillation, respectively. [b] Probably includes several % HT from diffusion out of quartz walls.

apparent difference seems to result from Gordus', *et al.*, normalizing on the basis that the observed activities represent 100% yield. If their results are normalized on the basis of our finding that only about 60% of the activity is observed under the given circumstances, the agreement with our values becomes satisfactory.

We have checked the effect of addition of I_2 *after* irradiation. The results observed are identical to those obtained in the runs where I_2 was absent.

The above results, which indicated that a one-step hot atom displacement mechanism was operative, suggested testing this idea by moderating the hot atoms with an excess of He^4. Preliminary, rather approximate data on runs in which He^4 was present in excess are given in the summary Table VI and will be discussed later.

A series of experiments similar to those on methane, but much less extensive, were carried out on ethane. These are summarized in Table V. With ethane, CH_3T becomes a minor and C_2H_5T a major product. Also there are three products, HT, CH_3T and C_2H_5T (instead of just HT and CH_3T as with methane) which are unaffected by the presence of iodine scavenger. Otherwise the same qualitative generalizations that can be made for the results on methane also appear to be largely true for ethane.

TABLE V

REACTION PRODUCTS OF RECOIL TRITIUM WITH GASEOUS ALKANES

Irradiation at ~5 × 10^{12} n./cm.²-sec., ~ 50°)

Tritiated product	Alkane irrad., % Methane[b]	Ethane[c]
Hydrogen	50.0	43.4
Methane	32.9	4.2
Ethane	6.4	29.4
Propane	4.0	8.1
Isobutane	1.5	0.6
n-Butane	1.1	9.4
Neopentane	0.6	0.0
Isopentane	1.1	1.8
n-Pentane	0.4	0.3
2,2-Dimethylbutane	1.2	0.2
2(?)-Methylpentane[a]	0.3	0.3
3(?)-Methylpentane[a]	0.3	1.6
n-Hexane	0	0.2

[a] Identification not confirmed. [b] Run C12 (normalized to average % HT observed). [c] Run C14 (normalized to average % HT observed).

TABLE VI

SUMMARY OF SOME SALIENT RESULTS IN GASEOUS METHANE SYSTEMS

Conditions: Flux, n./cm.² sec.	Added material	% Tritium in: HT	CH_3T	C_2H_5T	Higher labeled hydrocarbons
5 × 10^{12}		50.0	31.8	7.7	10.4
2 × 10^9		61.7	29.8	2.6	5.4
5 × 10^{12}	0.2 mm. I_2	28.2	27.5	0.1	0.4
5 × 10^{12}	0.99 mole fraction He^4 ~5 mm. Br_2	5 ± 5	~1	0	0

The detailed distributions of labeled species resulting from runs on both labeled methane and ethane are given in Table IV. There is a possibility that some labelled alkenes are formed, but being present only in trace amounts these may

TABLE VII

MECHANISM OF THE REACTION OF RECOIL TRITIUM WITH GASEOUS METHANE

T* denotes high kinetic energy tritium; italics denote end product.

A—Primary processes (hot)			
1	$T^* + CH_4 \longrightarrow \mathit{CH_3T} + H$	28%	56%
2	$\longrightarrow \mathit{HT}$ + etc.	28%	
3	$\longrightarrow CH_2T\cdot$ + etc.	4%	44%
4	$\longrightarrow CHT\cdot$ + etc.	0–6%	
5	$\longrightarrow CT\cdot$ + etc.		
6	$\longrightarrow T\cdot$ + etc.	34–40%	
			100%
B—Secondary processes (thermal)			
1	Abstraction $T\cdot + CH_4 \longrightarrow \mathit{HT} + CH_3\cdot$	22% at $\overline{nv} = 5 \times 10^{13}$ (~50°)	
		34% at $\overline{nv} = 2 \times 10^{9}$ (~25°)	
2	Reaction with radiation produced radicals		
	(a) $T\cdot + CH_3\cdot \longrightarrow CH_2T\cdot + H$		
	(b) $\longrightarrow \mathit{CH_3T}$		
	(c) $T\cdot + C_2H_5\cdot \longrightarrow C_2H_4T\cdot + H$		
	(d) $\longrightarrow \mathit{C_2H_5T}$	22% at $\overline{nv} = 5 \times 10^{13}$ (~50°)	
	(e) $CH_2T\cdot + CH_3\cdot \longrightarrow \mathit{C_2H_6T}$	10% at $\overline{nv} = 2 \times 10^{9}$ (~25°)	
	(f) $CH_2T\cdot + C_2H_5\cdot \longrightarrow \mathit{C_2H_7T}$		
	(g) $C_2H_4T\cdot$ + etc.		
	(h) etc.		
3	Reaction with radiation produced ions		
			44%

have been reduced to the corresponding alkanes by hydrogen atoms produced during the irradiation.

Discussion

The results given in Tables I and III led us to postulate a mechanism for the reaction of recoil tritium in the gas phase which involves a direct, one-step replacement reaction as the primary step. Any labeled species formed in this first, hot step can then undergo secondary, thermal reactions. For CH_4 the detailed mechanism is given in Table VII (T^* denotes a "hot" atom).

The secondary (or thermal) processes listed are those which the radical products of the primary process would be expected to undergo in irradiated methane. Hydrogen abstraction by T is important with combination reactions with radiation-produced species competing. The list of possible primary processes is quite short for methane, but only some of the simpler of the possible secondary reactions of thermal tritiated species with radiation produced radicals are listed. Secondary reactions with radiation produced ions also are possible but are not explicitly listed. It is noteworthy that the secondary processes given have all been studied independently and are all known to occur.[14] (But see discussion of reaction 2b below.)

In the presence of a radical scavenger, such as I_2, the primary reactions will be unaffected. However, the thermal T· and $CH_2T\cdot$ formed in them will no longer react by the secondary processes B, but instead will undergo preferential reaction with I_2 to form CH_3I and HI. The disappearance of higher labeled hydrocarbons, the diminished amount of HT, and the appearance of CH_2TI, in the presence of I_2, are thus a natural consequence of the mechanism.

The experimental results may now be used to try to estimate the per cent. of tritium participating in the various reactions of the postulated mechanism. The resulting values are given in Table VII. The percentages of CH_3T, HT and $CH_2T\cdot$ radical formed by the primary reaction are assumed to be equal to the percentages of CH_3T, HT and CH_2TI found in runs where I_2 was present. A lower limit for the amount of thermal T· formed by collision (classified for convenience as one of the primary reactions) is given by the increase in the yield of HT, at low flux, when I_2 is not present. An upper limit for CHT and CT is given by difference. ($CHTI_2$ was not observed as a product. However the reaction efficiency of CH_2 with CH_4 may be so high that at the pressure of I_2 used no CH_2I_2 would be formed.)

Competition between Secondary Reactions.—From these values summarized in Table VII it is estimated that 44% of the recoil tritium emerges from the primary reaction region as a chemically reactive species. Two types of secondary reactions are then expected to compete for these species (chiefly T·); H abstraction from CH_4 (Bl) and combination with radiation-produced species. A simple calculation indicates that such a competition should actually exist. From the neutron flux a very rough estimate of the radiation energy input into the system and thus of the approximate rate of radical production in the system may be made. Using a plausible value[14] for the rate of radical recombination, the radical concentration in the system may be obtained. From this a very approximate rate of combination of the tritiated radicals with the radiation-produced radicals is calculated. This value is of the same order of magnitude as the rate of H abstraction by T· from CH_4, as calculated from the data of Berlie and Le Roy[9] on the reaction $H + CH_4$. Unfortunately there are insufficient data to permit similar calculations on the importance of reaction with radiation-produced ions.

(14) E. W. R. Steacie, "Atomic and Free Radical Reactions," 2nd ed., Reinhold Publ. Corp., New York, N. Y., 1954, pp. 511, *et seq.*

These expectations of competitive secondary reactions are in good qualitative agreement with the observed effect of a drastic change of neutron flux (Table VI). In Table VII the percentages of tritium undergoing thermal H abstraction and combination with radiation-produced species have been calculated from the increase in the yields of HT and labeled hydrocarbons, respectively, when I_2 is not present. The ratio of H abstraction to reaction with radiation-produced species is seen to change from 1:1 at a flux of $\sim 5 \times 10^{12}$ n./cm.^{2} sec. to 2:1 at a flux of $\sim 2 \times 10^9$ n./cm.^{2}-sec. (This ratio should depend on the radical density and hence on the square root of the radiation density. However, no quantitative correlation is available because of the difficulty of estimating radiation density, especially in the low flux case where the $He^3(n,p)T$ reaction is no longer the only important source of radiation energy.)

The fact that only a qualitative correlation is observed may indicate the existence of a further type of secondary reaction. Thus, while it can be calculated using the known rate of hydrogen abstraction from methane[9] that few thermal tritium atoms will reach the walls, there is a possibility that the surface may have some indirect effects of an unknown nature. It should be emphasized that the yields given in Table VII only express a rough estimate.

Effect of Moderator.—The mechanism outlined above suggested that the importance of the primary reaction could be reduced or eliminated if the tritons were slowed down before encountering CH_4 molecules. Such a moderating effect can be produced by the addition of large amounts of He^4. The elimination of HT and CH_3T formed by the hot mechanism would result and instead the products formed would be those from the reaction of thermal T·. If, in addition to the large excess of He^4 moderator, I_2 or Br_2 are present as radical scavengers, all, or nearly all, of the tritium should undergo thermal reaction to form halides, and little or no labeled hydrocarbons should be formed. Preliminary data (Table VI) show that this is indeed the case in runs made at approximately $-50°$ using Br_2 as scavenger. This result would appear to lend very strong support to the mechanism postulated.

Effect of Temperature.—While a change in the temperature of the system should not affect the primary (hot) reaction of the recoil tritium, some effect on the relative importance of the competing secondary reactions would be expected. The H-abstraction reaction (B1, Table VII) has a large temperature coefficient[9] while combination with radiation-produced radicals[14] and possibly ions should have a very small one. Hence the ratio of thermally produced HT to labeled hydrocarbons should increase with increasing temperature (providing there is no compensating temperature coefficient governing the concentration of radiation-produced species). The results given in Table II which show no such dependence might therefore appear somewhat anomalous if our suggestion as to the types of competing secondary reactions is correct. It must be noted, however, that these runs were made at low radiation density, where combination with radiation-produced species is relatively uncommon. The expected effect, especially on the ratio HT/CH_3T, would therefore be small and may be within the experimental error.

The picture as regards the secondary reaction, as studied by variation of the temperature and addition of moderator, appears to be complex. It is receiving further study in an attempt to separate the various factors which seem to be involved.

Specific Effects in Secondary Reactions in Methane.—It is of interest to consider briefly in somewhat more detail the origin of the large number of labeled products (Table IV) which have been formed by reaction of thermal tritiated radicals with radiation produced species in methane. The small effect of I_2 on the yield of CH_3T at $\sim 50°$ indicates that thermal formation of this species is relatively rare. This is in agreement with calculations of Kimball[15] that methane formed by the union of a methyl radical and a hydrogen atom (reaction 2b, Table VII) has a very short lifetime and usually can survive only in the presence of a third body. Consistent with this explanation of the normally low yield of thermally produced CH_3T are the results on a single run on methane in a tube containing a large surface area in the form of quartz powder. In this run the yield of CH_3T rose to 37%, the highest value we have observed. Other workers[14] have found that when atomic hydrogen reacts with methyl radical exchange takes place. This means that in our system reaction 2a (Table VII) leading to CH_2T· is probably the most common radical reaction.

Higher labeled hydrocarbons can be produced by the type of radical reaction given in Table VII. It is also likely[16,17] that ions produced by radiation can react readily to build up polymeric species which then react with the tritiated radicals (reaction 3 Table VII). The decrease of yield with chain length in the higher labeled hydrocarbons (Table V) is plausible from almost any point of view. In the case of methane the distribution of activity between iso and normal compounds appears rather non-specific as might be expected in building up polymers from one-carbon units.

Reaction of Recoil Tritium with Ethane.—Our reaction mechanism of hot primary displacement reactions followed by certain secondary reactions appears to hold as well in the gaseous ethane system as it does in methane. A wider range of reactions analogous to those given in Table VII for methane, may be expected for ethane. Three, rather than two, stable products, HT, CH_3T and C_2H_5T may now be formed by direct hot reaction. As expected (see Table IV) these products are found even in the presence of I_2 radical scavenger. However, I_2 still substantially eliminates labeled higher hydrocarbons larger than the "parent" molecule and reduces the yield of HT.

The yield of the degradation product CH_3T is much smaller than that of C_2H_5T. This is consistent with earlier work on the reaction of recoil

(15) J. Kimball, *J. Chem. Phys.*, 5, 310 (1957).
(16) D. O. Schissler and D. P. Stevenson, *J. Chem. Phys.*, 24, 926 (1956).
(17) G. Meisels, W. Hamill and R. Williams, *ibid.*, 25, 790 (1957).

tritium in condensed phase[5,18] where the yield of the labeled "parent" molecule was found always to be much higher than that of labeled products formed by breaking C–C bonds.

The yield of thermal C_2H_5T from ethane appears to be slightly higher than in the case of CH_3T from methane. This would be plausible since the lifetime of C_2H_5T formed by the radical combination should be longer than that of CH_3T. Considering for the moment much more complex cases than methane and ethane, this type of consideration would indicate that in such systems appreciable amounts of the labeled form of the parent molecule and of the labeled degradation products, may be formed by the secondary, thermal type of process as well as by primary, hot displacement reaction.

Nature of Primary Displacement Reaction.—By the use of the mechanism postulated, it has thus been possible to correlate and explain in some detail a number of general as well as specific observed effects. It thus seems likely that a mechanism involving a high-energy one-step displacement as the primary step is a satisfactory and probably unique representation of the reaction of high energy hydrogen in the gas phase. We may briefly consider the nature of this primary displacement reaction.

Gorin, *et al.*,[8] have considered and have treated the case of an on-center collision between H atom and methane. They consider that this reaction will go by Walden inversion with an activation energy of 37 Kev. However, this is not the only possible mode of interaction. In an off-center collision the incoming H will essentially collide with a C–H bond rather than the central carbon atom. This can lead to the replacement of the struck H by the incoming one without Walden inversion. No direct evidence is presently available regarding which of these types of interactions is dominant. However, if a direct atomic replacement mechanism is also operative in the solid phase, our previous data on sugar systems[4] indicates that Walden inversion is not involved in the primary hot reaction.

The Hot Replacement Mechanism in Other Systems.—If direct hot replacement is the primary mechanism for the reaction of recoil tritium in the gas phase, it is of interest to explore the possibility that other hot-atom reactions proceed by a similar process. Our previous study of liquid alkanes offers the most direct comparison with the present data. Table VIII, comparing the chemical fate of recoil tritium in gaseous and condensed methane and ethane shows no major changes in the pattern of products. This suggests that the mechanism remains essentially unchanged by the phase change.

The changes that are observed in going to the liquid phase are the ones that would be expected as a result of the system becoming close packed, and also, in the case of methane, being at a much lower temperature.

In the condensed phase the medium can readily absorb excess energy and momentum from the collision complex and may thus increase the probability for the primary displacement processes. Of the secondary processes the reaction of T· with CH_3· (Table VII B2b) becomes more probable, since these fragments—resulting from the dissociation of a collision complex which had too high an internal energy to form CH_3T directly—may now be kept together by the "cage"[19] of surrounding molecules, and can thus reunite to form the labelled molecule.

The net effect of the condensed medium is then an increase in the yield of the labelled form of the molecule irradiated at the expense of the other products. The modifications imposed correspond to, and are experimentally indistinguishable from the "billiard-ball, radical cage" model proposed by Libby[20] and extended by Miller, Gryder and Dodson.[21]

TABLE VIII

EFFECT OF PHASE ON CHEMICAL FATE OF RECOIL TRITIUM

(Flux ~5 × 10^9 n./cm.^{2} sec.)

Labeled product	Recoil T + CH_4, % Gas (50°)	Liq. (−160°)	Recoil T + C_2H_6, % Gas (50°)	Liq. (−160°)
HT	50.0	39.1	43.4	41.7
CH_3T	31.8	48.6	3.8	5.4
C_2 hydrocarbons	7.7	5.8	27.5	41.5
C_3 hydrocarbons	4.0	4.2	9.7	5.3
C_4 and higher hydrocarbons	6.3	2.3	15.3	6.2

It appears that the direct displacement mechanism can account well for reactions of recoil tritium in general, provided that the properties of the condensed phase in providing a momentum and energy sink are taken into account. In agreement with this thesis is our previous observation that labeled product distributions in more complex condensed systems have qualitatively the same features as those observed in gaseous methane. Hoff and Rowland[18] have concluded already from their detailed studies of liquid alcohol and acetone that a non-radical primary displacement mechanism would provide a possible explanation for their observations. Particularly significant are their findings that a radical scavenger (diphenyl-picryl-hydrazyl) lowered the yield of HT and labile tritium and that the reactions unaffected by scavenger could all proceed by replacing a single group, preferably a hydrogen atom, with recoil tritium.

Although most recoil atoms studied in hot-atom chemistry are much heavier than T, their size and rate of energy loss at the end of their track should not be greatly different from recoil tritium. This raises the question of whether the mechanism we have suggested for recoil tritium is perhaps important in hot atom chemistry in general. Current theories[10,22] of hot-atom chemistry distinguish between a "hot" and a "diffusive" mechanism. The diffusive process is affected by the addition of radicals and evidently corresponds to our "secondary" processes. The "hot" process is generally thought[10,22] to involve reaction of the recoil atom at the end of its track with one of the radicals it has just produced and which is being held in the same solvent cage. But there appears to be no direct

(18) W. Hoff and F. Rowland, *J. Am. Chem. Soc.*, 79, 4887 (1957).

(19) J. Franck and E. Rabinowitch, *Trans. Faraday Soc.*, 30, 120 (1934).

(20) W. F. Libby, *J. Am. Chem. Soc.*, 69, 2523 (1947).

(21) Miller, Gryder and Dodson, *J. Chem. Phys.*, 18, 579, 865 (1950).

(22) M. Milman and P. Shaw, *J. Chem. Soc.*, 1303 (1957).

evidence in the field of hot-atom chemistry, which indicates that this actually is the essential mechanism of the "hot" or radical-scavenger independent step. It seems quite possible that the hot displacement mechanism (modified as discussed above for condensed phases) might account for the existing data on hot-atom reaction as well as or even better than the "caged radical" model and its variations.

Appendix

The Charge State of Recoil Tritium.—One of the chief objectives of this research has been to investigate the gas phase reactions of a recoil species which is unambiguously a hot atom, rather than an ion, in the energy range of chemical interest. As mentioned in the introduction, the failure of halogen recoil species to act as expected on the basis of conventional hot-atom theory is often explained[11] by the hypothesis that they are actually reacting as ions rather than as hot atoms. This is a possibility, though perhaps not generally a likely one, since in the formation of halogen recoils by (n,γ) reaction low energy γ-rays may be produced and internally converted. Because of their low recoil energy the resulting ions might not be able to undergo sufficient collisions to become neutralized before reacting to enter chemical combination.

We have earlier mentioned that recoil tritium should react as an atom. Willard,[3,11] however, has presented the alternative suggestion that the products observed in the interaction of recoil T with alkanes were probably formed by ion–molecule reactions involving T^+. The high efficiencies observed for reactions such as $H^+ + CH_4 \rightarrow CH_5^+$ observed by mass spectrometry are cited in support of this hypothesis.

We consider that the close agreement of our results with the predictions of the hot-atom mechanism proposed by us is significant. However, our main basis for believing that recoil tritium must become chemically incorporated by reaction as an atom is based on the theory and experimental evidence on the physics of the slowing-down of fast particles.

The triton is of course produced as a bare nucleus, and as long as it remains at very high energy it will remain so. According to the theory of Bohr,[23] as the ratio of the kinetic energy (E) of the nucleus to the ionization potential (ϵ_i) of the electron in question drops to approximately the ratio of the nuclear (M) to electron (m) masses, the electron capture cross-section of the nucleus (σ_c) increases to become equal to the ionization cross section of the corresponding atom (σ_e). Thus, when $E/\epsilon_i \sim M/m$, then $\sigma_e/\sigma_c = 1$. This prediction has been verified for proton beams in both gases and solids.[24-26] For a triton this energy corresponds to ~75 Kev. Since both σ_c and σ_e are large,[24] equilibrium is established quickly and the ratio σ_e/σ_c also represents the ratio of ions to atoms.

Due largely to mathematical difficulties no accurate values of σ_e/σ_c have been calculated for lower energies. There is, however, no disagreement that this ratio must monatomically decrease toward zero with decreasing energy. A very large body of experimental data[24,25,27] on the equilibrium ion to atom ratios at kinetic energies down to 3 Kev. support this expectation. In the kilo-volt range, the proportion of ions is invariably reduced to a few per cent.

Less experimental evidence is available for lower energies, but there is no reason to expect a change in the trend. Simons and co-workers[28] have studied the scattering of protons of <150 e.v. in hydrocarbons and report rapid neutralization.

Another approach to this problem is *via* the resonance rule[29] (adiabatic hypothesis) which gives a successful qualitative picture of the cross-section for charge exchange processes. For a reaction involving a net energy transfer ΔE, the maximum cross-section occurs when $\Delta E/h \sim v/a$, where v is the relative velocity of the colliding particles and a, the range of their interaction. Although this theory chiefly considers charge exchange between single atoms or ions, qualitatively correct answers may still be expected for the cases under consideration here. Table IX shows $|\Delta E|$'s of charge transfer reactions together with the corresponding relative energies at which the cross sections are at their maxima. It is thus seen that as a particle loses its energy in the terminal portion of its track the probability of a de-ionization reaction becomes maximal while an ionization reaction becomes even less probable. Further, the magnitude of the cross-section peaks for these charge transfer processes increases with decreasing energy. Thus since under almost any circumstances (except perhaps in metals) the neutralization reactions involve less energy than ionization, an ion slowed down from a fairly high energy by a large number of collisions must come to rest as an atom. Similar considerations indicate that unless the first excited state is extremely low, the atom will also be in its ground state.

TABLE IX

CHARGE TRANSFER PROCESSES OF TRITIUM IN METHANE

	Absolute energy of process (e.v.)	Relative kinetic energies for max. probability of reaction (e.v.)
$T + CH_4 \rightarrow T^+ + CH_4 + e^-$	13.5	~30,000
$T + CH_4 \rightarrow T^- + CH_4^+$	12.4	~25,000
$T^- + CH_4 \rightarrow T + CH_4 + e^-$	0.7	~90
$T^+ + CH_4 \rightarrow T + CH_4^+$	0.4	~30

The interest and criticisms of the Professors W. von E. Doering, F. S. Rowland and J. E. Willard were most helpful. The authors are most grateful to Brookhaven National Laboratory where the part of this work published earlier[3] was performed, for continued help and assistance.

(23) N. Bohr, *Dan. Mat. Fys. Medd.*, 18, No. 8 (1948).
(24) S. Allison and S. Warshaw, *Rev. Mod. Phys.*, 25, 779 (1953).
(25) J. A. Philips, *Phys. Rev.*, 97, 404 (1955).
(26) P. Stier, C. Barnett and G. Evans, *ibid.*, 96, 973 (1954).
(27) See for instance A. C. Whittier, *Can. J. Chem.*, 32, 275 (1954).
(28) J. H. Simons, *et al.*, THIS JOURNAL, 56, 837 (1952); *J. Chem. Phys.*, 18, 473 (1950); 13, 216, 221 (1945).
(29) Mott and Massey, "The Theory of Atomic Collisions," Oxford, 1949. Massey and Burhop, "Electronic and Ionic Impact Phenomenon," Oxford, 1952.

STIC-ILL

adonis only $16.00

From: Canella, Karen
Sent: Friday, October 24, 2003 7:40 PM
To: STIC-ILL
Subject: ill order 09/854,204

Art Unit 1642 Location 8E12(mail)

Telephone Number 308-8362

Application Number 09/854,204

1. Cell, 1984, Vol. 39, No. 3, part 2, pp. 499-509

2. Journal of Biological Chemistry, 2001, 276(8):5836-5840

3. Pharmaceutical Research, 1996, 13 (11): 1615-1623

4. Journal of Peptide Research, 1998, 51(3): 235-243

5. Neuroscience Letters 1998, 255 (1): 41-44

6. EMBO, 1990, 9 (3): 815-819

7. Journal of Organic Chemistry, 1997, 62 (5): 1356-1362

8. CAPLUS COPYRIGHT 2003 ACS on STN
ACCESSION NUMBER: 1981:454710 CAPLUS
DOCUMENT NUMBER: 95:54710
TITLE: Natural peptide lactones as ion carriers in membranes
AUTHOR(S): Oberbaeumer, Ilse; Feigl, Peter; Ruf, Horst; Grell, Ernst
CORPORATE SOURCE: Max-Planck-Inst. Biophys., Frankfurt, D-6000/71, Fed. Rep. Ger.
SOURCE: Struct. Act. Nat. Pept., Proc. Fall Meet. Ges. Biol. Chem. (1981), Meeting Date 1979, 523-38. Editor(s): Voelter, Wolfgang; Weitzel, Guenther. de Gruyter: Berlin, Fed. Rep. Ger.
CODEN: 45VYAS
DOCUMENT TYPE: Conference
LANGUAGE: English

9. CAPLUS COPYRIGHT 2003 ACS on STN
ACCESSION NUMBER: 1998:72644 CAPLUS
DOCUMENT NUMBER: 128:141012
TITLE: Rational design of peptides with enhanced membrane permeability
AUTHOR(S): Borchardt, Ronald T.
CORPORATE SOURCE: Department of Pharmaceutical Chemistry, The University of Kansas, Lawrence, KS, 66045, USA
SOURCE: Medicinal Chemistry: Today and Tomorrow, Proceedings of the AFMC International Medicinal Chemistry Symposium, Tokyo, Sept. 3-8, 1995 (1997), Meeting Date 1995, 191-196. Editor(s): Yamazaki, Mikio. Blackwell: Oxford, UK.
CODEN: 65ONAG
DOCUMENT TYPE: Conference
LANGUAGE: English

Article title	Esterase-sensitive cyclic prodrugs of peptides: Evaluation of an acyloxyalkoxy promoiety in a model hexapeptide
Article identifier	0724874196003367
Authors	Pauletti_G_M Gangwar_S Okumu_F_W Siahaan_T_J Stella_V_J Borchardt_R_T
Journal title	Pharmaceutical Research
ISSN	0724-8741
Publisher	Plenum
Year of publication	1996
Volume	13
Issue	11
Supplement	0
Page range	1615-1623
Number of pages	9
User name	Adonis
Cost centre	Development
PCC	$16.00
Date and time	Monday, October 27, 2003 8:01:50 AM

Pharmaceutical Research, Vol. 13, No. 11, 1996

Research Article

Esterase-Sensitive Cyclic Prodrugs of Peptides: Evaluation of an Acyloxyalkoxy Promoiety in a Model Hexapeptide

Giovanni M. Pauletti,[1] Sanjeev Gangwar,[1] Franklin W. Okumu,[1] Teruna J. Siahaan,[1] Valentino J. Stella,[1] and Ronald T. Borchardt[1,2]

Received June 14, 1996; accepted August 23, 1996

Purpose. To evaluate a cyclic acyloxyalkoxycarbamate prodrug of a model hexapeptide (H-Trp-Ala-Gly-Gly-Asp-Ala-OH) as a novel approach to enhance the membrane permeation of the peptide and stabilize it to metabolism. ***Methods.*** Conversion to the linear hexapeptide was studied at 37°C in aqueous buffered solutions and in various biological milieus having measurable esterase activities. Transport and metabolism characteristics were assessed using the Caco-2 cell culture model. ***Results.*** In buffered solutions the cyclic prodrug degraded chemically to the linear hexapeptide in stoichiometric amounts. Maximum stability was observed between pH 3–4. In 90% human plasma ($t_{1/2}$ = 100 ± 4 min) and in homogenates of the rat intestinal mucosa ($t_{1/2}$ = 136 ± 4 min) and rat liver ($t_{1/2}$ = 65 ± 3 min), the cyclic prodrug disappeared faster than in buffered solution, pH 7.4 ($t_{1/2}$ = 206 ± 11 min). Pretreatment of these media with paraoxon significantly decreased the degradation rate of the prodrug. When applied to the apical side of Caco-2 cell monolayers, the cyclic prodrug ($t_{1/2}$ = 282 ± 25 min) was significantly more stable than the hexapeptide ($t_{1/2}$ = 14 min) and at least 76-fold more able to permeate (P_{app} = 1.30 ± 0.15 × 10^{-7} cm/s) than the parent peptide ($P_{app} \leq 0.17 \times 10^{-8}$ cm/s). ***Conclusions.*** Preparation of a cyclic peptide using an acyloxyalkoxy promoiety reduced the lability of the peptide to peptidase metabolism and substantially increased its permeation through biological membranes. In various biological media the parent peptide was released from the prodrug by an apparent esterase-catalyzed reaction, sensitive to paraoxon inhibition.

KEY WORDS: esterase-sensitive prodrug; peptide delivery; Caco-2 cells; membrane permeability; enzymatic stability; chemical stability.

INTRODUCTION

Clinical development of orally active peptide drugs has been restricted by their unfavorable physicochemical properties, which limit their intestinal mucosal permeation, and their lack of stability against enzymatic degradation (1–3). Successful oral delivery of peptides will depend, therefore, on strategies designed to alter the physicochemical characteristics of these potential drugs, without changing their biological activity, in order to circumvent the intestinal epithelial cells. In general, it is accepted that size, charge, and lipophilicity are crucial physicochemical properties in determining the ability of a peptide to permeate the intestinal mucosa (4). Solution conformation might be another important parameter affecting the transfer of peptide drugs across biological membranes (5, 6).

One possible approach to altering the physicochemical properties of a peptide is to employ prodrug strategies. Prodrugs are pharmacologically inactive chemical derivatives of drugs designed to overcome pharmaceutical and/or pharmacokinetic problems (for reviews see (7) and (8)). The ideal prodrug of a peptide would exhibit enhanced membrane permeation characteristics and increased stability against metabolic degradation. After crossing the membrane barrier, the prodrug should undergo spontaneous or enzymatic transformation to release the peptide, which then can exhibit its pharmacological effect. By preparing cyclic prodrugs using the functional groups of the N- and C-terminal ends of a peptide, metabolic degradation mediated by exopeptidases should be minimized (9). In addition, cyclization of a peptide may also restrict the conformational flexibility of the molecule, leading to a more compact structure with altered physicochemical properties (10).

Recently, our laboratory reported the synthesis of a cyclic prodrug of a model hexapeptide (H-Trp-Ala-Gly-Gly-Asp-Ala-OH) using an acyloxyalkoxy promoiety (11). The degradation of this N-terminal to C-terminal linked cyclic prodrug was designed to occur by an esterase-catalyzed reaction (Scheme 1). Esterases represent a large family of isozymes with broad substrate specificity found in a variety of tissues (e.g., blood, liver, intestinal mucosa) from different species (12, 13). In this study, we have determined the stability of the cyclic acyloxyalkoxycarbamate prodrug in buffer solutions and in various biological milieus having measurable esterase activities. Transport and metabolism of this cyclic prodrug were assessed using a cell culture model (Caco-2) of the intestinal mucosa. Caco-2

[1] Department of Pharmaceutical Chemistry, 2095 Constant Ave., The University of Kansas, Lawrence, Kansas 66047.
[2] To whom correspondence should be addressed.

ABBREVIATIONS: HBSS, Hanks' balanced salt solution; DMEM, Dulbecco's modified Eagle medium; AP, apical; BL, basolateral.

0724-8741/96/1100-1615$09.50/0

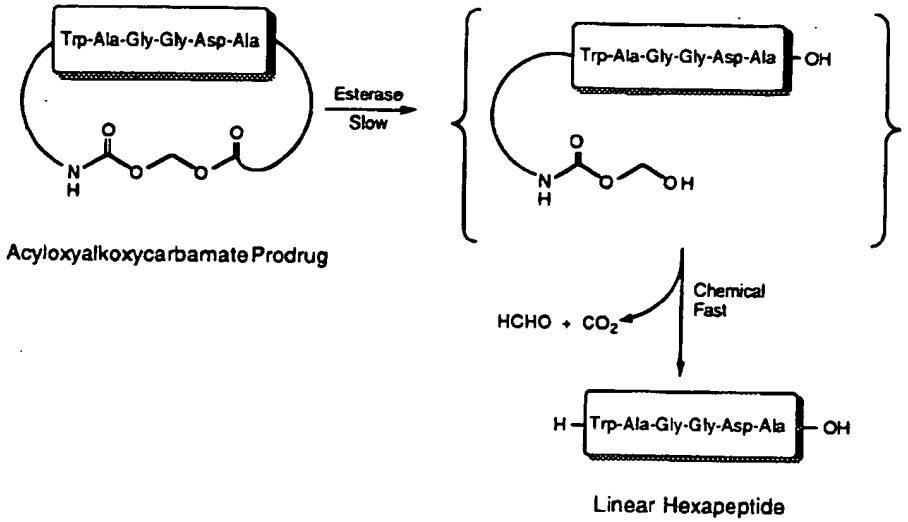

Scheme 1. Proposed mechanism for the release of the linear hexapeptide from the cyclic acyloxyalkoxycarbamate prodrug.

cells, which spontaneously undergo differentiation into confluent monolayers (14), have been shown to exhibit both the physical and metabolic barrier properties of intestinal mucosal cells to peptides (15–17). Our results are discussed in light of the physicochemical properties and the conformational structure of the cyclic prodrug.

MATERIALS

The cyclic acyloxyalkoxycarbamate prodrug was prepared as described elsewhere (11). The linear model hexapeptide, H-Trp-Ala-Gly-Gly-Asp-Ala-OH, was obtained by solid phase synthesis using standard Fmoc chemistry, purified by preparative HPLC (>98%), and characterized by FAB$^+$-MS and ^{1}H-NMR (10). Diethyl *p*-nitrophenyl phosphate (=paraoxon, approx. 90%), *p*-nitrophenyl butyrate (~98%), dimethyl sulfoxide (>99.5%), bestatin hydrochloride, captopril, Dulbecco's phosphate-buffered saline, and Hanks' balanced salts (modified) were purchased from Sigma Chemical Co. (St. Louis, MO). L-Glutamine 200 mM (100×), penicillin (10,000 U/ml), streptomycin (10,000 μg/ml), and non-essential amino acid 10 mM (100×) in 0.85% saline were obtained from Gibco BRL, Life Technologies (Grand Island, NY). Dulbecco's modified Eagle medium and trypsin/EDTA solution (0.25% and 0.02%, respectively, in Ca^{2+}- and Mg^{2+}-free Hanks' balanced salt solution) were purchased from JRH Biosciences (Lenexa, KS). Rat tail collagen (type 1) was obtained from Collaborative Biomedical Products (Bedford, MA), and fetal bovine serum from Atlanta Biologicals (Norcross, GA). D-1[^{14}C]Mannitol (spec. act. = 2.07 GBq/mmol) was purchased from Moravek Biochemicals (Brea, CA), and diprotin A was obtained from Bachem Feinchemikalien (Bubendorf, Switzerland). All other chemicals and solvents were of high purity or analytical grade and used as received.

METHODS

Cell Culture

Caco-2 cells were obtained from American Type Culture Collection (Rockville, MD) at passage 18. As described previously (14), cells were grown in a controlled atmosphere of 5% CO_2 and 90% relative humidity at 37°C in 150 cm^2 culture flasks using a culture medium consisting of Dulbecco's modified Eagle medium (DMEM) supplemented with 10% heat-inactivated fetal bovine serum, 1% non-essential amino acids, 100 μg/ml streptomycin, 100 U/ml penicillin, and 1% L-glutamine. When approximately 80% confluent (i.e., 3–5 days), cells were detached from the plastic support by partial digestion using trypsin/EDTA solution and either subcultured in new flasks or plated on collagen-coated polycarbonate membranes (Transwell®, 3 μm pore size, 24.5 mm diameter) at a density of 8.0 × 10^4 cells/cm^2. Caco-2 cells were fed with culture medium every other day for 7 days and then daily until transport experiments were performed (apical volume 1.5 ml, basolateral 2.6 ml). Cells were used in this study between passages 40 and 43.

Tissue Homogenate and Human Plasma

Rat Intestinal Homogenate

Male Sprague-Dawley rats (Animal Care Unit, The University of Kansas, Lawrence, KS) weighing 250–350 g were anesthetized with Metofane® and an abdominal incision was performed. The small intestine, from ~5 cm distal to the pylorus to ~5 cm proximal to the caecum, was immediately removed and rinsed with ice-cold oxygenated (95% O_2 and 5% CO_2) Hanks' balanced salt solution (HBSS), pH 7.4. After flushing out the intestinal contents with ice-cold oxygenated HBSS, segments of approximately 3 cm were isolated and cut open. The intestinal mucosa was scraped off with a glass slide by placing the everted intestine on a glass plate that was kept on a layer of ice. The mucosa was homogenized on ice with 10 ml HBSS using a 15 ml Wheaton glass homogenizer (15 strokes, pestle/wall clearance 0.25–0.76 mm). Aliquots of 1.5 ml were frozen and kept at −80°C until used. Before an experiment, the homogenate was quickly thawed and rehomogenized on ice with an equal volume of HBSS (10 strokes, pestle/wall clearance 0.64–0.75 mm). Cell debris and nuclei were removed at 4°C

by centrifugation for 10 min at 10,000 rpm (9000 × g) using a Marathon 21K/BR centrifuge (Hermle AG, Gosheim, FRG).

Rat Liver Homogenate

Rat livers were obtained from the same animals used to prepare the intestinal homogenate. The tissue was blotted to dryness and after weighing was sliced in small pieces with a scalpel. Homogenates were prepared in HBSS (1 ml per g tissue) as described for the preparation of rat intestinal homogenate.

Caco-2 Cell Homogenate

Confluent Caco-2 cell monolayers (21–28 days) were washed 3× with ice-cold HBSS and carefully scraped from the filter support with a rubber spatula. Cells of 6 monolayers were collected in 2 ml of ice-cold HBSS and homogenized on ice using a 15 ml Wheaton glass homogenizer (15 strokes, pestle/wall clearance 0.64–0.76 mm). Cell debris and nuclei were removed as described above.

Human Plasma

Human blood, stabilized with CPDA-1 solution USP, was obtained from the Topeka Blood Bank (Topeka, KS). Plasma was separated from the erythrocytes at 4°C by centrifugation for 10 min at 4700 rpm (2000 × g). For stability studies, human plasma was diluted to 90% (v/v) with HBSS, pH 7.4, in order to maintain the pH of the solution during the experiment.

Lipophilicity

The lipophilicities of the cyclic prodrug and the linear hexapeptide were estimated by determining their partition coefficients between 0.02 M phosphate buffer, pH 7.4, and an immobilized artificial membrane (IAM.PC.DD column, 10 cm × 4.6 mm I.D., Regis Technologies, Inc., Morton Grove, IL) according to Liu *et al.* (18). Aliquots (20 μl) of the peptide solutions (~15 μg/ml, in running buffer) were injected on the c lumn (flow rate 1.0 ml/min) and solutes detected with a UV detector (λ = 220 nm) or with a fluorescence detector as described below.

M lecular Size

The average hydrodynamic volumes of the peptides were estimated by high-resolution size exclusion chromatography performed in 0.02 M phosphate buffer, pH 7.4, with 0.25 M NaCl using a Superdex Peptide 10/30 HR column (10 × 300 mm, Pharmacia Biotech, Uppsala, Sweden). The peptide solutions (50 μl, ~10 μg/ml, in running buffer) were injected on the column (flow rate 1.0 ml/min), and solutes were detected with a UV detector at λ = 220 nm as described below.

Chemical Stability

The chemical stability of the cyclic acyloxyalkoxycarbamate prodrug was assessed at 37°C over the pH range 3.0–9.6. Solutions of the prodrug (~15 μg/ml) were prepared in buffers at an ionic strength of 0.5 M adjusted with NaCl. The buffers (0.1 M) used for each pH were as follows: potassium bitartrate at pH 3.0; sodium acetate at pH 4.0; sodium phosphate at pH 5.0–8.0; and sodium borate at pH 9.0 and 9.6. Samples were maintained at 37.0 ± 0.5°C in a temperature-controlled shaking water bath (60 rpm) in sealed vials. Periodically, 20 μl aliquots were removed and immediately analyzed by HPLC. Rate constants were calculated by linear regression from pseudo first-order plots of prodrug concentration vs. time measured for at least two half-lives.

Enzymatic Stability

The stability of the acyloxyalkoxycarbamate prodrug in various tissue homogenates and 90% human plasma was determined at 37°C in the presence and absence of paraoxon, a potent esterase inhibitor. Total esterase activity in the biological media was assessed using *p*-nitrophenyl butyrate (PNPB) as substrate. *p*-Nitrophenol, the final product of this enzymatic reaction, was quantitated spectrophotometrically at λ = 420 nm using a HP 8452 diode array spectrophotometer equipped with a temperature-controlled cuvet holder (25°C). Initial velocities were calculated by linear regression ($r^2 \geq 0.99$) and corrected for non-enzymatic hydrolysis. Esterase activities were expressed as units per milligram protein (U/mg protein). One unit represents the amount of enzyme that catalyzes the formation of 1 μmol *p*-nitrophenol per minute in HBSS, pH 7.4 (25°C). Conditions of linearity for the enzymatic hydrolysis of PNPB in HBSS, pH 7.4, (25°C) were maintained for 600 s between 0.02–2 U/ml. Total protein concentration in the biological media was determined using the Bio-Rad® Protein Assay (Bio-Rad Laboratories; Richmond, CA) with bovine serum albumin as standard.

The acyloxyalkoxycarbamate prodrug (final concentration ~24 μM) was incubated for 6 hours with 1 ml of homogenates of rat intestinal mucosa, rat liver, Caco-2 cells or 90% human plasma in a temperature-controlled (37.0 ± 0.5°C) shaking water bath (60 rpm). At various time points, aliquots (20 μl) were removed and the esterase activity immediately quenched by adding 150 μl of a freshly prepared 6 N guanidinium hydrochloride solution in acidified HBSS (HBSS containing 0.01% (v/v) phosphoric acid). Aliquots (150 μl) of that acidic mixture (pH ~3) were then transferred to an Ultrafree®-MC 5000 NMWL filter unit (Millipore, Bedford, MA) and centrifuged at 7500 rpm (5000 × g) for 60 min (4°C). Aliquots (50 μl) of the filtrates were diluted with mobile phase and injected on the HPLC column. Recoveries for the peptides were ≥97%.

The effect of an esterase inhibitor on the rate of degradation of the cyclic prodrug in the various biological media was determined using paraoxon. Paraoxon (final concentration 1 mM) was first preincubated with the respective biological matrix for 15 min at 37°C before adding the prodrug or PNPB. Apparent half-lives ($t_{1/2}$) for the disappearance of the prodrug were calculated from the rate constants obtained by linear regression ($r^2 \geq 0.97$) from pseudo first-order plots of prodrug concentration vs. time.

Transport Studies

Caco-2 cell monolayers grown on collagen-coated polycarbonate filters (Transwells®) were used for transport experiments between days 21 and 28. The integrity of each batch of cells was first tested by measuring the leakage of [^{14}C]-mannitol in representative cell monolayers (n = 3). Apical (AP)-to-basolateral (BL) flux for this paracellular marker never

exceeded values of 0.4%/hour. Routinely, cell monolayers were washed 3× with prewarmed HBSS, pH 7.4, and the peptide solution (~100 μM in HBSS) was applied to the donor compartment (AP, 1.5 ml or BL, 2.6 ml). HBSS was added to the receiver compartment. Samples (120 μl, receiver side; 20 μl, donor side) were removed at various times up to 180 min from both sides. The volume removed from the receiver side was always replaced with fresh, prewarmed HBSS. To stabilize the samples, an aliquot of acetonitrile and diluted phosphoric acid (final concentrations 10% (v/v) and 0.01% (v/v), respectively) was added. This acidic mixture (pH ~3) was immediately frozen in a dry-ice/acetone bath and kept at −80°C until HPLC analysis. Transport experiments, from the AP-BL side as well as from the BL-AP side, were performed in triplicate at 37°C in a shaking water bath (60 rpm). Permeation of the linear model hexapeptide through Caco-2 cell monolayers was assessed in the presence and absence of a "cocktail" of three peptidase inhibitors (i.e., 0.29 mM bestatin, 1 mM captopril, and 1 mM diprotin A).

HPLC Analysis

Chromatographic analyses were carried out on a Shimadzu LC-10A gradient system (Shimadzu, Inc., Tokyo, Japan) consisting of LC-10AD pumps, a SCP-6 controller, a SPD-10A UV detector, and a RF-535 fluorescence detector connected to LCI-100 integrators (Perkin-Elmer, Norwalk, CT). Samples from a refrigerated sample tray (4°C) were injected by a Perkin-Elmer ISS-100 autoinjector on a Dynamax C_{18} reverse-phase column (5 μm, 300 Å, 25 cm × 4.6 mm I.D., Rainin Instruments, Woburn, MA) equipped with a guard column. The fluorescence of the eluent was monitored at emission λ = 345 nm (excitation λ = 285 nm). Gradient elution of the peptides was performed at a flow rate of 1 ml/min from 10.8–74.0% (v/v) acetonitrile in water using trifluoroacetic acid (0.1%, v/v) as the ion-pairing agent. Under these conditions, the retention times of the linear model hexapeptide and the cyclic prodrug were 7.7 and 11.8 min, respectively.

Data Analysis

Permeability coefficients (P_{app}) of the linear model hexapeptide were calculated according to equation 1:

$$P_{app} = \frac{\Delta Q/\Delta t}{A \cdot c(0)} \quad (1)$$

where $\Delta Q/\Delta t$ = linear appearance rate of mass in the receiver solution, A = cross-sectional area (i.e., 4.71 cm^2), and $c(0)$ = initial peptide concentration in the donor compartment at $t = 0$.

Data analysis for the acyloxyalkoxycarbamate prodrug was based on the assumption that the change in the amount of the prodrug in the donor compartment is due only to passive diffusion from the donor to the receiver compartment and chemical hydrolysis in the donor compartment. Similarly in the receiver compartment, the change in mass of the prodrug is assumed to be related only to the passive diffusion of the prodrug from the donor to the receiver compartment and chemical hydrolysis in the receiver compartment. Under these conditions, the following equations were obtained using Laplace transformation:

$$\frac{M_D}{M_D(0)} = e^{-(A \cdot P_{app}/V_D + k)t} \quad (2)$$

$$\frac{M_R}{M_D(0)} = e^{-kt} - e^{-(A \cdot P_{app}/V_D + k)t} \quad (3)$$

V_D = volume of the donor compartment and k = rate constant characterizing the chemical hydrolysis of the cyclic prodrug during transport experiments. M_D and M_R represent the amount of prodrug in the donor and receiver compartments, respectively, and $M_D(0)$ = the initial amount of prodrug applied to the donor compartment at $t = 0$. P_{app} for the acyloxyalkoxycarbamate prodrug was obtained by a simultaneous curve-fitting procedure using equation 2 for the receiver and equation 3 for the donor compartment.

Statistical Analysis

The results of experiments performed in triplicate are presented as mean ±SD. Statistical significance was tested by one-way analysis of variance (ANOVA) using Tukey's family error at $p < 0.05$.

RESULTS

Chemical Stability

The degradation kinetics of the cyclic prodrug at 37°C was followed in aqueous buffered solutions, pH 3.0–9.6, for at least two half-lives. The only degradation product that appeared in the reaction mixture was the linear hexapeptide, which was stable at all pH values studied. Mass balance (≥97.2%) was achieved in all experiments. A representative time course of the disappearance of the cyclic prodrug and the appearance of the linear hexapeptide is presented in Fig. 2A. From the disappearance of the cyclic prodrug, degradation rate constants, k_{obs}, were calculated by linear regression of pseudo first-order plots ($r^2 \geq 0.98$). Fig. 1 shows a plot of the log k_{obs} vs. pH, which appears to consist of two distinct portions. Maximum stability of the cyclic prodrug was found at pH values ≤4

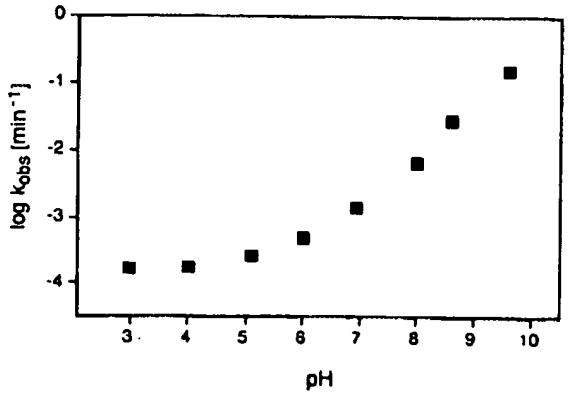

Fig. 1. The pH/rate profile for the chemical degradation of the cyclic prodrug determined in 0.1 M buffer solutions pH 3.0–9.6 (μ = 0.5 M) at 37°C. Apparent first-order rate constants, k_{obs}, were calculated from the disappearance of the prodrug as described in Materials and Methods.

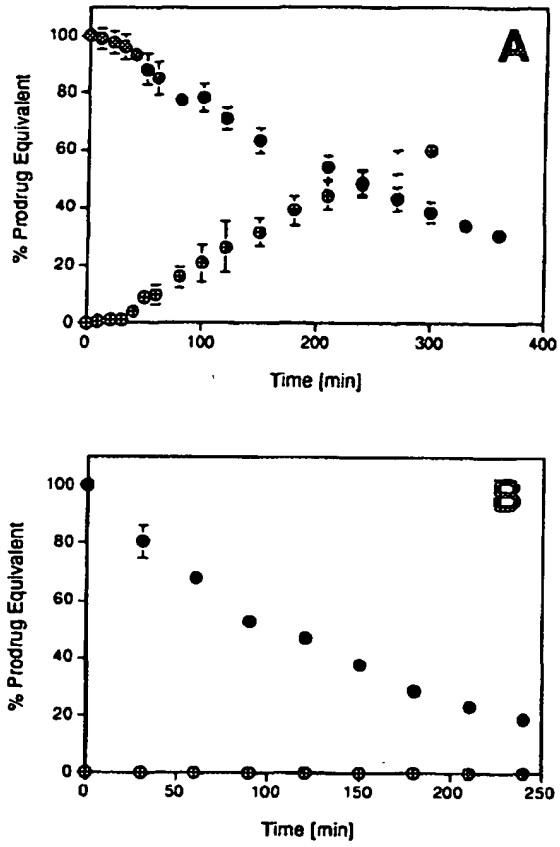

Fig. 2. Stability of the cyclic prodrug at 37°C in HBSS, pH 7.4, and 90% human plasma. Panel A shows the time course of the disappearance of the cyclic prodrug (•) and the appearance of the linear hexapeptide (⊕) in HBSS, pH 7.4; Panel B shows the result of a similar experiment performed in 90% human plasma. Experiments were performed in triplicate (average ± SD).

(k_{obs} = 1.61 × 10^{-4} min^{-1}). With increasing pH, the cyclic prodrug degrades progressively faster to the linear model hexapeptide. At pH values ≥8, the slope in the pH/rate-profile is approximately 1.

Enzymatic Stability

The acyloxyalkoxycarbamate prodrug was designed to undergo enzyme-catalyzed hydrolysis of the ester bond followed by two fast chemical steps to release the parent peptide (11) (see Scheme 1). Therefore, the stability of the cyclic prodrug was determined in various biological media (i.e., rat intestinal homogenate, rat liver homogenate, 90% human plasma and Caco-2 cell homogenate) having measurable esterase activities, and these rates were compared to the chemical degradation in HBSS, pH 7.4.

Comparison of the relative esterase activities present in these biological media as determined by PNPB hydrolysis reveals that rat intestinal homogenate contains the highest esterase activity per mg protein, followed by rat liver homogenate, Caco-2 cell homogenate and 90% human plasma. After a 15 min preincubation at 37°C with the esterase inhibitor paraoxon (1 mM), enzyme activities in all matrices were significantly reduced (Table I). However, the extent of inhibition was not related to the total enzyme activity measured in the absence of paraoxon, but seems to be species-dependent (rat >> human) and, within the same species (i.e., rat), tissue-specific (intestine > liver). In 90% human plasma, residual esterase activity after incubation with paraoxon was still 30% of the initial activity, whereas in rat liver homogenate only a minimum residual activity of 1.3% could be determined. In rat intestinal homogenate, no esterase activity at all was detectable after pretreatment with paraoxon.

Apparent half-lives for the disappearance of the cyclic prodrug in the various biological media are presented in Table I. With the exception of Caco-2 cell homogenate, the rate of disappearance of the cyclic prodrug in these biological media was substantially faster than in HBSS, pH 7.4. In Caco-2 cell homogenate, the cyclic prodrug disappeared at approximately the same rate as that observed in HBSS, although esterase activity was measured in this biological matrix.

In the presence of paraoxon, the disappearance of the cyclic prodrug in all biological media, except for Caco-2 cell homogenate, was significantly slower than in the absence of the esterase inhibitor. This indicates that the cyclic prodrug most likely degrades by hydrolysis of the ester bond mediated by esterases. However, it should be mentioned that in all biological media, mass balance for the conversion of the cyclic prodrug to the linear hexapeptide was not achieved. The amount of the linear hexapeptide never exceeded values of 0.05% of the prodrug equivalent as shown in Fig. 2B for the degradation of the cyclic prodrug in 90% human plasma. This can be explained by the fact that, in contrast to the experiments performed in aqueous buffered solutions, the linear hexapeptide rapidly degrades (e.g., $t_{1/2}$ in 90% human plasma = 3.7 min; data not shown) due to the presence of peptidases in these biological media.

Transport in Caco-2 Cell Monolayers

To determine the cell permeability characteristics of the linear hexapeptide and the cyclic prodrug, permeation of these peptides was assessed in Caco-2 cell monolayers, an *in vitro* model of the intestinal mucosa. Fig. 3A shows that the linear hexapeptide rapidly disappears from the AP side of Caco-2 cell monolayers ($t_{1/2}$ = 14 min), suggesting high susceptibility to enzymatic degradation by peptidases. To test this hypothesis, transport experiments were conducted in the presence of a mixture of three potent peptidase inhibitors (i.e., bestatin, captopril, and diprotin A) (19). Under these conditions, the disappearance of the linear hexapeptide was indeed slower, so that more than 70% of the initially applied peptide concentration was still present on the AP side of the monolayer after a 180 min incubation. The cyclic prodrug, in contrast, was significantly more stable than the linear hexapeptide when applied to the AP side of the Caco-2 cell monolayers (Fig. 3A). In the absence of peptidase inhibitors, 66.9 ± 1.0% of the prodrug initially added to the donor compartment was present after a 3-hr incubation period. A comparison of the disappearance rate f the cyclic prodrug from the AP side of Caco-2 cell monolayers ($t_{1/2}$ = 282 ± 25 min) with the respective rate determined f r the chemical hydrolysis of the cyclic prodrug in HBSS ($t_{1/2}$ = 206 ± 11 min, see Table I) revealed that the cyclic prodrug is

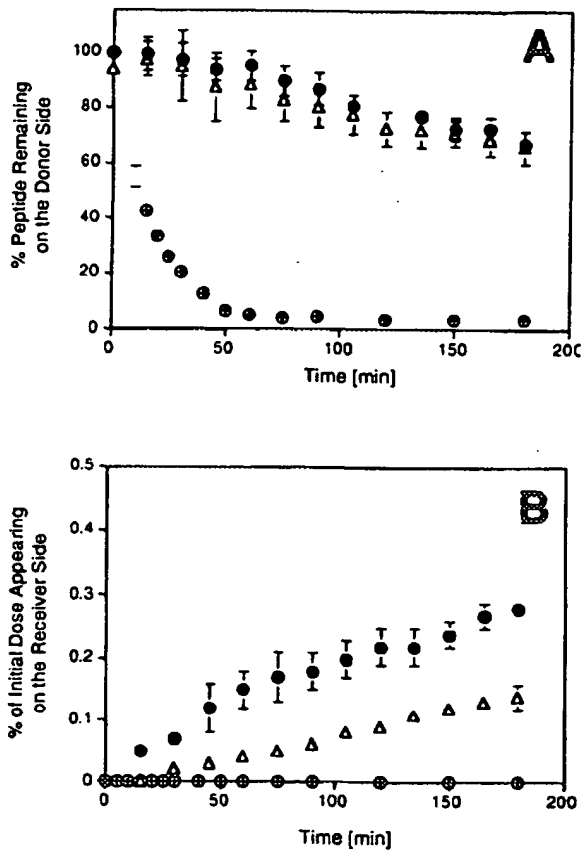

Fig. 3. Time course of disappearance of the cyclic prodrug (●) and appearance of the linear hexapeptide (in the presence (△) and absence (⊕) of peptidase inhibitors) when applied to the apical side of Caco-2 cell monolayers and incubated up to 3 hours at 37°C. Panel A shows time profiles of the peptides remaining in the donor compartment (i.e., apical side), and Panel B represents the peptides transported to the receiver compartment (i.e., basolateral side). Experiments were performed in triplicate (average ± SD).

metabolically stable when applied to the AP side of Caco-2 cell monolayers.

In the absence of peptidase inhibitors, the linear hexapeptide did not permeate the Caco-2 cell monolayer in measurable amounts (Fig. 3B). As a consequence, the apparent permeability coefficient (P_{app}) was estimated based on the analytical detection limit for the peptide (Table II). The intrinsic permeability of the linear hexapeptide was obtained from the linear flux (0.08%/hr) that was observed from the AP to the BL compartment and vice versa in the presence of the peptidase inhibitors. The cyclic prodrug, in contrast, was able to cross the cell barrier in the absence of peptidase inhibitors at an initial rate of 0.15%/hr (calculated within the first 45 min). At later time points, the increase in the amount of prodrug measured in the BL compartment deviates from linearity because the prodrug is undergoing chemical hydrolysis as described earlier in this paper. When compared to the P_{app} of the parent peptide, the cyclic prodrug is at least 76-fold more able to permeate than is the linear hexapeptide (Table II). Transport in the AP to BL direction was statistically not different from the transport in the opposite direction (i.e., BL-AP). The cyclic acyloxyalkoxycarbamate prodrug was also approximately 3 times more able to permeate than the linear model hexapeptide in the presence of potent peptidase inhibitors.

Physicochemical Properties

Physicochemical properties (lipophilicities and average hydrodynamic volumes) of the linear hexapeptide and the cyclic prodrug, which might be crucial in determining their permeation characteristics, were determined by chromatographic techniques and are shown in Table II. The negative log k'_{IAM} value determined for the linear peptide reflects moderate interaction between the hydrophobic portion of the immobilized phosphatidylcholine analogs and the peptide. Incorporating the peptide into the cyclic prodrug resulted in stronger interactions to the lipophilic stationary phase, as indicated by a larger log k'_{IAM} value. This suggests higher lipophilicity for the cyclic prodrug as compared to the linear hexapeptide.

Based on the capacity factors, K_d, that were determined for the peptides by high-resolution size exclusion chromatography (Table II), the cyclic prodrug appears to have a smaller molecular hydrodynamic volume than the linear hexapeptide, although its molecular weight is larger.

Table I. Apparent Half-Lives of the Cyclic Prodrug in HBSS, pH 7.4, Rat Intestinal Homogenate, Rat Liver Homogenate, 90% Human Plasma, and Caco-2 Cell Homogenate in the Presence and Absence of Paraoxon (1 mM) at 37°C

Incubation mixture	Specific activity[a] [U/mg protein]	Enzyme concentration [U/ml]		Apparent half-life[b] [min]	
		−paraoxon	+paraoxon	−paraoxon	+paraoxon
HBSS, pH 7.4	0	0	0	206 ± 11	201 ± 4
Caco-2 cell homogenate	0.29	0.48	n.d.	209 ± 8	n.d.
90% human plasma[c]	0.01	0.37	0.11	100 ± 4*	171 ± 13*
rat intestinal homogenate	7.37	10.32	0	136 ± 4*	215 ± 4
rat liver homogenate	1.53	13.77	0.18	65 ± 3*	193 ± 3

Note: n.d. = not determined. *Significantly different from the control in HBSS, pH 7.4 ($p < 0.05$).

[a] Determined at 25°C in HBSS, pH 7.4 using *p*-nitrophenyl butyrate as substrate.

[b] Calculated from apparent first-order rate constants.

[c] Human plasma diluted to 90% (v/v) with HBSS, pH 7.4.

Table II. Physicochemical Properties and Transport Characteristics Determined Through Caco-2 Cell Monolayers of the Cyclic Prodrug and the Linear Hexapeptide

Compound	MW	Size[a] [K_d]	Lipophilicity[b] [log k'_{IAM}]	Permeability coefficients, P_{app} [$\times 10^6$ cm/s]	
				AP-BL	BL-AP
H-Trp-Ala-Gly-Gly-Asp-Ala-OH	574	0.59	−1.10	<0.17	<0.17
H-Trp-Ala-Gly-Gly-Asp-Ala-OH + peptidase inhibitor "cocktail"[c]				4.05 ± 0.24	4.66 ± 0.60
Trp-Ala-Gly-Gly-Asp-Ala 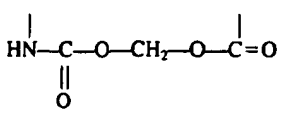	631	0.83	−0.32	12.97 ± 1.48[d]	11.59 ± 0.91[d]

[a] Determined by high-resolution size exclusion chromatography.
[b] Partition coefficient between 0.02 M phosphate buffer, pH 7.4, and an immobilized artificial membrane of phosphatidylcholine analogs (IAM.PC.DD).
[c] Bestatin 0.29 mM, captopril 1 mM, diprotin A 1 mM.
[d] Calculated from the cumulative flux in the receiver compartment that was corrected for chemical degradation of the prodrug in HBSS, pH 7.4 (see Materials and Methods).

DISCUSSION

A fundamental requirement of a prodrug is that it can be converted to the parent drug by either a chemical or enzymatic reaction (7). The acyloxyalkoxycarbamate prodrug described in this study was designed to release the model hexapeptide by enzymatic hydrolysis of the ester moiety (see Scheme 1). Since ester bonds are not only enzymatically but also chemically labile, we determined the stability of the cyclic prodrug both in buffered solutions, pH 3.0-9.6, and in biological media known to contain esterase activity.

With respect to chemical instability, this cyclic prodrug was more stable under moderate acidic conditions than in basic solutions (Fig. 1). The plateau region between pH 3 and 4 suggests spontaneous or water-catalyzed hydrolysis, whereas the progressively faster disappearance at pH values ≥5 implies a specific base-catalyzed hydrolysis of the ester moiety as the major degradation mechanism. It is important to note that the linear hexapeptide can be formed from the cyclic prodrug by chemical hydrolysis, i.e., in the absence of any esterase activity. Since the rate constants for the formation of the linear model hexapeptide (e.g., HBSS, pH 7.4, $t_{1/2}$ = 213 ± 13 min) were nearly identical with those obtained for the disappearance of the cyclic prodrug (e.g., HBSS, pH 7.4, $t_{1/2}$ = 206 ± 11 min), we concluded that the rate-determining step in the cascade of reactions leading to the release of the parent peptide is indeed the ester hydrolysis, followed by rapid elimination of formaldehyde and carbon dioxide (Scheme 1).

In a biological milieu, the cyclic prodrug would be expected to degrade to the linear hexapeptide by both chemical and enzyme-catalyzed reactions (Scheme 1). To assess the susceptibility of this prodrug to esterase-catalyzed hydrolysis, several biological media were selected and the rates of prodrug conversion determined. Based on the spectrophotometric assay using PNPB as a substrate, all biological media that were used in this study exhibited measurable levels of esterase activity (Table I). The specific esterase activity, however, was remarkably species-dependent and, within the same species, found to differ significantly between various tissues (Table I). Studies performed earlier with different substrates indicate that rat tissue, in general, exhibits much higher esterase activities than human tissues (12, 20, 21). Within the same species, liver, plasma and intestinal mucosa are considered the most important sites of metabolism for esterase-sensitive drugs, although the ranking order in activity is unquestionably affected by substrate specificity (22).

Apparent half-lives of the acyloxyalkoxycarbamate prodrug in human plasma and rat tissue homogenates were significantly less than in HBSS, pH 7.4. This suggests that the disappearance of the cyclic prodrug may be catalyzed by esterases. Due to rapid metabolism of the linear hexapeptide in biological media (*e.g.*, $t_{1/2}$ in 90% human plasma = 3.7 min; data not shown), it was not clear whether the disappearance of the cyclic prodrug was based on the mechanism proposed in Scheme 1 or mediated by endopeptidases. The latter pathway could be ruled out by the observation that a N-terminal-to-C-terminal-linked analog of the hexapeptide showed ≤0.3% degradation after a 6-hr incubation in rat liver homogenate (data not shown). Hence, we have reasonable confidence that the cyclic prodrug is converted to the linear model hexapeptide by an esterase-mediated reaction.

Additional experimental evidence for the proposed mechanism shown in Scheme 1 was obtained from studies using paraoxon, a potent esterase inhibitor. Apparent half-lives of the cyclic prodrug in 90% human plasma and rat tissue homogenates were significantly longer after preincubation with the potent esterase inhibitor. In Caco-2 cell homogenate, however, the rate of disappearance of the cyclic prodrug in the absence of paraoxon was not different than the chemical hydrolysis rate, in spite of the fact that this biological medium had high esterase activity (Table I). This suggests that the cyclic prodrug can be cleaved only by a certain family of isozymes that are present in 90% human plasma and rat tissue homogenates but not in

Caco-2 cells. Esterases that are sensitive to paraoxon inhibition are classified as B-esterases (23). Based on the almost complete inhibition of the enzymatic hydrolysis of PNPB in rat tissue homogenates in the presence of paraoxon, we conclude that these biological media contain predominantly B-esterases. Human plasma, in contrast, showed still more than 30% residual esterase activity after pretreatment with paraoxon, suggesting the presence of a considerable fraction of A-and/or C-esterases in this medium. Since the rate of disappearance of the cyclic prodrug in 90% human plasma in the presence of paraoxon was significantly different from chemical hydrolysis, the acyloxyalkoxycarbamate prodrug seems to have affinity for B-esterases as well as for "non"-B-esterases (i.e., A- and/or C-esterases). However, carboxypeptidases are also known to cleave ester bonds (24) and, therefore, it is not known whether the release of the parent peptide from the cyclic prodrug is mediated only by esterases.

The intestinal mucosa represents a significant barrier to oral delivery of peptides into the systematic circulation (1, 4). Tight intercellular junctions limit paracellular flux of a peptide (physical barrier), and peptidases associated with the brush-border membrane and the cytoplasm (metabolic barrier) rapidly metabolize peptides to their constituent amino acids (1–3). Therefore, it was of interest to investigate the transport and metabolism of the acyloxyalkoxycarbamate prodrug in Caco-2 cell monolayers, an *in vitro* model of the intestinal mucosa that has been shown to exhibit physical (14, 17) and metabolic (16) barrier properties similar to the *in vivo* situation.

As expected, the linear hexapeptide disappeared rapidly from the AP side of Caco-2 cell monolayers, indicating high susceptibility to peptidase metabolism (Fig. 3A). HPLC analysis revealed Trp and Trp-Ala as a major metabolites (data not shown). This suggests metabolism by aminopeptidases and dipeptidyl peptidase IV, respectively. Since the linear hexapeptide was not detected in the BL compartment, we investigated whether the metabolic or the physical barrier function of the intestinal mucosa is the major detriment to the permeation of this peptide. In the presence of a peptidase inhibitor "cocktail" that has been successfully used to stabilize the metabolism of delta sleep-inducing peptide (DSIP) on Caco-2 cells (19), approximately 70% of the initially applied amount of peptide remained after a 3-hr incubation. Under these conditions, a linear increase in the amount of peptide transported to the BL compartment was observed, indicating that the metabolic rather than the physical barrier properties restrict the permeation of the linear hexapeptide across Caco-2 cell monolayers.

The cyclic prodrug, in contrast, was significantly more stable than the linear hexapeptide when placed on the AP side of Caco-2 cell monolayers (Fig. 3A). This indicates that the cyclic prodrug approach using the acyloxyalkoxy promoiety can markedly reduce the lability of the peptide toward metabolic degradation mediated by intestinal peptidases. In addition, the cyclic prodrug appears to exhibit more favorable physicochemical properties to permeate the physical barrier of the intestinal mucosa. This conclusion was drawn from the observation that the permeation of the acyloxyalkoxycarbamate prodrug is approximately 3 times greater than the intrinsic permeability determined for the linear model hexapeptide in the presence of peptidase inhibitors. The cyclic prodrug was also ~3 times more permeable than the metabolically stable N-terminus acetylated and C-terminus amidated analog of the linear hexapeptide (10).

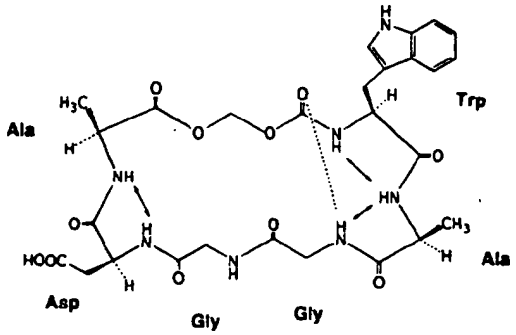

Fig. 4. Secondary structure of the cyclic prodrug in solution (with permission (25)). Dashed line indicates the intramolecular hydrogen bond of a β-turn and arrows symbolize the close proximity (≤ 4Å) of amide protons in the peptide backbone.

Structural analysis performed by CD as well as by one- and two-dimensional NMR spectroscopy revealed that the cyclic prodrug contains well defined elements of secondary structure (25), whereas the linear hexapeptide exists in a dynamic equilibrium between random coil and β-turns (10). Fig. 4 shows the secondary structure determined for the cyclic prodrug in solution (25). The cyclic nature of the prodrug seems to favor the formation of intramolecular hydrogen bonds. This might account for an overall higher lipophilicity index (i.e., log k'_{IAM}) of the cyclic prodrug as determined by IAM chromatography (Table II). In addition, cyclization of a linear molecule can also lead to a reduction in size. Based on the K_d values obtained by size exclusion chromatography (Table II), it appears that the cyclic prodrug is significantly smaller than compounds of equivalent molecular weight. As suggested by these results, the smaller and less hydrophilic cyclic prodrug comprises more favorable physicochemical properties to traverse biological membranes than does the linear model hexapeptide. With respect to the mechanism of permeation of the cyclic prodrug through Caco-2 cell monolayers, reduction in molecular size could have increased the paracellular flux of the peptide through aqueous pores, and/or the higher lipophilicity of the prodrug could have shifted its pathway of permeation to a larger contribution toward the transcellular route.

In conclusion, the experimental results presented in this paper illustrate that the use of the acyloxyalkoxy promoiety to prepare esterase-sensitive cyclic prodrugs may represent a promising approach in drug delivery to enhance the membrane permeation of peptides and, simultaneously, increase their metabolic stability.

ACKNOWLEDGMENTS

The authors would like to thank Dr. Norman F. H. Ho (Pharmacia & Upjohn Company, Kalamazoo, MI) for his valuable help in the data analysis and Manoj M. Nerurkar (Department of Pharmaceutical Chemistry, The University of Kansas) for his assistance in animal surgery. This work was supported by research grants from Glaxo, Inc., The United States Public Health Service (DA09315), Costar Corporation, and a fellowship to G. M. P. from the Swiss National Science Foundation.

REFERENCES

1. V. H. L. Lee and A. Yamamoto. *Adv. Drug Delivery Rev.* **4**:171–207 (1990).
2. V. Bocci. *Adv. Drug Delivery Rev.* **4**:149–169 (1990).
3. X. H. Zhou. *J. Controlled Release* **29**:239–252 (1994).
4. G. M. Pauletti, S. Gangwar, G. T. Knipp, M. M. Nerurkar, F. W. Okumu, K. Tamura, T. J. Siahaan, and R. T. Borchardt. *J. Controlled Release* **41**:3–17 (1996).
5. R. A. Gray, D. G. Vander Velde, C. J. Burke, M. C. Manning, C. R. Middaugh, and R. T. Borchadt. *Biochemistry* **33**:1323–1331 (1994).
6. W. A. Banks, A. J. Kastin, D. H. Coy, and E. Angulo. *Brain. Res. Bull.* **17**:155–158 (1986).
7. H. Bundgaard. *Adv. Drug Delivery Rev.* **8**:1–38 (1992).
8. R. Oliyai and V. J. Stella. *Ann. Rev. Pharmacol. Toxicol.* **32**:521–544 (1993).
9. J. K. McDonald and A. J. Barrett. *Mammalian Proteases: A Glossary and Bibliography*, Vol. 2, Exopeptidases, Academic Press, New York, 1986.
10. F. W. Okumu, G. M. Pauletti, D. G. Vander Velde, T. J. Siahaan, and R. T. Borchardt. *Pharm. Res.* **12**:S–302 (1995).
11. S. Gangwar, G. M. Pauletti, T. J. Siahaan, V. J. Stella, and R. T. Borchardt. *J. Org. Chem.* (submitted).
12. M. Inoue, M. Morikawa, M. Tsuboi, and M. Sugiura. *Jpn. J. Pharmacol.* **29**:9–16 (1979).
13. F. M. Williams. *Clin. Pharmacokinet.* **10**:392–403 (1985).
14. I. J. Hidalgo, T. J. Raub, and R. T. Borchardt. *Gastroenterology* **96**:736–749 (1989).
15. P. Artursson. *J. Pharm. Sci.* **79**:476–482 (1990).
16. M. Pinto, S. Robine-Leon, M.-D. Appay, M. Kedinger, N. Tradou, E. Dussaulx, B. Lacroix, P. Simon-Assmann, K. Haffen, J. Fogh, and A. Zweibaum. *Biol. Cell* **47**:323–330 (1983).
17. G. Wilson, I. F. Hassan, C. J. Dix, I. Williamson, R. Shah, and M. Mackay. *J. Controlled Release* **11**:25–40 (1990).
18. H. Liu, S. Ong, L. Glunz, and C. Pidgeon. *Anal. Chem.* **67**:3550–3557 (1995).
19. P. F. Augustijns and R. T. Borchardt. *Drug Metab. Dispos.* **23**:1372–1378 (1995).
20. C. S. Cook, P. J. Karabatsos, G. L. Schoenhard, and A. Karim. *Pharm. Res.* **12**:1158–1164 (1995).
21. W. N. Aldridge. *Biochem. J.* **53**:117–124 (1953).
22. K. Takahashi, S. Tamagawa, H. Sakano, T. Katagi, and N. Mizuno. *Biol. Pharm. Bull.* **18**:1401–1404 (1995).
23. W. N. Aldridge. *Biochem. J.* **53**:110–117 (1953).
24. D. S. Auld and B. Holmquist. *Biochemistry* **13**:4355–4361 (1974).
25. S. Gangwar, S. D. S. Jois, T. J. Siahaan, D. G. Vander Velde, V. J. Stella, and R. T. Borchardt. *Pharm. Res.* **13**: 1657–1662 (1996).

GH506.E5

MLC

STIC-ILL

From: Canella, Karen
Sent: Friday, October 24, 2003 7:40 PM
To: STIC-ILL
Subject: ill order 09/854,204

Art Unit 1642 Location 8E12(mail)

Telephone Number 308-8362

Application Number 09/854,204

1. Cell, 1984, Vol. 39, No. 3, part 2, pp. 499-509

2. Journal of Biological Chemistry, 2001, 276(8):5836-5840

3. Pharmaceutical Research, 1996, 13 (11): 1615-1623

4. Journal of Peptide Research, 1998, 51(3): 235-243

5. Neuroscience Letters 1998, 255 (1): 41-44

6. EMBO, 1990, 9 (3): 815-819

7. Journal of Organic Chemistry, 1997, 62 (5): 1356-1362

8. CAPLUS COPYRIGHT 2003 ACS on STN
ACCESSION NUMBER: 1981:454710 CAPLUS
DOCUMENT NUMBER: 95:54710
TITLE: Natural peptide lactones as ion carriers in membranes
AUTHOR(S): Oberbaeumer, Ilse; Feigl, Peter; Ruf, Horst; Grell, Ernst
CORPORATE SOURCE: Max-Planck-Inst. Biophys., Frankfurt, D-6000/71, Fed. Rep. Ger.
SOURCE: Struct. Act. Nat. Pept., Proc. Fall Meet. Ges. Biol. Chem. (1981), Meeting Date 1979, 523-38. Editor(s): Voelter, Wolfgang; Weitzel, Guenther. de Gruyter: Berlin, Fed. Rep. Ger.
CODEN: 45VYAS
DOCUMENT TYPE: Conference
LANGUAGE: English

9. CAPLUS COPYRIGHT 2003 ACS on STN
ACCESSION NUMBER: 1998:72644 CAPLUS
DOCUMENT NUMBER: 128:141012
TITLE: Rational design of peptides with enhanced membrane permeability
AUTHOR(S): Borchardt, Ronald T.
CORPORATE SOURCE: Department of Pharmaceutical Chemistry, The University of Kansas, Lawrence, KS, 66045, USA
SOURCE: Medicinal Chemistry: Today and Tomorrow, Proceedings of the AFMC International Medicinal Chemistry Symposium, Tokyo, Sept. 3-8, 1995 (1997), Meeting Date 1995, 191-196. Editor(s): Yamazaki, Mikio. Blackwell: Oxford, UK.
CODEN: 65ONAG
DOCUMENT TYPE: Conference
LANGUAGE: English

The EMBO J urnal vol.9 no.3 pp.815 - 819, 1990

Induction of non-bilayer lipid structures by functional signal peptides

J.A.Killian[1], A.M.Ph. de Jong[1], J.Bijvelt[2], A.J.Verkleij[3] and B.de Kruijff[1,3]

[1]Centre for Biomembranes and Lipid Enzymology, [2]Department of Molecular Biology and [3]Institute of Molecular Biology and Medical Biotechnology, University of Utrecht, Padualaan 8, 3584 CH Utrecht, The Netherlands

Communicated by L.L.M.van Deenen

Using ^{31}P NMR and freeze-fracture electron microscopy we investigated the effect of several synthetic signal peptides on lipid structure in model membranes mimicking the lipid composition of the *Escherichia coli* inner membrane. It is demonstrated that the signal peptide of the *E.coli* outer membrane protein PhoE, as well as that of the M13 phage coat protein, strongly promote the formation of non-bilayer lipid structures. This effect appears to be correlated to *in vivo* translocation efficiency, since a less functional analogue of the PhoE signal peptide was found to be less active in destabilizing the bilayer. It is proposed that signal sequences can induce local changes in lipid structure that are involved in protein translocation across the membrane.

Key words: model membranes/non-bilayer lipid structures/^{31}P NMR/protein translocation/signal peptides

Introduction

Proteins that are destined for export out of the cytoplasm of *Escherichia coli* cells are synthesized as precursor proteins with N-terminal extensions or signal sequences, which are essential for translocation of the protein across the inner membrane (for reviews, see Baker *et al.*, 1987; Briggs and Gierasch, 1986; Benson *et al.*, 1985; Gierasch, 1989). Although the 15–25 amino acids long signal sequences of various precursor proteins have no primary structure homology, they all consist of a positively charged N-terminal region followed by a stretch of ~10–15 hydrophobic amino acids and a more polar region containing the cleavage site (Von Heijne, 1985).

In recent years a number of biophysical studies have been carried out on the properties of signal peptides in order to get insight into the role of these sequences in protein translocation (Batenburg *et al.*, 1988a,b; Brüch *et al.*, 1989; Cornell *et al.*, 1989; Gierasch, 1989; Nagaraj *et al.*, 1987; Reddy and Nagaraj, 1989). However, in spite of extensive research in this area, the mechanism by which proteins translocate across membranes and the exact role of signal sequences therein is still not known. In principle, two types of translocation pathways have been postulated. One hypothesis, originally proposed for the analogous eukaryotic system, is that proteins translocate via proteinaceous pores (Blobel and Dobberstein, 1975; Rapoport, 1986). Such a pore-forming role has been recently proposed for the SecY protein, one of the components of the export machinery of *E.coli* (Watanabe and Blobel, 1989). Another possibility is that membrane lipids are directly involved in translocation of proteins across membranes (Wickner, 1979, 1988). The observation that the M13 phage procoat protein can cross a pure lipid bilayer in the absence of any proteinaceous factors (Geller and Wickner, 1985) strongly supports this possibility. Consistent with this hypothesis is the observation that phosphatidylglycerol (PG) is involved in translocation of the *E.coli* outer membrane protein PhoE (De Vrije *et al.*, 1988).

Evidently, translocation of a water-soluble protein across a lipid bilayer would be energetically unfavourable if the polar side chains were in contact with the hydrophobic lipid acyl chains. However, an attractive translocation pathway could be formed if locally and transiently an alternative, non-bilayer lipid structure were induced (Batenburg *et al.*, 1988b; Nesmeyanova, 1982). Such non-bilayer lipid intermediates have been proposed to play a role in a number of functional abilities of biological membranes and could be regulated, among other factors, by interactions between lipids and proteins or peptides (for reviews, see De Kruijff, 1987; De Kruijff *et al.*, 1985 and references therein). Since signal peptides can interact strongly with lipids (Batenburg *et al.*, 1988b; Cornell *et al.*, 1989; Gierasch, 1989; Nagaraj *et al.*, 1987), the possibility should be considered that signal sequences, in addition to their role in efficient targetting and possible other roles as discussed by Gierasch (1989), can act by locally inducing the formation of non-bilayer lipid structures which may be involved in translocation of proteins across the membrane.

We explored this possibility by studying the effect of several synthetic signal peptides on lipid structure in model membranes mimicking the lipid composition of the *E.coli* inner membrane. Using ^{31}P NMR and freeze-fracture electron microscopy it was investigated how membrane lipid organization is affected upon insertion of the signal peptide of the *E.coli* outer membrane protein PhoE and whether changes in lipid organization correlate with the functional activity of the signal sequence in protein translocation. The specificity of the process was further investigated by studying the effect of various other (signal) peptides as well as signal peptide fragments.

We will demonstrate here that the signal peptide of PhoE is extremely effective in inducing the formation of non-bilayer lipid structures in model membrane systems. This effect appears to be related to *in vitro* and *in vivo* translocation efficiency and is most likely a general property of signal peptides.

Our results support, but do not prove, the hypothesis that non-bilayer lipid structures are involved in protein translocation and suggest that signal sequences could act by inducing a local change in lipid structure that allows the protein to cross the membrane.

	-20 ↓ -1 ↓
PhoE signal p ptide	MKKSTLALVVMGIVASASVQA
Fragment Met^{-21}-Ala^{-1}	MKKSTLA
Fragment Met^{-21}-Gly^{-10}	MKKST'ALVVMG
Fragment Ile^{-9}-Ala^{-1}	IVASASVQA
N-formylat d signal peptide	f-MKKSTLALVVMGIVASASVQA
[Asp^{-19},Asp^{-20}] signal p ptide	MDDSTLALVVMGIVASASVQA
M13 coat signal p ptide	MKKSLVLKASVAVATLVPMLSFA

Fig. 1. Primary structure of the signal peptides and PhoE signal peptide fragments used in this study. The arrow at position −1 indicates the cleavage site of the signal sequence.

Results

In this study we investigated the effect of several signal peptides and signal peptide fragments on membrane lipid structure. The peptides (see Figure 1 for their structure) were introduced through the aqueous medium to model membranes composed of dioleoylphosphatidylethanolamine (DOPE) and dioleoylphosphatidylglycerol (DOPG) in a 3/1 m lar ratio to mimic the lipid composition of the *E.coli* inner membrane (Burnell *et al.*, 1980b). At 30°C these model membranes form stable bilayers, which give rise to a characteristic ^{31}P NMR spectrum (Seelig, 1977; Cullis and De Kruijff, 1979) with a low field shoulder and a high field peak, as shown in Figure 2A.

Addition of the PhoE signal peptide to these model membranes results in dramatic changes in ^{31}P NMR characteristics, that can be observed already at a very low molar ratio of peptide to lipid of 1/3200 (Figure 2B). Superimposed on the 'bilayer' signal a second component is visible, with a smaller overall linewidth, indicating that the motional characteristics of part of the lipids are strongly affected by the presence of the signal peptide.

Increasing the peptide/lipid ratio leads to further spectral changes, as illustrated in Figure 2B–D for peptide/lipid ratios ranging from 1/3200 to 1/200. The relative intensity of the second spectral component increases with the peptide/lipid ratio whereas its linewidth decreases. At the highest molar ratio of 1/200 a sharp 'isotropic' signal is observed which indicates that a change in lipid organization has occurred in which the lipids undergo fast isotropic motion with a correlation time of $<10^{-5}$/s^{-1} (Burnell *et al.*, 1980a). The occurrence of an isotropic ^{31}P NMR signal as in Figure 2D is commonly observed during a transition from a bilayer organization of lipids to a hexagonal H_{II} phase and in that case is indicative of the formation of type II non-bilayer structures (for review, see Lindblom, 1989), which are structures with a net concave surface curvature at the lipid/water interface. Interestingly, when pure lipid samples are incubated at elevated temperatures a similar change from a bilayer to isotropic ^{31}P NMR signal is observed as upon introduction of the signal peptide (not shown). This behavior has been described in detail in several analogous lipid systems and is typical for a temperature induced transition from a bilayer organization of lipids to a type II cubic structure (Lindblom, 1989). Thus, it is very likely that the isotropic ^{31}P NMR signal induced by the PhoE signal peptide represents a type II non-bilayer lipid organization. This is further supported by the observations that: (i) bilayer stabilization occurred upon incorporation of 5 mol% palmitoyllysophosphatidylcholine (LPC), a typical type I lipid, which on its own organizes in structures with a net convex surface curvature and therefore mitigates against the formation of type II structures (Madden and Cullis, 1982); and that (ii) after spinning the sample for 15 min at 30 000 *g* the isotropic signal was associated with the pellet, excluding the possibility (Burnell *et al.*, 1980a) that this signal originated from the formation of small vesicles.

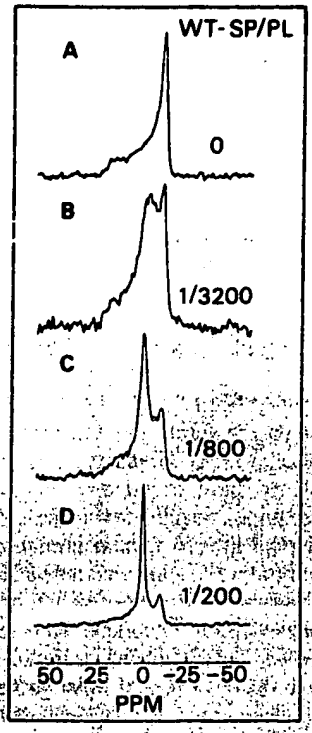

Fig. 2. ^{31}P NMR spectra of DOPE/DOPG (75/25 molar ratio) dispersions upon addition of PhoE signal peptide in various molar ratios of peptide to lipid as indicated in figure.

To further characterize the nature of the structures giving rise to the observed isotropic ^{31}P NMR signal, freeze-fracture electron microscopy was performed. As shown in Figure 3A and in accordance with the ^{31}P NMR results a control sample of pure lipid shows the presence of large vesicles (diameter 2000–20 000 Å). Addition of the PhoE signal peptide (1/200 molar ratio of peptide to lipid) clearly results in a change of morphology. The electron micrograph (Figure 3B) shows the presence of lipidic particles of ~120 Å in diameter as well as larger volcano-like protrusions (diameter ~300 Å), that most likely represent interbilayer fusion points. A very similar change in morphology as upon introduction of the signal peptide was observed in pure lipid samples after incubation at elevated temperatures (not shown). Since such a morphology typically occurs under conditions that induce a transition from a bilayer organization of lipids to a hexagonal H_{II} phase (Verkleij, 1984), the electron microscopy experiments are

Fig. 3. Electron micrographs of DOPE/DOPG (75/25 molar ratio) dispersions in the absence of peptide (A) and upon addition of PhoE signal peptide in a 1/200 molar ratio of peptide to lipid (B). Magnification: 37 000×.

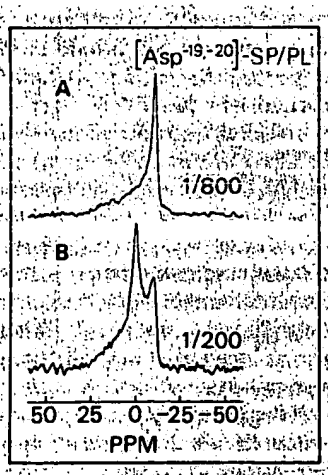

Fig. 4. ^{31}P NMR spectra of DOPE/DOPG (75/25 molar ratio) dispersions upon addition of PhoE [$Asp^{-19,-20}$] signal peptide in molar ratios of peptide to lipid of 1/800 (A) and 1/200 (B).

in full agreement with the ^{31}P NMR results, both indicating that the PhoE signal peptide induces the formation of type II non-bilayer lipid structures.

To investigate whether this effect of the signal peptide on lipid structure can be correlated to its functional activity, we next studied the effect of replacement of the positively charged lysine residues at the N terminus by aspartic acid, which modification in the signal sequence of prePhoE results in a decrease of the *in vivo* and *in vitro* translocation efficiency (Bosch *et al.*, 1989). Figure 4A shows that when

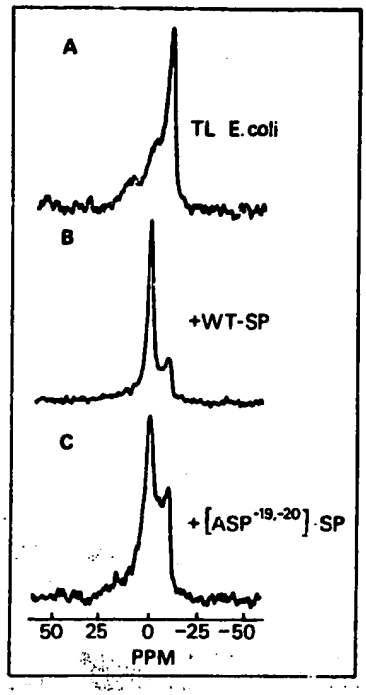

Fig. 5. ^{31}P NMR spectra of model membranes of the total lipid extract of *E.coli* cells in the absence of peptide (A) and upon addition of PhoE signal peptide (B) or PhoE [$Asp^{-19,-20}$] (C) signal peptide in a molar ratio of peptide to lipid of 1/100.

added in a molar ratio of peptide to lipid of 1/800 the PhoE [$Asp^{-19,-20}$] signal peptide is unable to perturb lipid structure under conditions at which the wild-type signal peptide induces a large isotropic signal (Figure 2C). Increasing the peptide/lipid ratio to 1/200 also for the [$Asp^{-19,-20}$] signal peptide results in the formation of an isotropic spectral component (Figure 4B) but with a relative intensity that is considerably less than that induced by the wild-type signal peptide under identical conditions (compare with Figure 2D). A qualitatively similar effect on lipid structure of both peptides was observed in model membranes composed of the total lipid extract of *E.coli* cells (Figure 5). Sucrose-density gradient centrifugation experiments of these samples showed a quantitative association of the wild-type signal peptide as well as of the [$Asp^{-19,-20}$] signal peptide with the model membranes (not shown) demonstrating that the differences in effect on lipid structure are not due to differences in binding affinity. In these *E.coli* lipid model membranes twice the amount of both signal peptides was required to induce approximately the same percentage of isotropic ^{31}P NMR signal as in the DOPE/DOPG mixtures. This lower efficiency of perturbation of the bilayer is most likely due to the more saturated character of the *E.coli* lipids.

The percentage of isotropic signal induced by the various signal peptides in DOPE/DOPG mixtures is quantified in Figure 6A. From this figure it is clear that the formylated form of the PhoE signal peptide (see Figure 1), which is expected to be the form in which the signal sequence functions *in vivo*, has a similar effect on lipid structure as the non-formylated signal peptide. Furthermore it was found that the signal peptide of the M13 coat protein (see Figure 1 for its chemical structure) also was able t induce an isotropic component in the DOPE/DOPG mixtures, indicating that this lipid structure perturbing activity is most likely

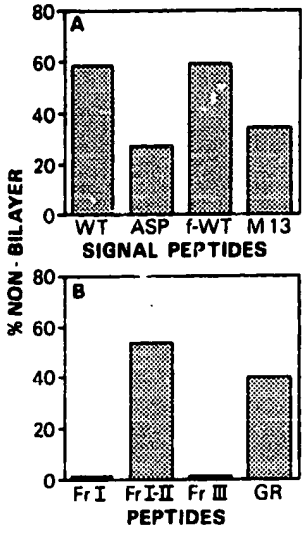

Fig. 6. Quantification of the relative amount of isotropic ^{31}P NMR signal induced in dispersions of DOPE/DOPG (75/25 molar ratio) by various signal peptides (**A**) and other peptides or signal peptide fragments (**B**) in a 1/200 molar ratio of peptide to lipid. **A**: PhoE signal peptide (WT), PhoE [$Asp^{-19,-20}$] signal peptide (ASP), N-formylated PhoE signal peptide (f-WT) and signal peptide of M13 coat protein (M13). **B**: signal peptide fragments Met^{-21}-Ala^{-15} (Fr I), Met^{-21}-Gly^{-10} (Fr I-II) and Ile^{-9}-Ala^{-1} (Fr III) and gramicidin A' (GR).

a general property of functional signal peptides. Although this peptide appeared to be less effective than the PhoE signal peptide, it should be realized that the extent of the effect of the signal peptide of the M13 coat protein on lipid structure cannot be directly compared on a functional level with that of the PhoE signal peptides, since it is not known whether the *in vivo* and *in vitro* translocation efficiency of the M13 procoat protein is similar to that of prePhoE in the same system.

To investigate which part of the PhoE signal peptide is responsible for its effect on lipid structure, ^{31}P NMR experiments were carried out using the various fragments of the peptide indicated in Figure 1. These experiments showed that neither the N-terminal positively charged fragment Met^{-21}-Ala^{-15}, nor the hydrophobic C-terminal fragment Ile^{-9}-Ala^{-1}, was able to induce the formation of an isotropic signal (Figure 6B). In contrast, the longer N-terminal fragment Met^{-21}-Gly^{-10} was found to induce an isotropic signal with an intensity rather similar to that induced by the intact signal peptide.

Addition of gramicidin A', a very strong promotor of the formation of type II lipid structures in model membrane systems (Killian and De Kruijff, 1986), also was found to result in the induction of an isotropic signal (Figure 6B), but with an efficiency that is less than that of the PhoE signal peptide (Figure 6A). This observation thus illustrates the strength of the lipid perturbing activity of the signal peptide.

Discussion

The results in this paper demonstrate a completely new property of signal peptides, i.e. their ability to induce the formation of type II non-bilayer lipid structures when introduced through the aqueous phase to model membranes mimicking the lipid composition of the *E.coli* inner membrane. Moreover, it is shown that this effect on lipid structure is most likely a general property of signal peptides, since it also is observed for the signal peptide of the M13 coat protein, which has a different translocation pathway (Ohno-Iwahita and Wickner, 1983) and does not require the proteinaceous factors that are known to be essential for efficient translocation of prePhoE (De Vrije *et al.*, 1988; Kusters *et al.*, 1989).

Furthermore, our results indicate that the type II non-bilayer lipid structure inducing activity of the signal peptides is related to their efficiency in protein translocation, since replacement of the two lysine residues at the N terminus of the signal sequence of prePhoE by aspartic acid results in a decrease of the rate of translocation across the *E.coli* membrane (Bosch *et al.*, 1989) and since similarly we demonstrated here that the PhoE [$Asp^{-19,-20}$] signal peptide is less effective than the wild-type signal peptide in inducing the formation of type II non-bilayer lipid structures in DOPE/DOPG mixtures as well as in model membranes composed of the total lipid extract of *E.coli* cells.

From the observations that this negatively charged mutant signal peptide affects lipid structure less than the wild-type PhoE signal peptide and that the positively charged N-terminal fragment of the PhoE signal peptide does not affect lipid structure at all, it can be concluded that overall hydrophobicity, the most evident requirement for functional signal sequences (Von Heijne, 1985; Gierasch, 1989), is also essential for the bilayer destabilizing activity of the signal peptides, whereas electrostatic interactions appear to determine the efficiency of the process. Of the various fragments of the PhoE signal peptide however, it was shown that fragment Met^{-21}-Gly^{-10}, but not the hydrophobic C-terminal fragment, was able to induce changes in lipid organization, demonstrating that hydrophobicity alone is not sufficient. In this respect it is interesting to note that fragment Met^{-21}-Gly^{-10} but not Ile^{-9}-Ala^{-1} was found to be capable of adopting an α-helical structure in apolar solvents (Batenburg *et al.*, 1988a), a property that has been shown to be essential for functional signal sequences (Briggs and Gierasch, 1984; Emr and Silhavy, 1983).

Summarizing, the results presented in this paper are consistent with our hypothesis as outlined in the Introduction, that signal sequences can act by inducing a local and transient formation of type II non-bilayer lipid structures that allow proteins to translocate across the membrane. However, we would like to emphasize that care should be taken in extrapolating the effects of signal peptides on lipid structure to their importance for *in vivo* protein translocation, since as yet nothing is known about the localization of signal sequences during translocation across membranes, nor is it clear whether a direct interaction occurs between the signal sequence of a precursor protein and membrane lipids.

Materials and methods

Materials

The PhoE signal peptide, its N-formylated derivative and PhoE [$Asp^{-19,-20}$] signal peptide were prepared by solid-phase synthesis by D.Olshevski (University of California, San Diego, CA). M13 coat signal peptide was from the same source and was a kind gift of Dr W.Wickner (University of California, LA). HPLC analysis, performed as described previously (Batenburg *et al.*, 1988a), indicated a >95% purity of the various signal peptides. Fragments Met^{-21}-Ala^{-15}, Met^{-21}-Gly^{-10} and Ile^{-9}-Ala^{-1} of the PhoE signal peptide were synthesized and purified as described by Batenburg *et al.* (1988a). The amino acid composition of the

various peptides was confirmed by amino acid analysis on a Kontron Liquimat III amino acid analyzer. Gramicidin was purchased from Sigma (St. Louis, MO) and used as such.

1,2-Dioleoyl-*sn*-glycero-3-phosphoglycerol (DOPG), 1,2-dioleoyl-*sn*-glycero-3-phosphoethanolamine (DOPE), and 1-palmitoyl-*sn*-glycero-3-phosphocholine (LPC) were obtained as described previously (Killian *et al.*, 1986). All lipids were judged pure from HPTLC using chloroform/methanol/water/ammonia (68/28/2/2, by vol.) as eluents. *E.coli* lipids were isolated as described before (Batenburg *et al.*, 1988b) from a culture of *E.coli* SD12 cells, grown at 37°C and harvested at the late logarithmic phase. The amount of lipids was quantified on the basis of the phosphate content of the total lipid extract according to Rouser *et al.* (1975).

All solvents and other reagents were of analytical grade.

Sample preparation

Lipid dispersions were prepared by lyophilizing mixtures of DOPE (15 μmol) and DOPG (5 μmol) or 20 μmol of *E.coli* lipids, from 1 ml benzene, followed by hydration in 1 ml 100 mM NaCl, 10 mM PIPES, 0.2 mM EDTA buffer, pH 7.4. The lipid mixtures were allowed to swell for 1 h at room temperature and then subjected to a minimum of five cycles of freeze-thawing.

All peptides were first dissolved in trifluoroacetic acid in a concentration of 50 mg/ml and then dried under a stream of N_2. Next, 5 mM stock solutions of the peptides were prepared in trifluoroethanol (TFE) which were used as such or which prior to addition to the lipid dispersion were diluted, such that each sample composed of DOPE and DOPG contained 2 vol% of TFE whereas to all *E.coli* lipid samples a total of 4 vol% of TFE was added. Increasing the amount of TFE to 4 vol% in these former samples did not affect the results. The peptide was added slowly, using a Hamilton syringe, and under gentle stirring to the lipid dispersion in a 5 ml polyethylene vial. The sample was then transferred to a 10 mm NMR tube and incubated at 30°C for 2 h. ^{31}P NMR spectra were recorded at 30°C as described below.

^{31}P NMR

^{31}P NMR experiments were carried out as described before (Chupin *et al.*, 1987) on a Bruker MSL 300 spectrometer at 121.4 MHz. Prior to Fourier transformation an exponential multiplication was applied to 2000 accumulated free induction decays, resulting in a 100 Hz linebroadening. Percentages of isotropic and bilayer signals were obtained by subtraction with an estimated maximal error of 5%. All spectra were scaled to the same height of the largest peak. No changes in total intensity were observed upon addition of the peptide.

Freeze-fracture electron microscopy

Immediately after incubation samples were rapidly frozen from room temperature with a Reichert Jung KF 80 plunge-freezing device (Sitte *et al.*, 1987) without the use of cryoprotectants. The freeze-fracture replicas were made in a Balzers 300 apparatus and analysed with a Philips 420 electron microscope.

Acknowledgements

The authors would like to thank Dr. A.M. Batenburg for synthesis and purification of the fragments of the PhoE signal peptide and Dr. G.J. de Vrije for critically reading the manuscript.

References

Baker,K., Mackman,N. and Holland,I.B. (1987) *Prog. Biophys. Mol. Biol.*, **49**, 89–115.

Batenburg,A.M., Brasseur,R., Ruysschaert,J.M., Van Scharrenburg,G.J.M., Slotboom,A.J., Demel,R.A. and De Kruijff,B. (1988a) *J. Biol. Chem.*, **263**, 4202–4207.

Batenburg,A.M., Demel,R.A., Verkleij,A.J. and De Kruijff,B. (1988b) *Biochemistry*, **27**, 5678–5685.

Benson,S.A., Hall,M.N., Silhavy,T.J. (1985) *Annu. Rev. Biochem.*, **54**, 101–134.

Blobel,G. and Dobberstein,B. (1975) *J. Cell. Biol.*, **67**, 835–851.

Bosch,D., De Boer,P., Bitter,W. and Tommassen,J. (1989) *Biochim. Biophys. Acta*, **979**, 69–76.

Briggs,M.S. and Gierasch,L.M. (1984) *Biochemistry*, **23**, 3111–3114.

Briggs,M.S. and Gierasch,L.M. (1986) *Adv. Prot. Chem.*, **38**, 109–180.

Bruch,M.D., McKnight,J. and Gierasch,L.M. (1989) *Biochemistry*, **28**, 8554–8561.

Burnell,E., Cullis,P.R. and De Kruijff,B. (1980a) *Biochim. Biophys. Acta*, **603**, 63–69.

Burnell,E., Van Alphen,L., Verkleij,A.J. and De Kruijff,B. (1980b) *Biochim. Biophys. Acta*, **597**, 492–501.

Chupin,V., Killian,J.A. and De Kruijff,B. (1987) *Biophys. J.*, **51**, 395–405.

Cornell,D.G., Dluhy,R.A., Briggs,M.S., Knight,C.J. and Gierasch,L.M. (1989) *Biochemistry*, **28**, 2789–2797.

Cullis,P.R. and De Kruijff,B. (1979) *Biochim. Biophys. Acta*, **559**, 399–420.

De Kruijff,B. (1987) *Nature*, **329**, 587–588.

De Kruijff,B., Cullis,P.R., Verkleij,A.J., Hope,M.J., Van Echteld,C.J.A. and Taraschi,T.F. (1985) In Martonos,A.N. (ed.), *The Enzymes of Biological Membranes (2nd ed.) Vol. 1*. Plenum Press, NY, pp. 131–204.

De Vrije,T., De Swart,R.L., Dowhan,W., Tommassen,J. and De Kruijff,B. (1988) *Nature*, **334**, 173–175.

Emr,S.D. and Silhavy,T.J. (1983) *Proc. Natl. Acad. Sci. USA*, **80**, 4599–4603.

Geller,B.L. and Wickner,W. (1985) *J. Biol. Chem.*, **260**, 13281–13285.

Gierasch,L.M. (1989) *Biochemistry*, **28**, 923–930.

Killian,J.A. and De Kruijff,B. (1986) *Chem. Phys. Lipids*, **40**, 259–284.

Killian,J.A., Van den Berg,C.W., Tournois,H., Keur,S., Slotboom,A., Van Scharrenburg,G.J.M. and De Kruijff,B. (1986) *Biochim. Biophys. Acta*, **857**, 13–27.

Kusters,R., De Vrije,T., Breukink,E. and De Kruijff,B. (1989) *J. Biol. Chem.*, **264**, 20827–20830.

Lindblom,G. (1989) *Biochim. Biophys. Acta*, **988**, 221–256.

Madden,T.D. and Cullis,P.R. (1982) *Biochim. Biophys. Acta*, **684**, 149–153.

Nagaraj,R., Joseph,M. and Reddy,G.L. (1987) *Biochim. Biophys. Acta*, **903**, 465–472.

Nesmeyanova,M.A. (1982) *FEBS Lett.*, **142**, 189–193.

Ohno-Iwahita,Y. and Wickner,W. (1983) *J. Biol. Chem.*, **258**, 1895–1900.

Rapoport,T.A. (1986) *CRC Crit. Rev. Biochem.*, **20**, 73–137.

Reddy,G.L. and Nagaraj,R. (1989) *J. Biol. Chem.*, **264**, 16591–16597.

Rouser,G., Eleischer,S. and Yamamoto,A. (1975) *Lipids*, **5**, 494–496.

Seelig,J. (1977) *Rev. Biophys.*, **10**, 353–418.

Sitte,H., Edelman,L. and Neumann,K. (1987) In Sternbrecht,P.A. and Zierold,K. (eds), *Cryotechniques in Biological Electron Microscopy*. Springer Verlag, Berlin, Heidelberg, pp. 87–113.

Verkleij,A.J. (1984) *Biochim. Biophys. Acta*, **779**, 43–63.

Von Heijne,G. (1985) *J. Mol. Biol.*, **184**, 99–105.

Watanabe,M. and Blobel,G. (1989) *Proc. Natl. Acad. Sci. USA*, **86**, 1895–1899.

Wickner,W. (1979) *Annu. Rev. Biochem.*, **48**, 23–45.

Wickner,W. (1988) *Biochemistry*, **27**, 1081–1086.

Received on November 7, 1989; revised on December 6, 1989

STIC-ILL NPL

From: Canella, Karen
Sent: Friday, October 24, 2003 7:40 PM
To: STIC-ILL
Subject: ill order 09/854,204

Art Unit 1642 Location 8E12(mail)

Telephone Number 308-8362

Application Number 09/854,204

1. Cell, 1984, Vol. 39, No. 3, part 2, pp. 499-509

2. Journal of Biological Chemistry, 2001, 276(8):5836-5840

3. Pharmaceutical Research, 1996, 13 (11): 1615-1623

4. Journal of Peptide Research, 1998, 51(3): 235-243

5. Neuroscience Letters 1998, 255 (1): 41-44

6. EMBO, 1990, 9 (3): 815-819

7. Journal of Organic Chemistry, 1997, 62 (5): 1356-1362

8. CAPLUS COPYRIGHT 2003 ACS on STN
ACCESSION NUMBER: 1981:454710 CAPLUS
DOCUMENT NUMBER: 95:54710
TITLE: Natural peptide lactones as ion carriers in membranes
AUTHOR(S): Oberbaeumer, Ilse; Feigl, Peter; Ruf, Horst; Grell, Ernst
CORPORATE SOURCE: Max-Planck-Inst. Biophys., Frankfurt, D-6000/71, Fed. Rep. Ger.
SOURCE: Struct. Act. Nat. Pept., Proc. Fall Meet. Ges. Biol. Chem. (1981), Meeting Date 1979, 523-38. Editor(s): Voelter, Wolfgang; Weitzel, Guenther. de Gruyter: Berlin, Fed. Rep. Ger.
CODEN: 45VYAS
DOCUMENT TYPE: Conference
LANGUAGE: English

9. CAPLUS COPYRIGHT 2003 ACS on STN
ACCESSION NUMBER: 1998:72644 CAPLUS
DOCUMENT NUMBER: 128:141012
TITLE: Rational design of peptides with enhanced membrane permeability
AUTHOR(S): Borchardt, Ronald T.
CORPORATE SOURCE: Department of Pharmaceutical Chemistry, The University of Kansas, Lawrence, KS, 66045, USA
SOURCE: Medicinal Chemistry: Today and Tomorrow, Proceedings of the AFMC International Medicinal Chemistry Symposium, Tokyo, Sept. 3-8, 1995 (1997), Meeting Date 1995, 191-196. Editor(s): Yamazaki, Mikio. Blackwell: Oxford, UK.
CODEN: 65ONAG
DOCUMENT TYPE: Conference
LANGUAGE: English

THE JOURNAL OF BIOLOGICAL CHEMISTRY

Vol. 276, No. 8, Issue of February 23, pp. 5836–5840, 2001
Printed in U.S.A.

Arginine-rich Peptides

AN ABUNDANT SOURCE OF MEMBRANE-PERMEABLE PEPTIDES HAVING POTENTIAL AS CARRIERS FOR INTRACELLULAR PROTEIN DELIVERY*

Received for publication, August 18, 2000, and in revised form, November 7, 2000
Published, JBC Papers in Press, November 17, 2000, DOI 10.1074/jbc.M007540200

Shiroh Futaki‡§, Tomoki Suzuki‡, Wakana Ohashi‡, Takeshi Yagami¶, Seigo Tanaka‡, Kunihiro Ueda‡, and Yukio Sugiura‡

From the ‡Institute for Chemical Research, Kyoto University, Uji, Kyoto 611-0011 and the ¶National Institute of Health Sciences, Setagaya-ku, Tokyo 158-8501, Japan

A basic peptide derived from human immunodeficiency virus (HIV)-1 Tat protein (positions 48–60) has been reported to have the ability to translocate through the cell membranes and accumulate in the nucleus, the characteristics of which are utilized for the delivery of exogenous proteins into cells. Based on the fluorescence microscopic observations of mouse macrophage RAW264.7 cells, we found that various arginine-rich peptides have a translocation activity very similar to Tat-(48–60). These included such peptides as the D-amino acid- and arginine-substituted Tat-(48–60), the RNA-binding peptides derived from virus proteins, such as HIV-1 Rev, and flock house virus coat proteins, and the DNA binding segments of leucine zipper proteins, such as cancer-related proteins c-Fos and c-Jun, and the yeast transcription factor GCN4. These segments have no specific primary and secondary structures in common except that they have several arginine residues in the sequences. Moreover, these peptides were able to be internalized even at 4 °C. These results strongly suggested the possible existence of a common internalization mechanism ubiquitous to arginine-rich peptides, which is not explained by a typical endocytosis. Using $(Arg)_n$ (n = 4–16) peptides, we also demonstrated that there would be an optimal number of arginine residues ($n \sim 8$) for the efficient translocation.

Recently, methods have been developed for the delivery of exogenous proteins into living cells with the help of membrane-permeable carrier peptides such as HIV-1[1] Tat-(48–60) and Antennapedia-(43–58) (1–11). By genetically or chemically hybridizing these carrier peptides, the efficient intracellular delivery of various oligopeptides and proteins was achieved. One of the most amazing examples is the Tat-β-galactosidase fusion protein (4), which has a molecular mass as high as 120 kDa. Intraperitoneal injection of the protein resulted in delivery of the protein with β-galactosidase activity to various tissues in mice, including the brain. The peptide-mediated approaches would allow the incorporation of peptides containing unnatural amino acids or nonpeptide molecules such as fluorescence probes. These methods would become powerful tools not only for therapeutic purposes as an alternative to gene delivery, but also for the understanding of the mechanisms behind fundamental cellular events, such as signal transduction and gene transcription.

Besides the potential of Tat-(48–60) as a protein carrier, the internalization mechanism of the peptide attracted our interest. For example, Tat-(48–60) (GRKKRRQRRRPPQ) is a highly basic and hydrophilic peptide, which contains 6 arginine and 2 lysine residues in its 13 amino acid residues. However, the peptide was reported to be translocated through the cell membranes in 5 min at a concentration of 0.1 μM (2). Internalization of the peptide was not inhibited even at 4 °C. The peptide is less toxic to cells than other basic membrane-interacting agents. The above features suggested that the internalization mechanism of Tat-(48–60) was completely different from the typical transmembrane mechanisms reported so far. Questions arise as to whether such an efficient translocation is specific for Tat-(48–60) and Antennapedia-(43–58) peptides and what is the mechanism of the highly efficient internalization. Based on experiments using synthetic peptides, we suggest the possible presence of a very similar translocation mechanism to Tat-(48–60) present among the various arginine-rich peptides. We also suggest the possible existence of the optimum chain length of arginine peptides for the internalization.

EXPERIMENTAL PROCEDURES

Peptide Synthesis and Fluorescent Labeling—All the peptides used in this study were chemically synthesized by Fmoc (9-fluorenylmethyloxycarbonyl)-solid-phase peptide synthesis on a Rink amide resin as reported previously (12). Fluorescent labeling of the peptides was conducted by the treatment with 1.5 eq of 5-maleimidofluorescein diacetate (Sigma) in dimethylformamide-methanol (1:2) for 3 h followed by reverse-phase HPLC purification. The fidelity of the products was ascertained by time-of-flight mass spectrometry.

Conjugation of Carbonic Anhydrase with Basic Peptides—Carbonic anhydrase in phosphate-buffered saline (PBS) was simultaneously treated with fluorescein-5(6)-carboxamidocaproic acid *N*-hydroxysuccinimide ester (Sigma) and *N*-(6-maleimidocaproyloxy)succinimide ester (Dojin) (15 eq, each) at room temperature for 1 h to introduce the fluorescein and the maleimide function to the protein. After the removal of the unreacted reagents by gel-filtration on a Sephadex G-25 (Amersham Pharmacia Biotech) column, the cysteine of the respective arginine-rich peptides was allowed to react with the maleimide moiety on the above fluorescein-labeled protein at room temperature for 16 h, and then the unreacted peptides were removed by gel-filtration. Based on the molecular weight estimation by SDS-polyacrylamide gel electro-

* This work was supported by grants-in-aid for scientific research from the Ministry of Education, Science, Sports and Culture of Japan and in part by the Mochida Memorial Foundation for Medical and Pharmaceutical Research. The costs of publication of this article were defrayed in part by the payment of page charges. This article must therefore be hereby marked "*advertisement*" in accordance with 18 U.S.C. Section 1734 solely to indicate this fact.

§ To whom correspondence should be addressed. Tel.: 81-774-38-3211; Fax: 81-774-32-3038; E-mail: futaki@scl.kyoto-u.ac.jp.

[1] The abbreviations used are: HIV, human immunodeficiency virus; HTLV-II, human T-cell lymphotrophic virus type-II; BMV, brome mosaic virus; FHV, flock house virus; HPLC, high performance liquid chromatography; PBS, phosphate-buffered saline; MTT, [3-(4,5-dimethylthiazol-2-yl)-2,5-diphenyl-2H-tetrazolium bromide; EMCS, *N*-(6-maleimidocaproyloxy)succinimide ester; NLS, nuclear localization sequence.

phoresis, one or two molecules of basic peptides and fluorescein per protein were incorporated, respectively.

Cell Culture—Mouse macrophage RAW264.7 cells were maintained in RPMI 1640 medium with 10% heat-inactivated fetal bovine serum. Cells were grown on 60-mm dishes and incubated at 37 °C under 5% CO_2 to ~70% confluence. A subculture was performed every 3–4 days.

Peptide Internalization and Visualization—For each assay, 4 × 10^4/ml cells were pelleted on a eight-well Lab-Tek-II chamber slide (Nalge Nunc) (250 μl/well) and cultured for 16 h. After complete adhesion, the culture medium was exchanged. The cells were incubated at 37 °C for 3 h with the fresh medium (250 μl) containing fluorescein-labeled peptides or proteins. The concentrations of the peptides and proteins were adjusted before addition to the cell based on their fluorescent intensity. Cells were washed three times with PBS, fixed with acetone-methanol (1:1) for 2 min at room temperature, washed three times with PBS again, and then mounted in fluorescent mounting medium containing 15 mM NaN_3 (Dako). The distribution of fluorescein-labeled peptides was analyzed on a Zeiss Axioskop fluorescence microscope using a 100× oil immersion lens.

Confocal Microscopy—Cells were grown, incubated with proteins, and fixed basically as described above. Cells were then treated with PBS containing 5 μM propidium iodide (200 μl) at room temperature for 30 min, washed four times with PBS, and mounted in glycerol:PBS (9:1) containing 1% *p*-phenylenediamine dihydrochloride. Data were obtained using a confocal scanning laser microscope MRC 1024 (Bio-Rad) equipped with a 60× oil immersion lens or LSM 510 (Zeiss) equipped with a 40× lens.

MTT Assay—The MTT assay was conducted basically in the same manner as reported previously (2). Cells (1 × 10^4/well) were cultured in 96-microtiter plates in RPMI 1640 medium with 10% heat-inactivated fetal bovine serum in the presence of peptides (HIV-1 Tat-(48–60): GRKKRRQRRRPPQ-amide; R_9-Tat: GRRRRRRRRRPPQ-amide; HIV-1 Rev-(34–50): TRQARRNRRRRWRERQR-amide; FHV coat-(35–49): RRRRNRTRRNRRRVR-amide) at 10 or 100 μM. Cells were incubated at 37 °C under 5% CO_2 for 24 h before addition of MTT (Sigma, 5 mg/ml in PBS) for 4 h. The precipitated MTT formazan was dissolved overnight in 0.04 N HCl in isopropanol (100 μl). The absorbance at 570 nm was then measured. Cell viability was expressed as the ratio of the A_{570} of cells treated with peptide over the control samples.

RESULTS

Uptake of Tat-(48–60) Analogs by the Macrophage Cell—To obtain insight into the translocation mechanisms of the Tat-(48–60) peptide, Tat-(48–60), its D-amino acid-substituted analog (D-Tat) and arginine-substituted analog (R_9-Tat), where residues corresponding to positions 49–57 were replaced with arginine, were synthesized (Fig. 1*a*). An extra cysteine amide was incorporated into the C terminus of each peptide for the fluorescent labeling. The peptides corresponding to nuclear localization sequences (NLS) derived from simian virus 40 (13) and nucleoplasmin (14) were also synthesized as references. Treatment of the peptides with 5-maleimidofluorescein diacetate gave the corresponding fluorescein-labeled peptides. Internalization of the peptides was monitored by fluorescence microscopic observation after a 3-h incubation of the peptides with mouse macrophage RAW 264.7 cells at 37 °C. As a result, D-Tat and R_9-Tat were internalized into the cell as efficiently as the Tat-(48–60) peptides, and localization into both the cytoplasm and nucleus was observed (Fig. 2). A similar internalization of the D-amino acid analog of Tat was reported by Huq *et al.* (15) using a linear peptide corresponding to residues 37–72. These results would contradict the idea that a specific receptor may play a crucial role in the translocation of the Tat-(48–60) peptide. On the other hand, the simian virus 40-derived and nucleoplasmin-derived peptides showed a much lower degree of internalization. These NLS-derived peptides are rich in lysine. The above results suggested that arginine residues would play an important role in the translocation.

Translocation of Various Arginine-rich Nucleic Acid-binding Peptides through the Macrophage Cell Membranes—Arginine-rich basic segments are used by a variety of RNA-binding proteins to recognize specific RNA structures (16). If arginine

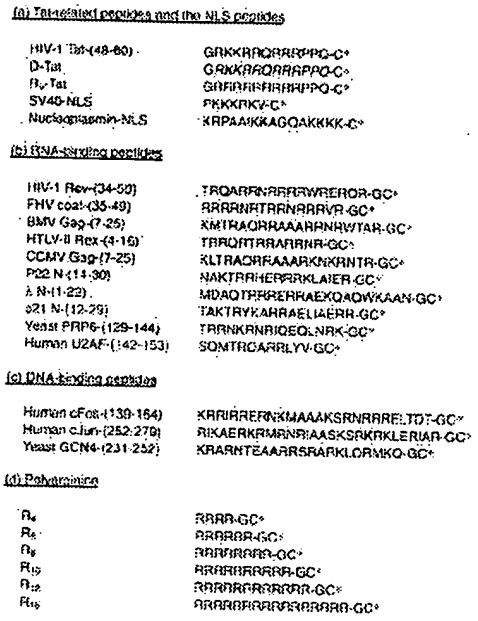

FIG. 1. **Structure of arginine-rich peptides used in this study.** C-terminal cysteine amide (C*) was fluorescein-labeled for monitoring the internalization of the peptides by fluorescence microscopy. D-Amino acids are denoted in *italics*. Cysteine residues corresponding to positions 154 and 269 in c-Fos and c-Jun were replaced by serine, respectively.

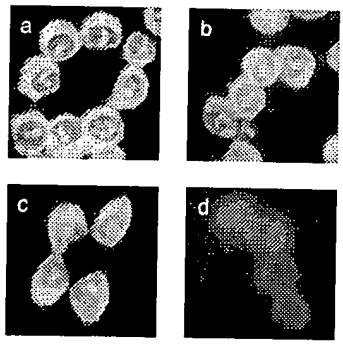

FIG. 2. **Translocation of the arginine-rich Tat-related peptides through the cell membranes.** RAW264.7 cells were treated with fluorescein-labeled peptides derived from HIV-1 Tat-(48–60) (*a*), R_9-Tat (*b*), D-Tat (*c*), and nucleoplasmin-NLS (*d*) (10 μM each) for 3 h.

in the sequence plays an important role in the translocation, peptides corresponding to these RNA-binding segments may translocate through the cell membranes. To test this hypothesis, 10 arginine-rich RNA-binding peptides bearing a C-terminal Gly-Cys-amide (Fig. 1*b*) were similarly prepared, fluorescein-labeled, and applied to the macrophage cells.

To our surprise, all the peptides other than the human U2AF-(142–153) peptide translocated through the cell membranes and accumulated in the cytoplasm and nucleus (Fig. 3). As judged from the fluorescent intensity, the efficiency of incorporation into the cells showed a tendency to correspond to the number of arginine residues in the sequence. Internalization activity of the HIV-1 Rev-(34–50), FHV coat-(35–49), HTLV-II Rex-(4–16), and BMV Gag-(7–25) peptides, which have more than seven arginine residues in their sequences, were comparable with that of the Tat-(48–60) peptide. Fluorescence was observed in the cells as early as 5 min after the addition of these peptides (1 μM) to the medium. Less extensive internalization was observed in the case of the λ N-(1–22), ϕ21 N-(12–29), and yeast PRP6-(129–144) peptides that have five arginine residues in their sequences. The fluorescent intensity

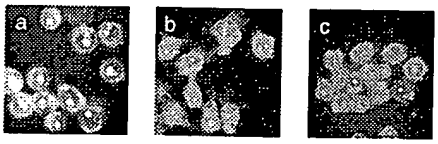

FIG. 3. **Difference in the translocation efficiency in the arginine-rich RNA-binding peptides after treatment of RAW264.7 cells with the fluorescein-labeled peptides derived from HIV-1 Rev-(34–50) (*a*), P22 N-(14–30) (*b*), and λ N-(1–22) (*c*) (10 μM each) for 3 h.**

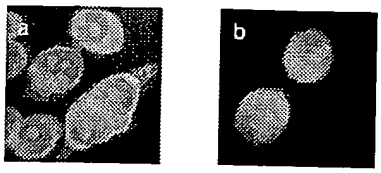

FIG. 4. **Translocation of DNA-binding peptides through the cell membranes.** RAW264.7 cells were treated with the fluorescein-labeled peptides derived from human c-Jun-(252–279) (*a*) and yeast GCN4-(231–252) (*b*) (1 μM each) for 3 h.

in the cells treated with the former peptides (0.1 μM) was judged not to be less than that in those treated with the latter peptides (10 μM). The P22 N-(14–30) and cowpea chlorotic mottle virus Gag-(7–25) peptides that have six arginine residues showed a moderate degree of translocation. HIV-1 Tat-(48–60) is reported to translocate through the cell membranes and accumulate in the nucleus, especially the nucleolus (2). A similar tendency was observed with the above peptides. Not only the RNA-binding peptides but also the DNA-binding peptides corresponding to the basic leucine zipper segments derived from cancer-related proteins, c-Fos and c-Jun, and the yeast transcription factor, GCN4, which were also rich in arginine (Fig. 1*c*), were internalized into the cells with almost the same efficiency as that of Tat-(48–60) (Fig. 4).

HIV-1 Tat-(48–60) was reported to induce little toxicity to HeLa cells (2). Using R_9-Tat, HIV-1 Rev-(34–50), and FHV coat-(35–49) peptides as representatives of the above arginine-rich peptides, cytotoxicity of the peptides was investigated. Determined by the MTT assay, the above peptides did not show a significant cytotoxicity to the macrophage cells during the treatment with a peptide (10 μM) for 24 h. At 100 μM, cell viability of the cells treated with R_9-Tat became 70%, whereas viability of those treated with other peptides as well as HIV-1 Tat-(48–60) was still greater than 95%. These results suggested that many of the arginine-rich peptides can be of low cytotoxicity as reported for the HIV-1 Tat-(48–60) peptide.

Consideration of the Translocation Mechanism of the Arginine-rich Peptides—The above experiments showed that a variety of arginine-rich RNA/DNA-binding peptides were able to translocate through the cell membranes. Little homology in these sequences was observed, except that they all have 5–11 arginine residues. Moreover, the D-amino acid substituted Rev-(34–50) peptide (1 μM) was internalized as efficiently as the L-peptide in 3 h (data not shown). Circular dichroism (CD) spectra of the HIV-1 Tat-(48–60), R_9-Tat, and FHV coat-(35–49) peptides in methanol were suggestive of their not having a significant secondary structure (Fig. 5), whereas the HIV-1 Rev-(34–50) peptide showed a spectrum typical of an α-helical peptide. The U2AF peptide, which was only slightly internalized into the cell, showed a spectrum very similar to that of the FHV coat-(35–49) peptide. These results were suggestive of the absence of even a common secondary structure in the membrane-permeable peptides. When the cells were incubated with a peptide (1 μM) at 4 °C for 30 min, no significant decrease in fluorescent intensity in the cell was observed using the HIV-1 Rev-(34–50), and FHV coat-(35–49) peptides (Fig. 6). These results suggested that typical endocytosis pathways so far established would not play a crucial role in the translocation of these arginine-rich peptides.

We next focused on the question whether the entry of arginine-rich peptides into the cells is one-way or not. The cells were treated with the HIV-1 Rev-(34–50) peptide (1 μM) for 3 h, then the medium was exchanged with a fresh one not containing the peptide. The fluorescence intensity from the cells 1 h later was almost comparable with or only slightly less than that of the cells just before the medium exchange. However, a

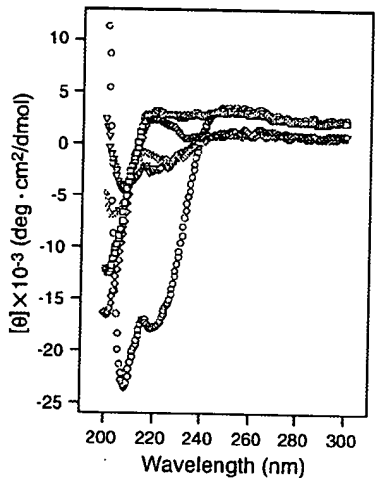

FIG. 5. **CD spectra of the arginine-rich peptides in methanol.** HIV-1 Tat-(48–60) (55 μM) (*square*), R_9-Tat (52 μM) (*diamond*), FHV coat-(35–49) (43 μM) (*upward triangle*), HIV-1 Rev-(34–50) (39 μM) (*circle*), and human U2AF-(142–153) (61 μM) (*downward triangle*).

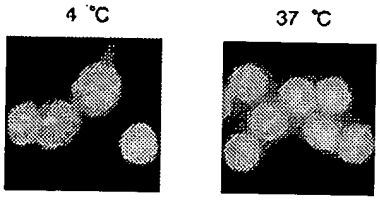

FIG. 6. **Effect of temperature on HIV-1 Rev-(34–50) peptide internalization.** The cells were incubated with the peptide (1 μM) for 30 min at 4 °C or at 37 °C. In the former case, the cells were preincubated at 4 °C for 1 h before addition of the peptide. All the following procedures were also conducted at 4 °C until the completion of the fixation.

substantial decrease in the fluorescence intensity was recognized in the cells 6 h later, and complete disappearance of the fluorescence was observed 24 h later. To examine if the above results were due to the leakage of the peptide from the cells, the medium was analyzed by an HPLC equipped with a fluorescence spectrophotometer. No peak was detected at the retention time corresponding to the peptide; however, peaks were observed that eluted at positions identical with those of the peptide treated with trypsin (data not shown). Therefore, we concluded that the decrease in fluorescence intensity of the cells mainly resulted from the degradation of the peptides, and not from the leakage of the intact peptide. The question whether the ingested peptide had a certain effect on the cell growth was also examined. The above HIV-1 Rev-(34–50)-treated cells were harvested 24 h later and counted. The cell number for the peptide-treated cells was comparable with that for the control cells (without peptide treatment). Thus, the peptide-ingesting cells were judged to remain viable to divide with little effect by the peptide. It would be plausible that the peptide evenly distributes in each of the daughter cells upon

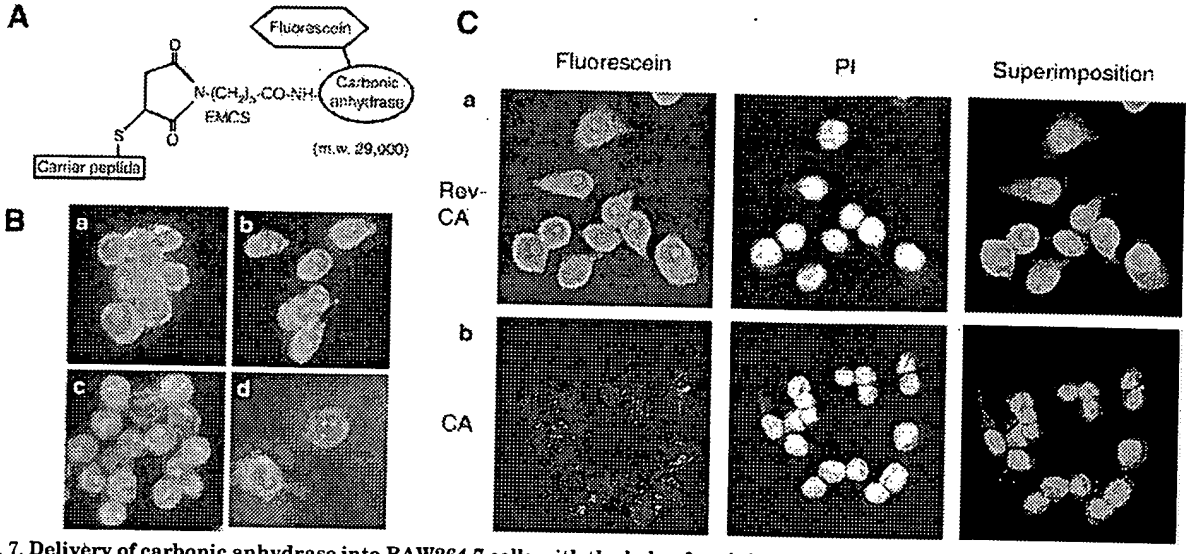

FIG. 7. **Delivery of carbonic anhydrase into RAW264.7 cells with the help of arginine-rich basic peptides.** *A*, schematic representation of the conjugates. *B*, fluorescence microscopy of the cells treated with carbonic anhydrase conjugated with the HIV-1 Rev-(34–50) (*a*), FHV coat-(35–49) (*b*), and HIV-1 Tat-(48–60) (*c*) peptides (1 μM each) for 3 h, respectively. Accumulation of the HIV-1 Rev-(34–50)-carbonic anhydrase conjugate in the cytosol and nucleus was also observed by the fluorescence microscopy of the cells without fixation (protein concentration: 10 μM) (*d*). *C*, confocal microscopic observation of the cells treated with carbonic anhydrase conjugated with the HIV-1 Rev-(34–50) peptide (1 μM) with nucleus staining by propidium iodide (*PI*) (*a*). The protein without the carrier peptides (1 μM) did not show a significant accumulation in the nucleus (*b*).

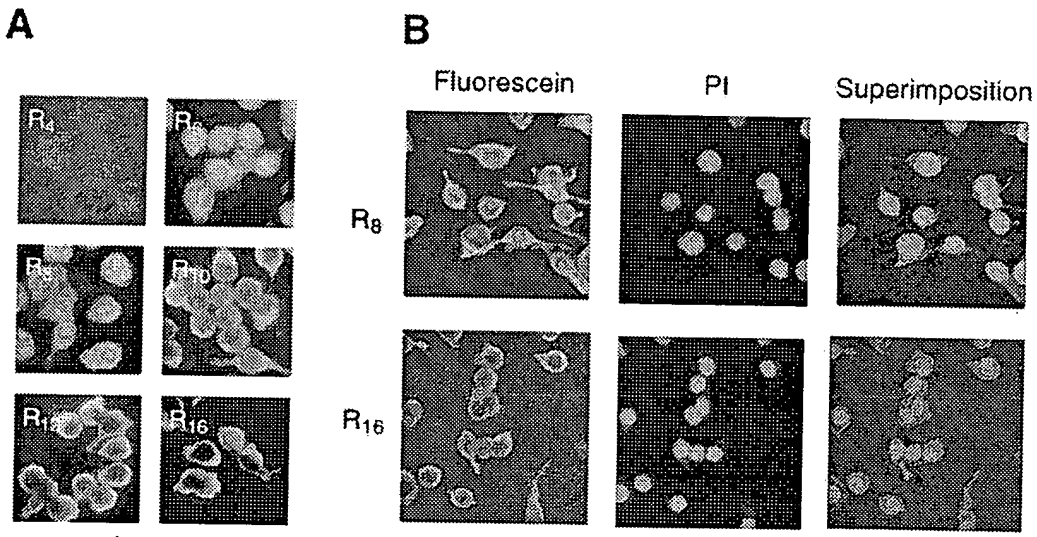

FIG. 8. **Fluorescence microscopic observation of the cells treated with polyarginine peptides (1 μM) for 3 h (*A*), and confocal microscopic observation of the cells treated with carbonic anhydrase conjugated with the R_8 or R_{16} peptides (1 μM) with nucleus staining by propidium iodide (*PI*) (*B*).**

cell division, since significant differences in the florescence intensity were not observed among the adjoining cells 6 h later. Considering the doubling time of the cell, which was estimated to be about 18 h, a certain amount of cells must have divided within the 6 h. If the peptides would preferentially stay in one of the daughter cells upon cell division, a certain discrepancy in the fluorescence intensity will be observed among the adjacent cells. However, further study will be necessary to adequately address this question.

Applicability of the Arginine-rich Peptides to the Intracellular Protein Delivery—To examine the applicability of the above basic peptides as protein carriers, we prepared basic peptide-protein conjugates. Carbonic anhydrase (29 kDa) was selected as a model protein. Basic peptide-carbonic anhydrase conjugates were prepared using *N*-(6-maleimidocaproyloxy)succinimide ester (EMCS) as a cross-linking agent (17) (Fig. 7*A*). A fluorescein moiety was introduced into the protein using the fluorescein-5(6)-carboxamidocaproic acid *N*-hydroxysuccinimide ester simultaneously with EMCS. As judged from the SDS-polyacrylamide gel electrophoresis of the conjugates, one to two molecules of the basic peptide and fluorescein moiety were introduced into a molecule of carbonic anhydrase, respectively. Carbonic anhydrase was successfully delivered into the cells with the help of the HIV-1 Rev-(34–50), FHV coat-(35–49), and R_9-Tat peptides as efficiently as with the HIV-1 Tat-(48–60) peptide (Fig. 7*B*). Accumulation of the conjugates in the cytosol and nucleus was also observed by fluorescence microscopy of the cells without fixation (Fig. 7*B*). Confocal microscopic analysis of these conjugates demonstrated both cytoplasmic and nuclear localization and not just attachment to the cellular membranes (Fig. 7*C*). On the other hand, fluorescein-labeled pro-

tein without a carrier peptide was located in a limited part of the cytosol (Fig. 7*C*). This result suggested that the protein was captured in the endosomes and was not able to be released into the cytosol. Myoglobin (17 kDa) was also introduced into the cell with the help of these carrier peptides (data not shown).

Effect of the Length of Arginine Chain on the Internalization—The above data strongly suggested the importance of arginine residues in the internalization. The possible existence of the unique internalization mechanism common in these arginine-rich peptides was also suggested. We then examined the effect of the number of arginine residues in the sequences. For simplification, peptides that are composed of 4–16 residues of arginine were prepared (Fig. 1*d*). To their C termini, the Gly-Cys-amide segment was also attached for the fluorescein labeling. These results are shown in Fig. 8*A*. Considerable difference was recognized on the translocation efficiency and intracellular localization among these peptides. R_4 showed extremely low translocation activity. R_6 and R_8 exhibited the maximum internalization and accumulation in the nucleus. What is interesting is that the degree of internalization decreased as the chain length further increased. For the R_{16}, internalization of the peptide was not significant. The same kind of difference was recognized in the experiments using the conjugates of carbonic anhydrase with the arginine peptides (Fig. 8*B*). A similar tendency was observed on the protein delivery using R_8 and R_{16} as the carrier molecules. Based on the confocal laser microscopic observations, the R_8-carbonic anhydrase conjugate was efficiently internalized into the macrophage cells and accumulation in the nucleus was observed as was seen in the case of the HIV-1 Rev-(34–50) conjugate. In contrast, the R_{16}-conjugate seemed to mainly reside on the cell membranes after a 3-h incubation with the conjugate, but significant accumulation in the nucleus was not observed.

DISCUSSION

In this report, we have shown that not only Tat-(48–60) but also various arginine-rich peptides were able to translocate through the mouse macrophage membranes. These peptides include the D- and arginine-substituted HIV-1 Tat-(48–60) analogs, RNA-binding peptides derived from proteins, such as HIV-1 Rev, HTLV-II Rex, BMV Gag, and FHV coat proteins, and the DNA-binding segments from c-Fos, c-Jun, and the GCN4 proteins. There seems a common or very similar mechanism for the internalization among these peptides. The mechanism is explained neither by adsorptive-mediated endocytosis nor by receptor-mediated endocytosis because the peptides were internalized by the cell at 4 °C, and there seemed little homology both in the primary and secondary structures among these membrane-permeable peptides except that they have several arginine residues in the sequences. These results strongly suggest the possible presence of the common and undefined internalization mechanisms ubiquitously laying among the arginine-rich basic peptides. As one more new finding concerning the features of the internalization, we have shown that the number of arginine residues has a significant influence on the method of internalization and that there seems to be an optimal number of arginine residues for the internalization. There still remain questions why such efficient translocation is possible for the arginine-rich peptides. Possible hydrogen bond formation of arginine with lipid phosphates (18) or interaction with extracellular matrices such as heparan sulfate (19) may be involved in the initial step during the mechanism. However, as was seen in the case of the R_{16} peptide, it is not enough to explain the mechanism only by considering adsorption of peptides on the membranes.

Tat-(48–60) has been reported to carry various proteins into the cells not only into cultured cells but also into the various organs of a living mouse (4). As the arginine-rich peptides examined here seem to have a similar ability as carriers of proteins, further study of the arginine-based peptides may result in finding peptides penetrating to some specific cells by themselves or with the help of other address peptides.

The results obtained here not only shed light on the possible presence of new types of ubiquitous transmembrane mechanisms for the arginine-rich peptides, but also on the development of novel carrier molecules for the intracellular protein delivery.

Acknowledgments—We are grateful to Drs. S. Tanaka and Y. Sugimoto (Kyoto University) and Professor H. Harashima (Hokkaido University) for helpful discussions.

REFERENCES

1. Fawell, S., Seery, J., Daikh, Y., Moore, C., Chen, L. L., Pepinsky, B., and Barsoum, J. (1994) *Proc. Natl. Acad. Sci. U. S. A.* **91**, 664–668
2. Vives, E., Brodin, P., and Lebleu, B. (1997) *J. Biol. Chem.* **272**, 16010–16017
3. Nagahara, H., Vocero-Akbani, A. M., Snyder, E. L., Ho, A., Latham, D. G., Lissy, N. A., Becker-Hapak, M., Ezhevsky, S. A., and Dowdy, S. F. (1998) *Nat. Med.* **4**, 1449–1452
4. Schwarze, S. R., Ho, A., Vocero-Akbani, A., and Dowdy, S. F. (1999) *Science* **285**, 1569–1572
5. Schwarze, S. R., and Dowdy, S. F. (2000) *Trends Pharmacol. Sci.* **21**, 45–48
6. Derossi, D., Joliot, A. H., Chassaing, G., and Prochiantz, A. (1994) *J. Biol. Chem.* **269**, 10444–10450
7. Derossi, D., Calvet, S., Trembleau, A., Brunissen, A., Chassaing, G., and Prochiantz, A. (1996) *J. Biol. Chem.* **271**, 18188–18193
8. Derossi, D., Chassaing, G., and Prochiantz, A. (1998) *Trends Cell Biol.* **8**, 84–87
9. Lin, Y. Z., Yao, S., Veach, R. A., Torgerson, T. R., and Hawiger, J. (1995) *J. Biol. Chem.* **270**, 14255–14258
10. Rojas, M., Yao, S., and Lin, Y. Z. (1996) *J. Biol. Chem.* **271**, 27456–27461
11. Rojas, M., Donahue, J. P., Tan, Z., and Lin, Y. Z. (1998) *Nat. Biotechnol.* **16**, 370–375
12. Futaki, S., Ishikawa, T., Niwa, M., Kitagawa, K., and Yagami, T. (1997) *Bioorg. Med. Chem.* **5**, 1883–1891
13. Kalderon, D., Roberts, B. L., Richardson, W. D., and Smith, A. E. (1984) *Cell* **39**, 499–509
14. Görlich, D., and Mattaj, I. W. (1996) *Science* **271**, 1513–1518
15. Huq, I., Ping, Y.-H., Tamilarasu, N., and Rana, T. M. (1999) *Biochemistry* **38**, 5172–5177
16. Tan, R., and Frankel, A. D. (1995) *Proc. Natl. Acad. Sci. U. S. A.* **92**, 5282–5286
17. Tachibana, R., Harashima, H., Shono, M., Azumano, M., Niwa, M., Futaki, S., and Kiwada, H. (1998) *Biochem. Biophys. Res. Commun.* **251**, 538–544
18. Calnan, B. J., Tidor, B., Biancalana, S., Hudson, D., and Frankel, A. D. (1991) *Science* **252**, 1167–1171
19. Chang, H. C., Samaniego, F., Nair, B. C., Buonaguro, L., and Ensoli, B. (1997) *AIDS* **11**, 1421–1431

STIC-ILL

From: Canella, Karen
Sent: Friday, October 24, 2003 7:40 PM
To: STIC-ILL
Subject: ill order 09/854,204

Art Unit 1642 Location 8E12(mail)

Telephone Number 308-8362

Application Number 09/854,204

1. Cell, 1984, Vol. 39, No. 3, part 2, pp. 499-509

2. Journal of Biological Chemistry, 2001, 276(8):5836-5840

3. Pharmaceutical Research, 1996, 13 (11): 1615-1623

4. Journal of Peptide Research, 1998, 51(3): 235-243

5. Neuroscience Letters 1998, 255 (1): 41-44

6. EMBO, 1990, 9 (3): 815-819

7. Journal of Organic Chemistry, 1997, 62 (5): 1356-1362

8. CAPLUS COPYRIGHT 2003 ACS on STN
ACCESSION NUMBER: 1981:454710 CAPLUS
DOCUMENT NUMBER: 95:54710
TITLE: Natural peptide lactones as ion carriers in membranes
AUTHOR(S): Oberbaeumer, Ilse; Feigl, Peter; Ruf, Horst; Grell, Ernst
CORPORATE SOURCE: Max-Planck-Inst. Biophys., Frankfurt, D-6000/71, Fed. Rep. Ger.
SOURCE: Struct. Act. Nat. Pept., Proc. Fall Meet. Ges. Biol. Chem. (1981), Meeting Date 1979, 523-38. Editor(s): Voelter, Wolfgang; Weitzel, Guenther. de Gruyter: Berlin, Fed. Rep. Ger.
CODEN: 45VYAS
DOCUMENT TYPE: Conference
LANGUAGE: English

9. CAPLUS COPYRIGHT 2003 ACS on STN
ACCESSION NUMBER: 1998:72644 CAPLUS
DOCUMENT NUMBER: 128:141012
TITLE: Rational design of peptides with enhanced membrane permeability
AUTHOR(S): Borchardt, Ronald T.
CORPORATE SOURCE: Department of Pharmaceutical Chemistry, The University of Kansas, Lawrence, KS, 66045, USA
SOURCE: Medicinal Chemistry: Today and Tomorrow, Proceedings of the AFMC International Medicinal Chemistry Symposium, Tokyo, Sept. 3-8, 1995 (1997), Meeting Date 1995, 191-196. Editor(s): Yamazaki, Mikio. Blackwell: Oxford, UK.
CODEN: 65ONAG
DOCUMENT TYPE: Conference
LANGUAGE: English

ELSEVIER

Neuroscience Letters 255 (1998) 41–44

Neuroscience Letters

Strong suppression of feeding by a peptide containing both the nuclear localization sequence of fibroblast growth factor-1 and a cell membrane-permeable sequence

Ai-Jun Li[a,1], Hiroyuki Tsuboyama[a,b,1], Akiko Komi[a], Masahiko Ikekita[b], Toru Imamura[a,b,*]

[a]Biosignaling Department, National Institute of Bioscience and Human Technology, Tsukuba, 305-8566, Japan
[b]Department of Applied Biological Science, Science University of Tokyo, Noda, 278-8510, Japan

Received 30 July 1998; received in revised form 25 August 1998; accepted 26 August 1998

Abstract

Earlier studies have shown that fibroblast growth factor (FGF)-1 in the brain regulates feeding behavior. In the present study, food intake in rats was strongly suppressed by an infusion into the lateral cerebroventricle of a synthetic peptide (26 amino acids) which contains both the N-terminal nuclear localization sequence (NLS) of FGF-1 and a recently identified membrane-permeable sequence. When the NLS motif in the peptide was destroyed by mutations of two lysine residues, the mutant peptide failed to affect eating. The results suggest that the NLS of FGF-1 plays an important role in FGF-1-induced feeding suppression and they introduce a novel compound for feeding regulation. © 1998 Elsevier Science Ireland Ltd. All rights reserved

Keywords: Eating; FGF-1; Nuclear localization sequence; Water intake; Rat

Fibroblast growth factors (FGFs) were originally identified as mitogens for fibroblasts and endothelial cells in culture, but they are now recognized to be multipotent regulators of many pathophysiological events. Many FGF family members, including FGF-1 (acidic FGF) and FGF-2 (basic FGF), are present throughout the central nervous system, and they have diverse effects in the brain. They have neurotrophic effects on many types of neurons [1,18], enhance long-term potentiation in the hippocampus [16,17] and facilitate learning and memory [8], and regulate feeding behavior [13]. Studies have shown that FGF-1 and FGF-2 are endogenous satiety substances in the brain. The FGF-1 and FGF-2 concentration in rat cerebrospinal fluid was dramatically increased by either food intake or an intraperitoneal (i.p.) glucose injection [4], while a third ventricle (3V) injection of FGF-1 or -2 significantly suppressed rat food intake [2,4,15]. This FGF-induced feeding suppression has been shown to be due to an inhibition of the activity of glucose-sensitive neurons in the lateral hypothalamic area (LHA) [13].

Although the FGF receptor (FGFR), FGFR-1, found on the LHA neurons plays a critical role in this feeding inhibition [7], studies with synthesized FGF-1 fragments have indicated that small peptide fragments containing the N-terminus of FGF-1, such as FGF-1-(1–15), [Ala[16]]FGF-1-(1–29), [Ser[16]]FGF-1-(1–29), and [Glu[16]]FGF-1-(1–29), also inhibit food intake when infused into the 3V of rats [7,15]. Such inhibition is not observed with the C-terminal fragment, FGF-1-(114–140). As these N-terminal small peptides are unlikely to bind to FGFR (to judge from previous studies), it is possible that part of the FGF-induced feeding inhibition is exerted through an FGFR-independent mechanism. Interestingly, the N-terminus of FGF-1 contains a nuclear localization sequence (NLS) (FGF-1-(7–13) in Fig. 1) that has been shown to be important for the mitogenic activity of FGF-1 [5]. An FGF-1 mutant that lacks the NLS fails to induce DNA synthesis and cell proliferation at concentrations sufficient to induce intracellular receptor-mediated tyrosine phosphorylation and *c-fos* expression [5]. Furthermore, a recent study demonstrated

* Corresponding author. Tel.: +81 298 546072; fax: +81 298 546095; e-mail: imamura@nibh.go.jp
[1] These two authors contributed equally to this work.

0304-3940/98/$19.00
PII S0304-3940(98)00701-0

that synthetic peptides containing both this NLS and a cell membrane-permeable sequence had the potential to stimulate DNA synthesis in an FGFR-independent manner after they were delivered into living NIH 3T3 cells [9]. In the present study, we investigated the effect on food intake exerted by a synthetic peptide (a 26 amino acid peptide, named SA peptide, which contains both the NLS of FGF-1 and a cell membrane-permeable sequence).

All the animals received humane care according to NIBH standard protocol. Male Wistar rats (Clea, Japan) weighing from 250–300 g were used. The rats were maintained in individual cages with a 12:12 h light-dark cycle (lights on at 0700 h) at a room temperature of 24–25°C. Powdered food (Rat chow, CE-2, Clea, Japan) and tap water were given ad libitum except between 1800 and 1900 h. Under pentobarbital sodium anesthesia (50 mg/kg, i.p.), a 23-gauge stainless steel guide cannula (15 mm long) was implanted into the left lateral cerebroventricle (LCV) according to a rat brain atlas (A: –0.6; L: 1.4; H: 3.8–4.0 mm) [14]. Synthetic peptides (as shown in Fig. 1) and recombinant human FGF-1 (R & D Systems, USA) were used. They were dissolved in 0.15 M NaCl containing 50 μg/ml heparin and 1 mg/ml bovine serum albumin. After 1 week recovery from the implantation, food and water intakes in the nighttime (1900–0700 h) and daytime (0700–1800 h) periods were measured every day. After an injection of 5 μl FGF-1 or peptide into the LCV (via a Hamilton syringe and within a 5-min period between 1830 to 1900 h), the changes in food and water intakes (between those on the infusion day and those on the last preinfusion day) were compared in order to elucidate the effect of FGF components on feeding and drinking behavior. After the experiments, the cannula site was determined in histologically stained 50 μm coronal brain slices after an LCV infusion of pontamine sky blue (2%, 5 μl) [7]. Only rats in which the cannula was inserted directly into the LCV were used for the data analysis. All results are expressed as the mean ± SEM. The statistical analysis was performed using a one-way analysis of variance (ANOVA) followed post-hoc by Fisher's protected least significant difference

	1 13
N-terminus of FGF-1:	FNLPPGNYKKPKL
NLS:	NYKKPKL
SA:	AAVALLPAVLLALLAPAAANYKKPKL
SB:	AAVALLPAVLLALLAPAAANYEEPKL
S:	AAVALLPAVLLALLAPAAA

Fig. 1. Structure of the N-terminus of FGF-1 and its related peptides (as used in the present study). The cell membrane-permeable hydrophobic sequence is underlined, the NLS of FGF-1 is double underlined, and the residues mutated in the NLS are indicated by asterisks.

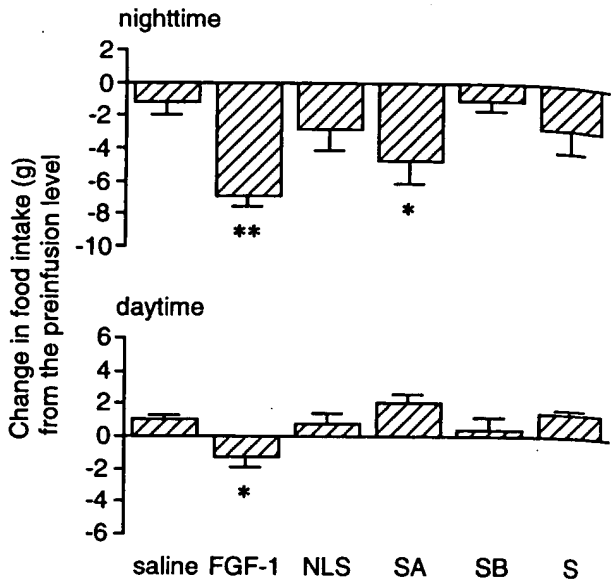

Fig. 2. Effect of an LCV infusion (13 pmol/5 μl per rat) of FGF-1 or its related peptides prior to the dark period on food intake in rats. The changes in the nighttime and daytime food intakes between the infusion and last preinfusion days are shown (mean ± SEM). *$P < 0.01$; **$P < 0.001$ (vs. saline group); one-way ANOVA followed post-hoc by Fisher's PLSD test (n = 4–12 rats in each group).

(PLSD) test. Differences were considered to be significant if $P < 0.05$.

Using the cell membrane-permeable import method [9,10], we synthesized several FGF-1-related peptides (Fig. 1). Among these peptides, SA peptide is composed of 26 amino acids, and contains both a cell membrane-

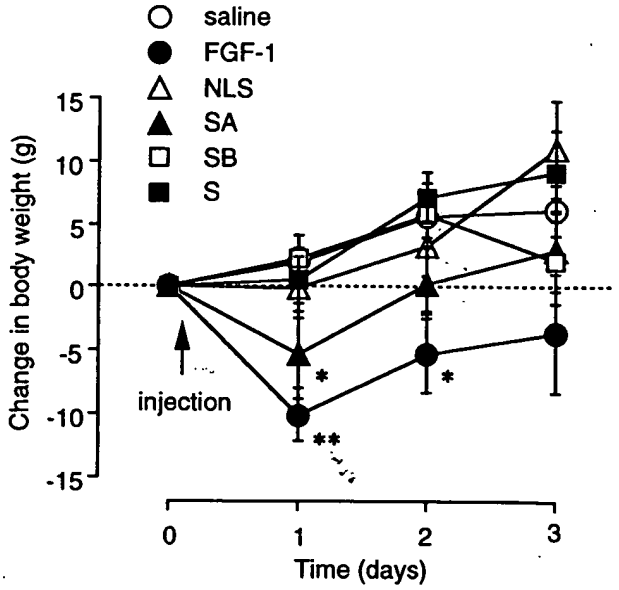

Fig. 3. Body weight changes (vs. that on the last preinfusion day) following an FGF-1 or peptide infusion. FGF-1 or a related peptide (13 pmol/5 μl per rat) was injected prior to the dark period as indicated by the arrow. *$P < 0.01$; **$P < 0.001$ (vs. saline group); one-way ANOVA followed post-hoc by Fisher's PLSD test (n = 4–12 rats in each group).

permeable sequence (16 amino acids) and the NLS of FGF-1 (7 amino acids) separated by a spacer (Ala-Ala-Ala). As control peptides, SB peptide (26 amino acids), which is identical to SA peptide except that two lysine residues in the NLS of SA peptide are mutated into two glutaminic acids, S peptide (19 amino acids), which is identical to SA peptide except that it lacks the FGF-1 NLS, and NLS peptide (7 amino acids) were used in the present study.

Fig. 2 shows the changes in food intake between the infusion and last preinfusion days following an infusion of FGF-1-related peptide or FGF-1 into the LCV in rats. One-way ANOVA indicated significant differences in both nighttime and daytime food intakes ($F(5,32) = 4.695, 3.980$ and $P < 0.003, 0.007$, respectively). SA peptide (13 pmol/rat, $n = 6$), like FGF-1 (13 pmol/rat, $n = 5$), significantly inhibited the nighttime food intake when compared with the saline-infused ($n = 12$) rats ($P < 0.01, 0.001$, respectively). FGF-1 also suppressed the daytime food intake ($P < 0.01$). Body weight gain (Fig. 3) was found to be decreased by the infusion of SA or FGF-1 when measured 24 h after the infusion ($P < 0.01, P < 0.0001$, respectively compared with the saline group). This feeding inhibition by SA peptide occurred in a dose-dependent manner (Fig. 4). The percentage inhibition by SA peptide of the nighttime food intake (vs. the last preinfusion day) was −26.6 ± 5.8% at 52 pmol ($n = 3$), −23.6 ± 7.0% at 13 pmol ($n = 5$), −16.5 ± 5.9% at 3.3 pmol ($n = 7$), and −5.3 ± 4.0% at 0 pmol (saline group). However, SB peptide ($n = 6$), in which the NLS motif is destroyed, failed to suppress food intake ($P > 0.8$ and $P > 0.2$, respectively for nighttime and daytime food intakes). Even at a higher dose, SB peptide (130 pmol/rat, $n = 3$) had no effect on feeding (data not shown). The cell membrane-permeable sequence (S peptide in Fig. 1) itself had no effect on feeding ($n = 5, P > 0.3$ and $P > 0.5$, respectively for nighttime and daytime food intakes). Thus, the present results indicate an important role for the NLS in FGF-1 on the feeding suppression induced by FGF-1. The FGF-1 NLS peptide at the same concentration did not affect food intake in the present study ($n = 4$, $P > 0.9$ and $P > 0.7$, respectively for nighttime and daytime food intakes). This is consistent with the observation that the NLS peptide is not mitogenically active without the cell membrane-permeable sequence (A. Komi, unpublished data).

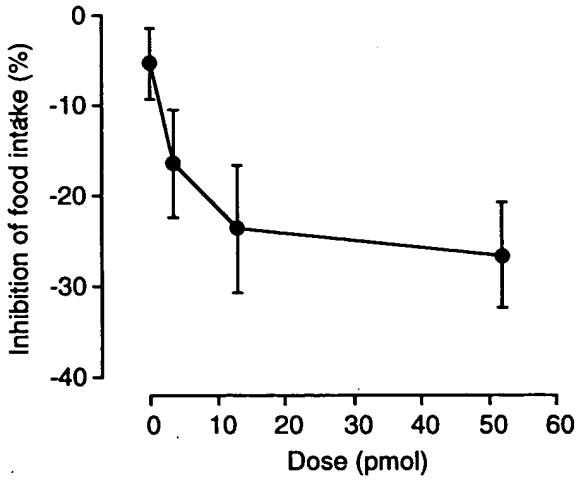

Fig. 4. Dose-dependent suppression of rat food intake by LCV infusion of SA peptide. SA peptide (3.3, 13, 52 pmol/rat) or saline (5 μl/rat) was injected prior to the dark period. Ordinate, inhibition of the nighttime food intake (expressed as a percentage change relative to that on the last preinfusion day; $n = 3$–12 rats for each group).

Table 1
Change in water intake from the preinfusion level following an injection of FGF-1 or its related peptides

Treatment	N	Nighttime	Daytime
Saline	12	−0.31 ± 1.1	1.3 ± 0.7
FGF-1	5	−12.3 ± 2.1**	−0.7 ± 1.2
SA	6	−8.4 ± 3.1*	1.2 ± 0.7
SB	6	−1.5 ± 2.2	1.2 ± 1.3
S	5	−4.9 ± 3.0	1.0 ± 0.4
NLS	4	−5.2 ± 1.4	0.8 ± 1.2

Data are the mean ± SEM (ml). FGF-1 or a related peptide (13 pmol/rat) or saline (5 μl/rat) was injected into the lateral ventricle prior to the dark period. N, number of rats for each group. *$P < 0.01$; **$P < 0.001$ compared with the saline group (one-way ANOVA followed post-hoc by Fisher's PLSD test).

Drinking behavior was also inhibited by the infusions. One-way ANOVA indicated a significant difference in the nighttime ($F(5,32) = 4.696$ and $P < 0.003$), but not in the daytime water intake ($F(5, 32) = 0.635$ and $P > 0.6$) among all the groups. As summarized in Table 1, an LCV infusion of SA peptide or FGF-1 significantly inhibited water intake in the nighttime when compared with saline-infusion ($P < 0.01$ and $P < 0.001$, respectively). These results are consistent with previous reports on FGF-1 and -2, and FGF-1 peptides [7,15]. However, it remains unclear whether this drinking suppression is a result of feeding inhibition or of a direct action on the mechanism regulating water intake [7,15].

Previous studies have shown that several peptides encompassing the FGF-1 N-terminus inhibit food intake in rats when injected into the 3V [7,15]. However, their potency for inducing feeding suppression was only about 1/50 to 1/200 of that of the wild-type FGF-1 [7,15]. The present study shows that by comparison with these peptides, SA peptide exerts a far stronger inhibitory effect on food intake. The potency with which SA peptide (13 pmol/rat) inhibited the nighttime food intake was 75.0% of that of FGF-1 (13 pmol/rat). As the cell membrane-permeable sequence itself had no effect on feeding (Fig. 2), this increased potency of SA peptide appears likely to be due to a more effective intracellular delivery of the FGF-1 NLS. It is intriguing to speculate that the feeding suppressive activity of SA peptide is exerted through the same signaling pathway as that for the intracellularly localized FGF-1 protein. However, it is unclear at present whether the suppressive activity is specific to FGF-1 NLS. An earlier study on the ability of SA

peptide to stimulate DNA synthesis in cultured fibroblasts revealed that other NLSs, such as those of v-Rel protein and of NF-κB p50 protein, also stimulated DNA synthesis when fused with a cell membrane-permeable sequence [10]. A preceding study showed that if the NLS in FGF-1 was functionally substituted by histone 2B NLS, the mitogenic activity of FGF-1 was recovered [5]. Evaluation of peptides containing these NLSs for their feeding regulatory activity would expand our understanding of the feeding regulatory mechanism in the brain. The results further suggest that a cell membrane-permeable transport method may be a useful approach for carrying peptides into the cytoplasm both in vitro [9,10] and in vivo.

The hypothalamus, especially the chemosensitive neurons in the LHA and ventromedial nucleus (VMH), is the most important site for feeding regulation [6,12]. The following studies, taken together, strongly suggest that the target site in the brain for FGF-induced feeding suppression is the LHA: (1) when ^{125}I-FGF-1 or ^{125}I-FGF-2 was infused into the rat LCV, the cell bodies of LHA neurons, but not those of VMH neurons were labeled [3]; (2) the neuronal activity of glucose-sensitive neurons in the LHA was inhibited by electrophoretic application of FGF-1 through an activation of protein kinase C, while VMH neurons did not respond [13]; and (3) FGFR-1 is present in LHA neurons, but not in VMH neurons [11]. However, the target site for SA peptide is still unclear. The present observation that the feeding suppression induced by SA peptide has a similar time-course to that induced by FGF-1 suggests that the LHA may be the site of action of SA peptide. As SA peptide that has been injected into the LCV appears to diffuse widely throughout the hypothalamus, it seems likely that LHA neurons respond to the incorporated SA peptide more strongly than VMH neurons (or that VMH neurons do not respond at all to SA peptide), thus leading to an inhibition of feeding. However, this interpretation remains hypothetical and needs to be examined further.

In summary, the present results strongly suggest that in addition to the FGF receptor-dependent pathway, an important role in FGF-1-induced feeding suppression is performed by the NLS of FGF-1. The present study introduces a novel compound for feeding regulation, and predicts that the cell membrane-permeable transport method will be an effective approach for carrying peptides into the cytoplasm in vivo.

We thank Dr. Masatoshi Takita at NIBH for his technical help, and Dr. R. Timms for his help in preparing this manuscript. This work was partly supported by an AIST-HFSP grant and an STA-COE grant to T.I., and an STA fellowship from JST to A.-J.L.

[1] Anderson, K.J., Dam, D., Lee, S. and Cotman, C.W., Basic fibroblast growth factor prevents death of lesioned cholinergic neurons in vivo, Nature, 332 (1988) 360–361.

[2] De Saint Hilaire, Z. and Nicolaïdis, S., Enhancement of slow wave sleep parallel to the satiating effects of acidic fibroblast growth factor in rats, Brain Res. Bull., 29 (1992) 525–528.

[3] Ferguson, I.A. and Johnson, E.M. Jr., Fibroblast growth factor receptor-bearing neurons in the CNS: identification by receptor-mediated retrograde transport, J. Comp. Neurol., 313 (1991) 693–706.

[4] Hanai, K., Oomura, Y., Kai, Y., Nishikawa, K., Shimizu, N., Morita, H. and Plata-Salamán, C.R., Central action of acidic fibroblast growth factor in feeding regulation, Am. J. Physiol., 256 (1989) R217–R223.

[5] Imamura, T., Engleka, K., Zhan, X., Tokita, Y., Forough, R., Roeder, D., Jackson, A., Maier, J.A.M., Hla, T. and Maciag, T., Recovery of mitogenic activity of a growth factor mutant with a nuclear translocation sequence, Science, 249 (1990) 1567–1570.

[6] Le Magnen, J., Body energy balance and food intake: a neuroendocrine regulatory mechanism, Physiol. Rev., 63 (1983) 314–386.

[7] Li, A.-J., Oomura, Y., Hori, T., Aou, S., Sasaki, K., Kimura, H. and Tooyama, I., Fibroblast growth factor receptor-1 in the lateral hypothalamic area regulates food intake, Exp. Neurol., 137 (1996) 318–323.

[8] Li, A.-J., Oomura, Y., Sasaki, K., Tooyama, I., Hanai, K., Kimura, H. and Hori, T., A single pre-training glucose injection induces memory facilitation in rodents performing various tasks: contribution of acidic fibroblast growth factor, Neuroscience, 85 (1998) 785–794.

[9] Lin, Y.-Z., Yao, S. and Hawiger, J., Role of the nuclear localization sequence in fibroblast growth factor-1-stimulated mitogenic pathways, J. Biol. Chem., 271 (1996) 5305–5308.

[10] Lin, Y.-Z., Yao, S., Veach, R.A., Torgerson, T.R. and Hawiger, J., Inhibition of nuclear translocation of transcription factor NF-κB by synthetic peptide containing a cell membrane-permeable motif and nuclear localization sequence, J. Biol. Chem., 270 (1995) 14255–14258.

[11] Matsuo, A., Tooyama, I., Isobe, S., Ooyama, Y., Akiguchi, I., Hanai, K., Kimura, J. and Kimura, H., Immunohistochemical localization in the rat brain of an epitope corresponding to the fibroblast growth factor receptor-1, Neuroscience, 60 (1994) 49–66.

[12] Oomura, Y., Ooyama, H., Sugimori, M., Nakamura, T. and Yamada, Y., Glucose inhibition of the glucose-sensitive neuron in the rat lateral hypothalamus, Nature, 247 (1974) 284–286.

[13] Oomura, Y., Sasaki, K., Suzuki, K., Muto, T., Li, A.-J., Ogita, Z.-I., Hanai, K., Tooyama, I., Kimura, H. and Yanaihara, N., A new brain glucosensor and its physiological significance, Am. J. Clin. Nutr., 55 (1992) 278S–282S.

[14] Paxinos, G. and Watson, C., The Rat Brain in Stereotaxic Coordinates, Academic Press, New York, 1982.

[15] Sasaki, K., Li, A.-J., Oomura, Y., Muto, T., Hanai, K., Tooyama, I., Kimura, H., Yanaihara, N., Yagi, H. and Hori, T., Effects of fibroblast growth factors and related peptides on food intake by rats, Physiol. Behav., 56 (1994) 211–218.

[16] Sasaki, K., Oomura, Y., Figurov, A. and Yagi, H., Acidic fibroblast growth factor facilitates generation of long-term potentiation in rat hippocampal slices, Brain Res. Bull., 33 (1994) 505–511.

[17] Terlau, H. and Seifelt, W., Fibroblast growth factor enhances long-term potentiation in the hippocampal slice, Eur. J. Neurosci., 2 (1990) 973–977.

[18] Walicke, P.A., Basic and acidic fibroblast growth factors have trophic effects on neurons from multiple CNS regions, J. Neurosci., 8 (1988) 2618–2627.

STIC-ILL

From: Canella, Karen
Sent: Friday, October 24, 2003 7:40 PM
To: STIC-ILL
Subject: ill order 09/854,204

Art Unit 1642 Location 8E12(mail)

Telephone Number 308-8362

Application Number 09/854,204

1. Cell, 1984, Vol. 39, No. 3, part 2, pp. 499-509

2. Journal of Biological Chemistry, 2001, 276(8):5836-5840

3. Pharmaceutical Research, 1996, 13 (11): 1615-1623

4. Journal of Peptide Research, 1998, 51(3): 235-243

5. Neuroscience Letters 1998, 255 (1): 41-44

6. EMBO, 1990, 9 (3): 815-819

7. Journal of Organic Chemistry, 1997, 62 (5): 1356-1362

8. CAPLUS COPYRIGHT 2003 ACS on STN
ACCESSION NUMBER: 1981:454710 CAPLUS
DOCUMENT NUMBER: 95:54710
TITLE: Natural peptide lactones as ion carriers in membranes
AUTHOR(S): Oberbaeumer, Ilse; Feigl, Peter; Ruf, Horst; Grell, Ernst
CORPORATE SOURCE: Max-Planck-Inst. Biophys., Frankfurt, D-6000/71, Fed. Rep. Ger.
SOURCE: Struct. Act. Nat. Pept., Proc. Fall Meet. Ges. Biol. Chem. (1981), Meeting Date 1979, 523-38. Editor(s): Voelter, Wolfgang; Weitzel, Guenther. de Gruyter: Berlin, Fed. Rep. Ger.
CODEN: 45VYAS
DOCUMENT TYPE: Conference
LANGUAGE: English

9. CAPLUS COPYRIGHT 2003 ACS on STN
ACCESSION NUMBER: 1998:72644 CAPLUS
DOCUMENT NUMBER: 128:141012
TITLE: Rational design of peptides with enhanced membrane permeability
AUTHOR(S): Borchardt, Ronald T.
CORPORATE SOURCE: Department of Pharmaceutical Chemistry, The University of Kansas, Lawrence, KS, 66045, USA
SOURCE: Medicinal Chemistry: Today and Tomorrow, Proceedings of the AFMC International Medicinal Chemistry Symposium, Tokyo, Sept. 3-8, 1995 (1997), Meeting Date 1995, 191-196. Editor(s): Yamazaki, Mikio. Blackwell: Oxford, UK.
CODEN: 65ONAG
DOCUMENT TYPE: Conference
LANGUAGE: English

J. Peptide Res. 51, 1998, 235–243
Printed in the United States of America - all rights reserved

JOURNAL OF PEPTIDE RESEARCH
ISSN 1397-002X

Conformational and topological requirements of cell-permeable peptide function

CAIGAN DU, SONGYI YAO, MAURICIO ROJAS and YAO-ZHONG LIN

Department of Microbiology and Immunology, Vanderbilt University School of Medicine, Nashville, Tennessee, USA

Received 3 July, revised 9 September, accepted for publication 16 November 1997

Cell-permeable peptide import recently was developed to deliver synthetic peptides into living cells for studying intracellular protein functions. This import process is mediated by an N-terminal carrier sequence which is the hydrophobic region of a signal peptide. In this study, the conformational consequence of the interaction of cell-permeable peptides with different mimetic membrane environments was investigated by circular dichroism analysis. We showed that cell-permeable peptides adopted α-helical structures in sodium dodecyl sulfate (SDS) micelles or aqueous trifluoroethanol (TFE). The potency of these peptides in forming helical structures is higher in an amphiphilic environment (SDS) than in a hydrophobic environment (TFE), suggesting that some hydrophilic molecules associated with the cell membrane may be involved in peptide import. We also studied topological requirements of cell-permeable peptide function. We demonstrated that peptides containing the carrier sequence in their C-termini can also be imported into cells efficiently. This important discovery can avoid repetitious synthesis of the membrane-translocating sequence for peptides with different functional cargoes and is potentially useful for developing a cell-permeable peptide library. Finally, we showed that, when a retro version of the carrier sequence was used, the peptide lost its translocating ability despite retaining a high content of α-helical structure in mimetic membrane environments. This suggests that the propensity of peptides to adopt a helical conformation is required but not sufficient for cellular import and that other structural factors such as the side-chain topology of the carrier sequence are also important. Our studies together contribute to the more rational design of useful cell-permeable peptides. © Munksgaard 1998.

Key words: cell-permeable peptide import; circular dichroism; membrane-translocating sequence; peptide delivery

The newly developed method of cell-permeable peptide import is an easy and nondestructive method for introducing synthetic peptides into living cells (1). It has been used successfully to probe functionally relevant domains of intracellular proteins and to influence protein-protein interactions involved in signal transduction pathways. Examples thus far include studies of the transcription factor-κB (1), fibroblast growth factor-1 (2), epidermal growth factor receptor (3), $\alpha_{IIB}\beta_3$ integrin receptor (4) and Shc adaptor protein (5). These studies have demonstrated unequivocally that the hydrophobic signal sequences can serve as efficient carriers for delivering peptides of interest (the cargoes) into living cells for functional characterization.

Signal peptide sequences mediate protein secretion and are composed of a positively charged N-terminus (n-region), a central hydrophobic core (h-region) and a carboxyl-terminal cleavage site (c-region) recognized by a signal peptidase (for reviews see 6–9). Many examples of export pathways mediated by signal sequences suggest that secretory proteins are transported across eukaryotic endoplasmic reticulum or bacterial cytoplasmic membranes through a hydrophilic protein-conducting channel formed by many membrane proteins, such as SecA and SecY proteins (for reviews see 10–13). Experimental evidence also has suggested that the signal sequences interact directly with membrane lipids (6, 14–23). This interaction is believed to be crucial for the initiation of membrane export (24). The data from CD studies show that various signal peptides can adopt an α-helical conformation in mimetic membrane environments (25–31). It is suggested that a helical

Abbreviations: CD, circular dichroism; DMEM, Dulbecco's modified Eagle's medium; EGF, epidermal growth factor; EGFR, epidermal growth factor receptor; FBS, fetal bovine serum; HEPES, *N*-2-hydroxyethylpiperazine-*N*′-ethanesulfonic acid; PBS, phosphate-buffered saline; SDS, sodium dodecyl sulfate; TFE, trifluoroethanol.

hairpin structure makes the signal peptide prone to interaction with membrane lipid (25–27, 32) and this lipid interaction then unloops the signal sequence, resulting in a transmembrane conformation (17). *In vivo* and *in vitro* experiments have established evidence that the h-region in the signal sequence plays a central role in helix structure formation and membrane transport (15, 33–37). Although h-regions derived from different proteins do not share sequence homology, they usually are made of a block of 7–16 hydrophobic amino acid residues (9). This suggests that the length of a h-region is not critical to its membrane transport activity. The hydrophobic residues found in the h-regions are often those which have the propensity for forming α-helical conformation, such as leucine and alanine. Mutation and deletion of the residues within the h-region, particularly those that are hydrophobic, often lead to impairment of protein export (9). Proline and glycine residues frequently are found in the middle and/or the end of the h-regions. They are believed to act as helix breakers and are important for forming turn structures in the signal peptides. Replacement of these residues with helix-stabilizing residues leads to less efficient protein export (28, 31).

In our cell-permeable peptide design, the h-region of a signal sequence is placed in the N-terminus of the peptide and is used as a carrier for peptide import (1). Different h-regions endowed peptides with similar cell membrane permeabilities (1, 4), irrespective of the lack of sequence homology among them. These observations suggest that characteristics such as hydrophobicity and structural conformation play an important role in mediating cell-permeable peptide import. The first aim of this study was to determine the conformational requirements of cell-permeable peptides for their interaction with cellular membranes. To achieve this, we used circular dichroism to analyze the conformational behavior of cell-permeable peptides in both heterogeneous amphiphilic and homogenous hydrophobic membrane-mimetic environments. The second objective of this study was to investigate the correlation between the membrane-translocating activity and the topology of cell-permeable sequences. For this purpose, we synthesized several structurally modified peptides and characterized their cellular import behavior and functional activities. These studies are of importance to a more rational design of various cell-permeable peptides.

EXPERIMENTAL PROCEDURES

Cell culture and peptide synthesis

NIH 3T3 cells and SAA cells (NIH 3T3 cells overexpressing human EGFR) were grown in Dulbecco's modified Eagle's medium (DMEM) (Cellgro, AK) containing 10% FBS. Peptides listed in Fig. 1 were synthesized by a stepwise solid-phase peptide synthesis method (38, 39) using *tert*-butyloxycarbonyl (Boc) protection.

ANL:	^{1}NYKKPKL^{7}
SA:	^{1}AAVALLPAVLLALLAPAAANYKKPKL^{26}
r-SA1:	^{1}NYKKPKLAAAAAVALLPAVLLALLAP^{26}
r-SA2:	^{1}NYKKPKLAAA*PALLALLVAPLLAVAA*^{26}
SP1068:	^{1}AAVALLPAVLLALLAPLPVPE$_p$YINQSV^{27}
r-SP1068:	^{1}LPVPE$_p$YINQSVAAVALLPAVLLALLAP^{27}

FIGURE 1

Amino acid sequences of the synthetic peptides studied. The cell membrane translocating (carrier) sequence is underlined and functional cargo sequences are in boldface. The retro version of the cell membrane translocating sequence is italicized. $_p$Y stands for phosphorylated tyrosine.

For phosphotyrosine-containing peptides, Boc-Tyr (PO_3Me_2) was used (3, 5). Synthetic peptides were cleaved from the resin and deprotected by HF or trifluoromethanesulfonic acid/CF_3COOH/dimethyl sulfide/*m*-cresol (1:5:3:1, v/v), extracted into 6 M urea in 0.1 M Tris-HCl, pH 8.2, dialyzed against 0.1 M Tris-HCl, purified by C_{18} reverse-phase HPLC (2.5 × 30 cm) eluted with 0.045% CF_3COOH/aqueous acetonitrile at a flow rate of 7 mL/min (1, 3, 5, 39). The purified peptides were then lyophilized for chemical characterizations and the use of biological assays. The purity of the peptides was verified by mass spectrometry analysis and analytic HPLC. All peptides had good solubilities in DMEM and other culture media. No additive such as dimethyl sulfoxide was required for dissolving the peptides.

Circular dichroism spectroscopy

Far-UV circular dichroism (CD) spectra were acquired using a JASCO J-720 spectropolarimeter. The pure peptide was first dissolved in 60% acetonitrile containing 0.05% trifluoroacetic acid and lyophilized by rapid freezing followed by drying under high vacuum. The stock peptide solution was made by hydrating the dry peptide in H_2O containing HCl (pH 2.5) and was vortexed completely before use. The aqueous SDS and TFE solutions were made by dissolving SDS (ICN, CA; ultra pure) or diluted TFE (Fluka, Ronkonkoma, NY) in H_2O containing HCl (pH 2.5). Finally, 10 μM peptide solutions were made in SDS or TFE solutions and vortexed before measurement. All CD measurements were performed at 25°C from 250 to 190 nm using a 1-mm path length. Data sets were recorded typically using a scan rate of 50 nm/min and a response time of 1 sec. An average of five scans was calculated, the baseline subtracted, and finally smoothed. The mean residue ellipticity, [θ], was calculated in units of degrees cm^2/dmol. The secondary structure content of each peptide was estimated by curve fitting the spectra to reference polylysine spectra (40), which is concentration independent and reproducible.

Translocation of ^{125}I-labeled peptides into cells
Tyrosine-containing SA peptide and its analogs were radiolabeled with ^{125}I by the IODO-GEN method (Pierce Chemical Co., Rockford, IL) as described (1, 2). The specific activities of ^{125}I-labeled SA, r-SA1 and r-SA2 peptides were 3.1×10^4, 3.0×10^4 and 2.5×10^4 cpm/ng, respectively. NIH 3T3 cells grown in DMEM containing 10% FBS were subcultured on a 60-mm dish and incubated for 3 days. The confluent monolayers (1.6×10^6 cells) on each dish were washed twice with Hanks' buffered salt solution (Cellgro, AK) and treated with 3 ng of labeled peptide in DMEM containing 10% FBS at 37°C for the indicated times.The cells were washed eight times with PBS, twice with 2 M NaCl/25 mM HEPES (pH 7.4) and twice with 2 M NaCl/20 mM sodium acetate (pH 4.0) until no radioactivity could be detected in the washings. The washed cells were lysed in lysis buffer (10 mM Tris-HCl, pH 7.0, 0.1 mM ethylenediaminetetraacetic acid, 1 mM phenylmethylsulfonyl fluoride, 1 mM dithiothreitol and 1% Triton X-100), and the radioactivity in the cell lysates was counted in a Packard Auto-Gamma counter.

Mitogenic assay
Confluent NIH 3T3 cells grown on a 96-well plate were transferred to a low serum medium (DMEM containing 0.5% FBS) for 2 days. The tested peptides were added to the serum-starved cells in fresh low serum medium. [^{3}H]Thymidine was added after 16 h, and 4 h later, the cells were washed with PBS, treated with 10% trichloroacetic acid, washed and solubilized with 0.15 M NaOH. The radioactivity of the solution was determined in a liquid scintillation counter (2).

Indirect immunofluorescence assay
Confluent SAA cells grown on chamber slides (Nunc, Naperville, IL) were treated with 0.5 mL peptide solution (50 μg/mL) in DMEM containing 20 mM HEPES and 0.1% bovine serum albumin at 37°C for 30 min. The peptide-treated cells were washed and fixed; intracellular peptides were detected by an indirect immunofluorescence assay using anti-SP1068 peptide antibodies and rhodamine-labeled goat anti-rabbit IgG (Kirkegaard and Perry Laboratories, Gaithersburg, MD) as described (1–3). Coverslips with stained cells were mounted in Poly/Mount (Polysciences, Warrington, PA) and analyzed in a fluorescence microscope using a 100× oil immersion lens.

In vivo *inhibition of EGF-induced EGFR/Grb2 protein-protein association by cell-permeable SP1068 and r-SP1068 peptides*
SAA cells were grown to 95% confluence in DMEM containing 10% FBS, serum-starved for 18 h and then treated with or without peptides (100 μg/mL or as specified) in DMEM containing 20 mM HEPES and 0.1% bovine serum albumin for 30 min as described (3). Subsequently, cells were stimulated with or without hEGF (50 ng/mL, Intergen, Purchase, NY) for 10 min and then washed extensively with cold PBS, 2 M NaCl/25 mM HEPES, pH 7.4, and 2 M NaCl/20 mM sodium acetate, pH 4.0, to remove extracellularly associated peptides. Cell lysates (0.5 mL; 0.3 mg/mL) were incubated with 1 μg of anti-Grb2 antibody. The immunocomplexes were precipitated with protein A-Sepharose (Sigma Chemical Co., St. Louis, MO). Immunoprecipitates were separated on SDS-polyacrylamide gel electrophoresis, transferred to nitrocellulose membranes, and probed with antibodies as indicated, followed by horseradish peroxidase-linked anti-rabbit or anti-mouse antibodies according to ECL protocol (3).

RESULTS

Conformational behavior of cell-permeable peptides in membrane mimetic conditions
To study the conformational behavior of cell-permeable peptides on their interaction with cell membranes, we analyzed their structures by circular dichroism in different membrane mimetic conditions. Micelles of SDS serve as an experimental model of the heterogeneous amphiphilic environment of a membrane lipid-aqueous interface, whereas TFE aqueous solution can mimic the homogeneous hydrophobic face of the membrane. The cell-permeable SA peptide was used as a model peptide (Fig. 1) for this conformational study. Our previous study demonstrated its efficiency in translocating the membrane of living cells and its functional activity in intracellular compartments (2). This peptide contained the h-region of the signal sequence of Kaposi fibroblast growth factor (as the carrier) in its amino-terminal segment, a spacer region of Ala-Ala-Ala, and the nuclear localization sequence of fibroblast growth factor-1 (as the functional cargo) in the carboxyl-terminal segment.

The SA peptide had great solubility in aqueous solutions containing various concentrations of SDS and TFE. Four different concentrations of SDS micelles (5, 50, 100, 550 mM), which mimic a membrane environment, were used to induce the formation of an SA peptide secondary structure. Figure 2 represents CD spectra of the SA peptide (10 μM) in various SDS micelle concentrations. The minimum at about 208 nm and a shoulder at 222 nm is characteristic of an α-helical conformation. This pattern was nearly invariant from 5 to 550 mM SDS, although the spectrum at 550 mM had a more negative ellipticity. In contrast, the spectrum of the SA peptide indicated a predominantly random coil conformation in the aqueous solution containing no SDS micelles. The relative secondary structure contents of cell-permeable SA peptide are shown in Table 1. They were estimated by curve fitting the spectra to reference polylysine spectra (40). In 5 mM SDS (detergent/peptide molar ratio, 500:1), the α-helix content of the peptide was 57%. The elevated

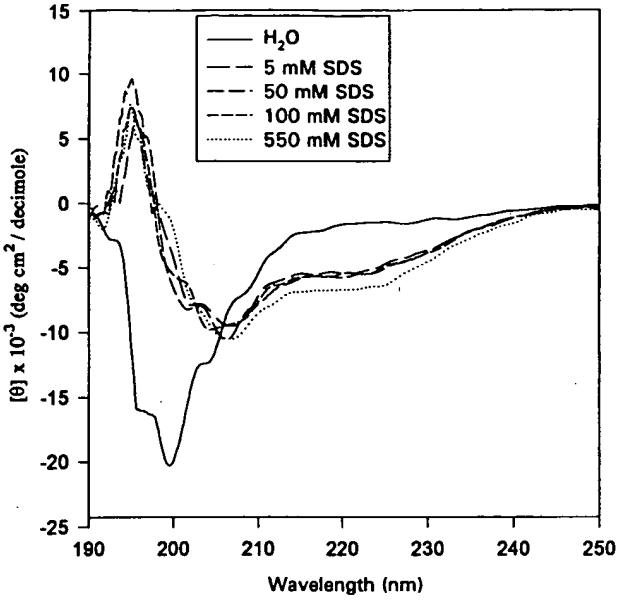

FIGURE 2

CD spectra of the cell-permeable SA peptide on interaction with different concentrations of SDS micelles.

α-helical structure in SDS micelles agreed with reduced levels of β-structure and random coil conformations. This indicates that cell-permeable SA peptide can conform to a strong α-helical structure even in a weak amphiphilic environment. In 500 mM SDS, the α-helix content remained at a similar level, but the β-structure level increased. However, the SA peptide adopted a predominant random coil conformation when SDS concentrations were smaller than 5% (not shown). These data suggest that cell-permeable peptides were in dynamic equilibrium among different structural conformations, which can be shifted toward a highly α-helical form when peptides in the aqueous phase approach the cell membrane.

To compare the induced secondary structures of cell-permeable peptides in amphiphilic and hydrophobic environments, we further analyzed the CD spectra of the SA peptide in aqueous solutions containing TFE. Four different TFE concentrations (10, 20, 30, 50%) were used to examine their effect on the induction of α-helix conformation. In 10% TFE, the CD spectrum of the SA peptide reflected a high content of random coil conformation, which did not differ significantly from that in the aqueous solution containing no TFE (Fig. 3). In highly hydrophobic conditions (20–50% TFE), the SA peptide showed a CD pattern similar to that in an amphiphilic environment (SDS micelles), with a minimum at about 207 nm and a shoulder at 222 nm, indicating the presence of an α-helical structure. Therefore, conformational transition of the peptide occurred between 10% and 20% TFE. The peptide spectrum had a more negative ellipticity in 30% than in 20% TFE, but the negativity did not increase in 50% TFE (Fig. 3; see also Table 2 for the contents of different structures). These results suggest that the induction of peptide helical conformation by TFE is concentration dependent, reaching a plateau at a concentration of 30% (3 M, TFE/peptide molar ratio, 3×10^5 to 1). This result is consistent with the finding by Baldwin and his colleagues (41), which demonstrates that the average helix propensity of peptides increases from 0 to 25% TFE but levels off at higher TFE concentrations. The TFE solutions used for our CD studies were acidic (pH 2.5). To determine the effect of pH in peptide conformation, we further analyzed the CD spectra of the SA peptide in 50% TFE in sodium phosphate buffer (pH 7.4). Our results showed that SA peptide still adopted a predominantly helical conformation at neutral pH (61% α-helix, 24% β-structure and 15% random coil).

TABLE 1

Secondary structure content of SA peptide in SDS micelles

SDS (mm)	α-Helix (%)[a]	β-Structure (%)	Random coil (%)
0	22	23	55
5	57	9	34
50	46	13	41
100	44	18	38
550	55	16	29

[a]Secondary structure content calculated from CD spectra, fitted to Greenfield-Fasman reference data (40).

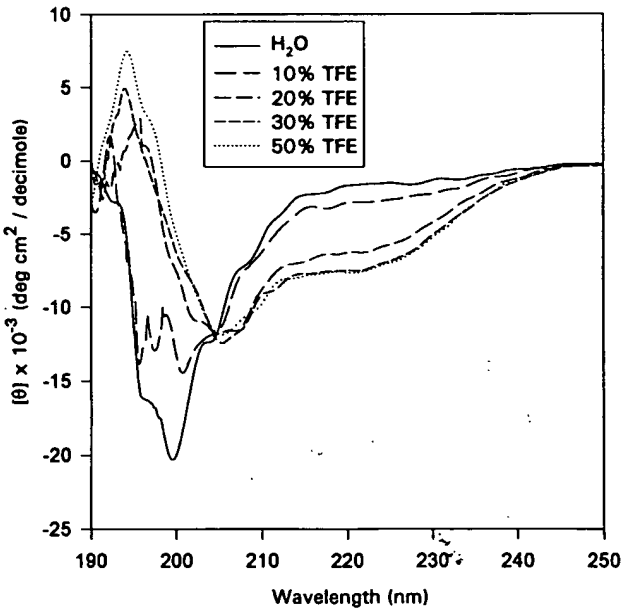

FIGURE 3

CD spectra of the cell-permeable SA peptide on interaction with different concentrations of TFE.

TABLE 2
Secondary structure content of SA peptide in TFE/H_2O

TFE (%)	α-Helix (%)	β-Structure (%)	Random coil (%)
0	22	23	55
10	29	26	45
20	43	23	34
30	46	23	31
50	47	24	29

TABLE 3
Secondary structure content of r-SA1 and r-SA2 peptides on interaction with mimetic membrane environments

	α-Helix (%)		β-Structure (%)		Random coil (%)	
Environment	r-SA1	r-SA2	r-SA1	r-SA2	r-SA1	r-SA2
H_2O	26	19	18	23	56	58
SDS (550 mM)	69	64	23	6	8	30
TFE (50%)	45	45	32	25	23	30

Comparing the effective concentrations of SDS and TFE as well as the secondary structure contents shown in Tables 1 and 2, it appears that the helix-forming potential of cell-permeable peptides in TFE solution was lower than in SDS micelles. The observed difference in α-helical content of a cell-permeable peptide on interaction with a heterogeneous amphiphilic and a homogeneous hydrophobic environment is probably caused by the hydrophilic specificity of the peptide-lipid interaction.

The ANL peptide is an SA peptide analog (2) that lacks the hydrophobic signal sequence (see Fig. 1 for the sequence). Its CD spectra showed a predominantly random conformation (>60%) even at high concentrations of SDS or TFE (not shown), indicating that α-helical conformation of a cell-permeable peptide in a membrane mimetic environment is contributed mainly by its hydrophobic signal sequence.

Effect of the location of the hydrophobic signal sequence on peptide import function

To determine the topology of the cell-membrane translocation sequence, we prepared an SA peptide analog (r-SA1, Fig. 1) in which the hydrophobic signal sequence (the carrier) was placed in the C-terminus of the peptide and the functional sequence (the cargo) was located in the N-terminus. The carrier and the cargo were separated by a spacer region of Ala-Ala-Ala. The CD spectra of the modified peptide in SDS micelles showed a double minimum at 208 nm and 222 nm, a pattern similar to that of the SA peptide except for more negative ellipticity (not shown), indicating a strong α-helical conformation in the amphiphilic environment. Curve-fitting of this spectrum consistently revealed that the helix content of the r-SA1 peptide was higher than that of the SA peptide (Table 3), suggesting that more residues of the r-SA1 peptide were probably involved in helical structure formation (see "Discussion"). To examine the membrane-translocating activity of the r-SA1 peptide, it was radiolabeled with ^{125}I and its uptake by living NIH 3T3 cells was measured. As shown in Fig. 4A, a time-dependent cellular import of r-SA1 peptide was observed when cells were incubated with the radiolabeled peptide. However, it was less potent than the ^{125}I-SA peptide (6.5% vs 15.5% at 4 h, Fig. 4A). Considering that the tyrosine residue for ^{125}I-labeling is located in different regions of the SA and r-SA1 peptides (see Fig. 1), the lower import activity of radiolabeled r-SA1 peptide may be caused by the interference of its bulky N-terminal ^{125}I group during peptide transport. This idea is supported by previous studies indicating that a free, preferably positively charged, N-terminal region of a signal sequence is required for efficient membrane transport (9, 42). To verify the cellular import activity of r-SA1 peptide, we examined unlabeled r-SA1 peptide for its functional activity, which depends strictly on its cellular permeability. We previously demonstrated that SA peptide was mitogenic when it was taken up by NIH 3T3 cells because it carried a functional cargo of the FGF-1 nuclear localization sequence (for details of the functional study, see Ref. 2). The r-SA1 peptide containing the same cargo sequence was also expected to be functional if its cellular import was as efficient as that of the SA peptide. As assessed in a thymidine incorporation assay (see Fig. 4B), r-SA1 peptide did not differ significantly from its SA peptide analog in stimulating mitogenic effects, suggesting that SA and r-SA1 peptides are similar in their cellular import activities. Therefore, the location of the hydrophobic signal sequence may not be crucial to the import activity of cell-permeable peptides.

To verify this finding, we investigated another known cell-permeable peptide (SP1068) containing the same N-terminal carrier sequence but a different cargo sequence, the EGFR autophosphorylation Tyr1068 site (Fig. 1) (3). We knew that this peptide could compete with intracellular EGFR for binding to the endogenous signaling protein Grb2 in EGF-stimulated SAA cells (see Ref. 3 for details). Thus, we prepared a SP1068 peptide analog (r-SP1068, Fig. 1) in which the relative positions of the carrier and the cargo regions in the peptide sequence were exchanged. We first examined whether r-SP1068 peptide with a C-terminal hydrophobic signal sequence can be taken up as efficiently as its SP1068 analog by living SAA cells. In cells treated with r-SP1068 peptide, intracellular peptide was observed in a staining pattern similar to that of SP1068-treated cells, as detected by an indirect immunofluo-

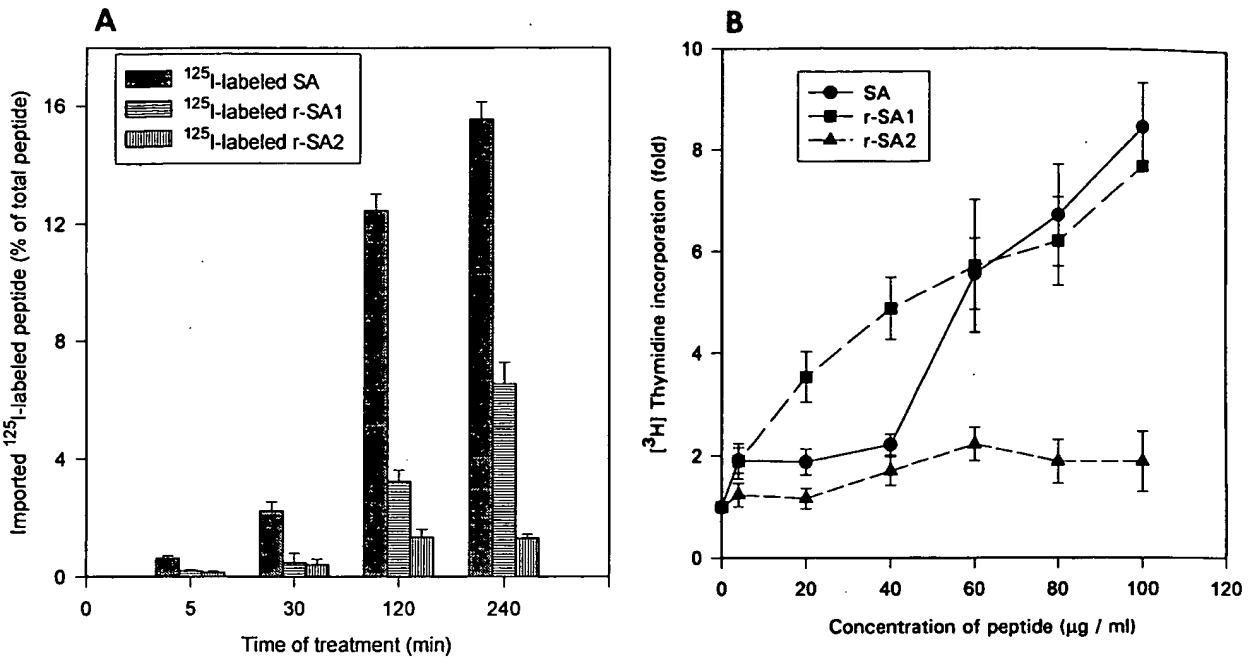

FIGURE 4

(A) Cellular import of ^{125}I-labeled SA, r-SA1 and r-SA2 peptides. Confluent NIH 3T3 cells were treated with ^{125}I-labeled peptides for the indicated times and washed extensively; radioactivities associated with the cell lysates were counted. (B) [^{3}H]Thymidine incorporation by NIH 3T3 cells stimulated by SA, r-SA1 and r-SA2 peptides. Serum-starved cells were incubated with various amounts of peptides. After 16 h, [^{3}H]thymidine was added, and 4 h later, the cells were washed, solubilized and the [^{3}H]thymidine incorporation determined. Data from both panels are the mean ± S.D. of triplicate samples and calculated as multiplicity of counts in the tested sample over a control sample (untreated cells). The experiment was repeated three times with similar results.

rescence assay using an anti-SP1068 peptide antibody (Fig. 5A). This result suggests that r-SP1068 peptide can be imported as efficiently into living cells as SP1068 peptide. We further tested the modified peptide for its functional activity in intracellular compartments. As shown in Fig, 5B, it was similar to its SP1068 peptide analog in inhibiting EGF-induced EGFR/Grb2 association. These results indicate that synthetic peptides containing the hydrophobic signal sequence in their C-termini are also capable of penetrating cell membranes, and thereby are useful for functional study of intracellular proteins.

Other topological requirements for cell-permeable peptide functions

Retro and retroenantio analogs of natural peptides have been used to design potentially bioactive molecules with different side-chain topology and/or chirality (43–49). To determine whether the direction of the sequence order and the side-chain topology of a cell-permeable region is crucial to peptide import activity, we prepared a retro peptide analog of the r-SA1 peptide (see r-SA2 peptide in Fig. 1). The carrier sequence of this peptide contained the same amino acids linked by normal peptide bonds, but in a reverse order (n, $n-1$, ..., 3, 2, 1), numbered from the N-terminus of the sequence. Therefore, r-SA1 and r-SA2 peptides have a noncomplementary side-chain topochemistry in their carrier sequences. As shown in Table 3, the CD spectra of the retro peptide still reflected a primary α-helix conformation in both amphiphilic (SDS) and hydrophobic (TFE) conditions, similar to that of the r-SA1 peptide analog. However, a significant difference in CD profiles between the two peptides was observed in their β-structures and random coil conformations. Table 3 showed that r-SA2 had a relatively lower content of β-structure and, in turn, a higher portion of random coil conformation in amphiphilic condition. The cellular import assay using ^{125}I-labeled peptides indicated that the reversal of the amide bonds of the hydrophobic signal sequence impairs cell membrane permeability, because the import activity of the r-SA2 peptide was negligible as compared with the SA and r-SA1 peptides (Fig. 4A). Consistent with its lack of cellular import, r-SA2 peptide also was not functional in the mitogenic assay (Fig. 4B). Together, these results suggest that a high content of α-helix conformation of the hydrophobic signal sequence is necessary but not sufficient for the induction of peptide cellular import. Other structural factors such as the topochemistry of the side-chains of the carrier sequence may play a role in peptide import.

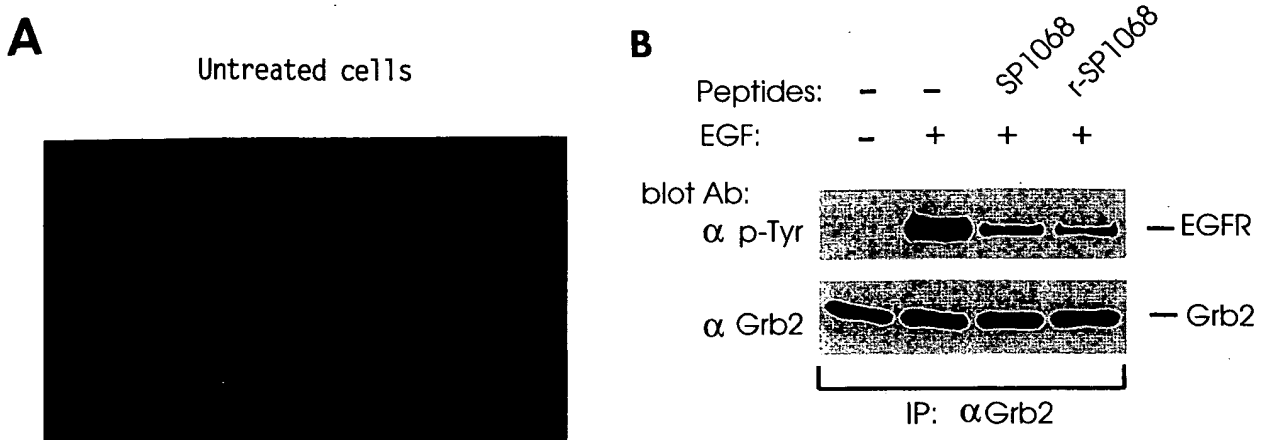

FIGURE 5

(A) Demonstration of the intracellular SP1068 and r-SP1068 peptide in SAA cells by fluorescence microscopy analysis. Confluent SAA cells were treated at 37°C with 100 μg/mL of peptide or diluent for 30 min. Intracellular peptides were detected by indirect immunofluorescence assay using anti-SP1068 peptide antibody and rhodamine-labeled anti-rabbit antibody and analyzed in a fluorescence microscope using a ×100 oil immersion lens. (**B**). *In vivo* inhibition of EGF-induced protein-protein interactions between EGFR and Grb2 by cell-permeable SP1068 and r-SP1068 peptides. Serum-starved SAA cells were treated with or without peptides (100 μg/mL) for 30 min followed by EGF (50 ng/mL) for an additional 10 min. Immunoprecipitation of the cell lysates was carried out with anti-Grb2 antibody. The immunoprecipitates (IP) were subjected to immunoanalysis with anti-Grb2 and anti-phosphotyrosine (α-pTyr) antibodies.

DISCUSSION

Delivery of synthetic cell-permeable peptides into living cells is mediated by the hydrophobic region (h-region) of the signal sequence (1). Different h-regions can bestow similar membrane-translocating activities on peptides (1–5). Functional application studies of cell-permeable peptides have suggested that the length and properties of flanking peptide sequences (the functional cargoes) do not affect the peptide-transporting activities. For example, the size of the cargoes used thus far ranges from 10 to 25 residues, which can be basic, acidic or modified, such as tyrosine-phosphorylated peptides (1–5). Immunofluorescence microscopy and immunoelectron microscopy analysis have suggested that cell-permeable peptides enter cells by free membrane penetration (Du *et al.*, unpublished results), which does not seem to involve either receptor-mediated endocytosis or a specific proteinaceous channel. Therefore, it is possible that cellular uptake of these peptides is initiated and promoted simply by the interactions between peptides and membrane lipids. In this study, we investigated the possible correlation between the appearance of secondary structures and the translocation activity of cell-permeable peptides. Our results showed that the cell-permeable peptide encompassing the h-region of the signal sequence as a carrier adopted an α-helical structure in membrane-mimetic environments. This helical structure induction is likely to result in a conformation essential for the peptide membrane import. The helical structure of the cell-permeable peptide was more predominant in a heterogeneous amphiphilic environment (SDS micelles) than in a homogeneous hydrophobic environment (TFE aqueous solution). This environmental specificity of the peptide suggests a possible interaction of the cell-permeable peptide with hydrophilic head groups of the cell membrane lipid, which may be involved in the initial stage of peptide penetration through the membrane.

We also determined the effect of the location of the hydrophobic signal sequence on peptide import function. When the cell-permeable peptide was modified by synthesizing the hydrophobic region in its carboxyl terminus, it still adopted an α-helical structure in the membrane mimetic environment and was able to penetrate across the cell membrane. Consistent with this, functional assays showed that the modified peptides were as active as their parent peptide analogs. The sequence topology of the parent and modified peptides suggests that the terminal attachments of the carrier sequence (hydrophobic signal sequence) do not significantly affect peptide-translocating activity. Considering that the peptide synthesis is conducted in the direction of the C- to N-terminus (38), development of peptides with a C-terminal cell-permeable sequence can avoid repetitious synthesis of the carrier sequence for peptides with different functional cargoes, thus greatly facilitating the usage of the cell-permeable peptide import technology by our scientific community. Also, this finding is potentially useful for developing a cell-permeable peptide library to detect functional motifs of various proteins.

We finally examined whether the peptide bond direction of the hydrophobic signal sequence is crucial for peptide import activity. When the cell-permeable r-SA1 peptide was converted by synthesizing the carrier sequence in a reverse order (n, $n-1$, ... 3, 2, 1), the retro peptide (r-SA2) did not penetrate across the cell membrane of living cells, as determined by both import and functional assays. If the retro r-SA2 peptide is rotated 180° in plane, the side-chains of its carrier sequence will have the mirror image of the r-SA1 peptide but the amide bond direction will be –NHCO– instead of –CONH–. Thus, it can be suggested that the side-chain topology and/or the peptide amide bond direction of the carrier sequence are required for peptide import function. Because the side-chain setting of the retro peptide topologically resembles that of the D-isomer of the r-SA1 peptide, further examination of the cellular import activity of the enantio and retroenantio analogs of the r-SA1 peptide will determine the exact functional roles of the side-chain topology and peptide bond direction.

All three SA peptide analogs showed significant but different contents of α-helical structure in membrane-mimetic environments. Using the IG computer program to predict the secondary structure of the peptides by the Chou and Fasman algorithm, it was shown that α-helical structure starts from residue 1 to residue 15 with a propensity of 1.231 in the SA cell-permeable peptide. This sequence represents exactly the hydrophobic carrier region of the SA peptide. However, in the r-SA1 peptide, containing the same carrier sequence in its C-terminal region, the α-helical structure location extends to its spacer and functional cargo sequences, starting from residue 6 to residue 25 with a propensity of 1.255. These calculated results fit well with our CD data showing that the r-SA1 peptides had a higher content of helix conformation (69%) in 550 mM SDS micelles compared with its SA peptide analog (55%). Because both SA and r-SA1 peptides have similar import and functional activities, efficient transport is not necessarily proportional to the content of α-helical structure. This assertion is supported by the example of the retro r-SA2 peptide which has a similar propensity (1.213) and residue numbers (residues 6–25) for forming α-helix structure as predicted by the computer calculation. However, the r-SA2 peptide was not active in cellular import despite its high α-helix content in SDS (Table 3). The difference in the predicted structure between active r-SA1 and inactive r-SA2 peptides is their β-structure content in an amphiphilic environment. In 550 mM SDS micelles, r-SA2 peptide displayed a lower β-structure (6%) than r-SA1 (23%). Although it remains to be determined

whether a significant amount of β-structure is required for efficient transport, these results again suggest that the peptide bond direction and/or the side-chain topology of the carrier sequence segment are important for forming a membrane-translocating conformation. A helical hairpin structure with a short loop is important for the signal peptide to interact with the lipid during the initial stage of membrane export. It is possible that the helix-loop-helix conformation is also required for peptide import. The import impairment of the r-SA2 peptide may be the result of its inability to form such a membrane-translocating conformation.

ACKNOWLEDGMENTS

This research was supported by the American Cancer Society Research Development Grant RD392 and by the NIH RO1 GM52500. We thank Dr. J. Donahue for his helpful suggestion, Dr. L. Zhang for his useful advice in CD measurements, Dr. G. Carpenter for SAA cell lines, Drs. J. Hawiger and J. P. Tam for review of the manuscript, and C. Walter for editorial assistance.

REFERENCES

1. Lin, Y.-Z., Yao, S., Veach, R.A., Torgerson, T.R. & Hawiger, J. (1995) *J. Biol. Chem.* **270**, 14255–14258
2. Lin, Y.-Z., Yao, S. & Hawiger, J. (1996) *J. Biol. Chem.* **271**, 5305–5308
3. Rojas, M., Yao, S. & Lin, Y.-Z. (1996) *J. Biol. Chem.* **271**, 27456–27261.
4. Liu, X.-Y., Timmons, S., Lin, Y.-Z. & Hawiger, J. (1996) *Proc. Natl. Acad. Sci. USA* **93**, 11819–11824
5. Rojas, M., Yao, S., Donahue, J.P. & Lin, Y.-Z. (1997) *Biochem. Biophys. Res. Commun.* **234**, 675–680
6. Briggs, M.S. & Gierasch, L.M. (1986) *Adv. Protein Chem.* **38**, 109–180
7. Gierasch, L.M. (1989) *Biochemistry* **28**, 923–930
8. von Heijne, G. (1985) *J. Mol. Biol.* **184**, 99–105
9. von Heijne, G. (1990) *J. Membr. Biol.* **115**, 195–201
10. Rapoport, T.A. (1992) *Science* **258**, 931–936
11. Gilmore, R. (1993) *Cell* **75**, 589–592.
12. Sanders, S.L. & Schekman, R. (1992) *J. Biol. Chem.* **267**, 13791–13794
13. Nunnari, J. & Walter, P. (1992) *Curr. Opin. Cell Biol.* **4**, 573–580.
14. Geller, B.L. & Wickner, W. (1985) *J. Biol. Chem.* **260**, 13281–13285
15. Briggs, M.S., Gierasch, L.M., Zlotnick, A., Lear, J.D. & DeGrado, W.F. (1985) *Science* **228**, 1096–1099
16. De Vrije, T., de Swart, R.L., Dowhan, W., Tommassen, J. & de Kruijff, B. (1988) *Nature* **334**, 173–175
17. De Vrije, T., Batenburg, A.M., Killian, J.A. & De Kruijff, B. (1990) *Mol. Microbiol.* **4**, 143–150
18. Jones, J.D., McKnight, C.J. & Gierasch, L.M. (1990) *J. Bioenerg. Biomembr.* **22**, 213–232
19. Killian, J.A., de Jong, A.M. Ph., Bijvelt, J., Verkleij, A.J. & de Kruijff, B. (1990) *EMBO J.* **9**, 815–819
20. Phoenix, D.A., Kusters, R., Hikita, C., Mizushima, S. & De Kruijff, B. (1993) *J. Biol. Chem.* **268**, 17069–17073.
21. Phoenix, D.A., De Wolf, F.A., Staffhorst, R.W.H.M., Hikita, C., Mizushima, S. & De Kruijff, B. (1993) *FEBS Lett.* **324**, 113–116
22. Kusters, R., Dowhan, W. & De Kruijff, B. (1991) *J. Biol. Chem.* **266**, 8659–8662
23. Kusters, R., Breukink, E., Gallusser, A., Kuhn, A. & De Kruijff, B. (1994) *J. Biol. Chem.* **269**, 1560–1563
24. De Kruijff, B. (1994) *FEBS Lett.* **346**, 78–82
25. Briggs, M.S. & Gierasch, L.M. (1984) *Biochemistry* **23**, 3111–3114
26. Batenburg, A.M., Brasseur, R., Ruysschaert, J.M., Van Scharrenburg, G J.M., Slotboom, A.J., Demel, R.A. & De Kruijff, B. (1988) *J. Biol. Chem.* **263**, 4202–4207
27. Batenburg, A.M., Demel, R.A., Verkleij, A.J. & de Kruijff, B. (1988) *Biochemistry* **27**, 5678–5685
28. Yamamoto, Y., Ohkubo, T., Kohara, A., Tanaka, T., Tanaka, T. & Kikuchi, M. (1990) *Biochemistry* **29**, 8998–9006
29. Hoyt, D.W. & Gierasch, L.M. (1991) *Biochemistry* **30**, 10155–10163
30. Rizo, J., Blanco, F.J., Kobe, B., Bruch, M.D. & Gierasch, L.M. (1993) *Biochemistry* **32**, 4881–4894
31. Chupin, V., Killian, J.A., Breg, J., De Jongh, H.H.J., Boelens, R., Kaptein, R. & De Kruijff, B. (1995) *Biochemistry* **34**, 11617–11624
32. McKnight, C.J., Briggs, M.S. & Gierasch, L.M. (1989) *J. Biol. Chem.* **29**, 17293–17297
33. Kendall, D.A., Bock, S.C. & Kaiser, E.T. (1986) *Nature* **321**, 706–708
34. Kendall, D.A. & Kaiser, E.T. (1988) *J. Biol. Chem.* **263**, 7261–7265
35. Yamamoto, Y., Taniyama, Y., Kikuchi, M. & Ikehara, M. (1987) *Biochem. Biophys. Res. Commun.* **149**, 431–436
36. Bird, P., Gething, M.-J. & Sambrook, J. (1990) *J. Biol. Chem.* **265**, 8420–8425
37. Chou, M.M. & Kendall, D.A. (1990) *J. Biol. Chem.* **265**, 2873–2880
38. Merrifield, R.B. (1963) *J. Am. Chem. Soc.* **85**, 2149–2154
39. Lin, Y.-Z., Caporaso, G., Chang, P.Y., Ke, X.H. & Tam, J.P. (1988) *Biochemistry* **27**, 5640–5645
40. Greenfield, N. & Fasman, C.D. (1969) *Biochemistry* **8**, 4108–4116
41. Luo, P. & Baldwin, R.L. (1997) *Biochemistry* **36**, 8413–8421
42. von Heijne, G. (1984) *EMBO J.* **3**, 2315–2318
43. Jameson, B.A., McDonnell, J.M., Marini, J.C. & Korngold, R. (1994) *Nature* **368**, 744–746
44. Guichard, G., Benkirane, N., Zeder-Lutz, G., Van Regenmortel, M.H.V., Briand, J.-P. & Muller, S. (1994) *Proc. Natl. Acad. Sci. USA* **91**, 9765–9769
45. Merrifield, R.B., Javvadi, P., Andreu, D., Ubach, J., Boman, A. & Boman, H.G. (1995) *Proc. Natl. Acad. Sci. USA* **92**, 3449–3453
46. Prelog, V. & Gerlach, H. (1964) *Helv. Chim. Acta* **47**, 2288.
47. Shemyakin, M.M., Ovchinnikov, Y.A. & Ivanov, V.T. (1968) *Angew. Chem. Int. Ed. Engl.* **8**, 492–499
48. Goodman, M. & Chorev, M. (1979) *Acc. Chem. Res.* **12**, 1–7
49. Chorev, M. & Goodman, M. (1993) *Acc. Chem. Res.* **26**, 266–273

Address:

Dr. *Yao-Zhong Lin*
Department of Microbiology and Immunology
Vanderbilt University School of Medicine
Nashville, TN 37232-2363
USA
Phone: (615) 343-8277
Fax: (615) 343-7392
E-mail: Liny@ctrvax.vanderbilt.edu.

L17 ANSWER 26 OF 26 CAPLUS COPYRIGHT 2003 ACS on STN
ACCESSION NUMBER: 1981:454710 CAPLUS
DOCUMENT NUMBER: 95:54710
TITLE: Natural **peptide** lactones as ion carriers in membranes
AUTHOR(S): Oberbaeumer, Ilse; Feigl, Peter; Ruf, Horst; Grell, Ernst
CORPORATE SOURCE: Max-Planck-Inst. Biophys., Frankfurt, D-6000/71, Fed. Rep. Ger.
SOURCE: Struct. Act. Nat. Pept., Proc. Fall Meet. Ges. Biol. Chem. (1981), Meeting Date 1979, 523-38. Editor(s): Voelter, Wolfgang; Weitzel, Guenther. de Gruyter: Berlin, Fed. Rep. Ger.
CODEN: 45VYAS
DOCUMENT TYPE: Conference
LANGUAGE: English
AB Membrane activity and physicochem. properties of the streptogramin antibiotics: virginiamycin S1 [23152-29-6], mikamycin B [3131-03-1], and viridogrisein [**299-20-7**] are discussed.
IT **299-20-7**
RL: BIOL (Biological study)
(cell membrane activity and physicochem. properties of)
RN 299-20-7 CAPLUS
CN Etamycin A (8CI, 9CI) (CA INDEX NAME)

NTE modified (modifications unspecified)

SEQ 1 TLXXIAX

Absolute stereochemistry.

L17 ANSWER 24 OF 26 CAPLUS COPYRIGHT 2003 ACS on STN
ACCESSION NUMBER: 1996:746841 CAPLUS
DOCUMENT NUMBER: 126:98787
TITLE: Esterase-sensitive cyclic prodrugs of **peptides** : evaluation of an acyloxyalkoxy promoiety in a model hexapeptide
AUTHOR(S): Pauletti, Giovanni M.; Gangwar, Sanjeev; Okumu, Franklin W.; Siahaan, Teruna J.; Stella, Valentino J.; Borchardt, Ronald T.
CORPORATE SOURCE: Dep. Pharmaceutical Chem., Univ. Kansas, Lawrence, KS, 66047, USA
SOURCE: Pharmaceutical Research (1996), 13(11), 1615-1623
CODEN: PHREEB; ISSN: 0724-8741
PUBLISHER: Plenum
DOCUMENT TYPE: Journal
LANGUAGE: English

AB The purpose of the study was to evaluate a cyclic acyloxyalkoxycarbamate prodrug of a model hexapeptide (H-Trp-Ala-Gly-Gly-Asp-Ala-OH) as a novel approach to enhance the membrane permeation of the peptide and stabilize it to metab. Conversion to the linear hexapeptide was studied at 37.degree.C in aq. buffered solns. and in various biol. milieus having measurable esterase activities. Transport and metab. characteristics were assessed using the Caco-2 cell culture model. In buffered solns. the cyclic prodrug degraded chem. to the linear hexapeptide in stoichiometric amts. Maximum stability was obsd. between pH 3-4. In 90% human plasma (t1/2 = 100 .+-. 4 min) and in homogenates of the rat intestinal mucosa (t1/2 = 136 .+-. 4 min) and rat liver (t1/2 = 136 .+-. 4 min) and rat liver (t1/2 = 65 .+-. 3 min), the cyclic prodrug disappeared faster than in buffered soln., pH 7.4 (t1/2 = 206 .+-. 11 min). Pretreatment of these media with paraoxon significantly decreased the degrdn. rate of the prodrug. When applied to the apical side of Caco-2 cell monolayers, the cyclic prodrug (t1/2 = 282 .+-. 25 min) was significantly more stable than the hexapeptide (t1/2 = 14 min) and at least 76-fold more able to permeate (Papp = 1.30 .+-. 0.15 .times. 10-7 cm/s) than the parent peptide (Papp .ltoreq. 0.17 .times. 10-8 cm/s). Prepn. of a cyclic peptide using an acyloxyalkoxy promoiety reduced the lability of the peptide to peptidase metab. and substantially increased its permeation through biol. membranes. In various biol. media the parent peptide was released from the prodrug by an apparent esterase-catalyzed reaction, sensitive to paraoxon inhibition.

IT **185348-61-2**
RL: BPR (Biological process); BSU (Biological study, unclassified); PRP (Properties); BIOL (Biological study); PROC (Process)
(**membrane permeability** and stability of cyclic prodrug of model hexapeptide)

RN 185348-61-2 CAPLUS
CN 1-6-Delta sleep-inducing peptide (rabbit), N-[(hydroxymethoxy)carbonyl]-, (6.fwdarw.1)-lactone (9CI) (CA INDEX NAME)

NTE cyclic

SEQ 1 AGGDAXW

L17 ANSWER 20 OF 26 CAPLUS COPYRIGHT 2003 ACS on STN
ACCESSION NUMBER: 1998:133304 CAPLUS
DOCUMENT NUMBER: 128:291642
TITLE: Conformational and topological requirements of cell-permeable **peptide** function
AUTHOR(S): Du, Caigan; Yao, Songyi; Rojas, Mauricio; Lin, Yao-Zhong
CORPORATE SOURCE: Department of Microbiology and Immunology, Vanderbilt University School of Medicine, Nashville, TN, USA
SOURCE: Journal of Peptide Research (1998), 51(3), 235-243
CODEN: JPERFA; ISSN: 1397-002X
PUBLISHER: Munksgaard International Publishers Ltd.
DOCUMENT TYPE: Journal
LANGUAGE: English

AB Cell-permeable peptide import recently was developed to deliver synthetic peptides into living cells for studying intracellular protein functions. This import process is mediated by an N-terminal carrier sequence which is the hydrophobic region of a signal peptide. In this study, the conformational consequence of the interaction of cell-permeable peptides with different mimetic membrane environments was investigated by CD anal. We showed that cell-permeable peptides adopted .alpha.-helical structures in sodium dodecyl sulfate (SDS) micelles or aq. trifluoroethanol (TFE). The potency of these peptides in forming helical structures is higher in an amphiphilic environment (SDS) than in a hydrophobic environment (TFE), suggesting that some hydrophilic mols. assocd. with the cell membrane may be involved in peptide import. We also studied topol. requirements of cell-permeable peptide function. We demonstrated that peptides contg. the carrier sequence in their C-termini can also be imported into cells efficiently. This important discovery can avoid repetitious synthesis of the **membrane-translocating** sequence for peptides with different functional cargoes and is potentially useful for developing a cell-permeable peptide library. Finally, we showed that, when a retro version of the carrier sequence was used, the peptide lost its translocating ability despite retaining a high content of .alpha.-helical structure in mimetic membrane environments. This suggests that the propensity of peptides to adopt a helical conformation is required but not sufficient for cellular import and that other structural factors such as the side-chain topol. of the carrier sequence are also important. Our studies together contribute to the more rational design of useful cell-permeable peptides.

IT **131089-11-7P**
RL: BPR (Biological process); BSU (Biological study, unclassified); PRP (Properties); SPN (Synthetic preparation); BIOL (Biological study); PREP (Preparation); PROC (Process)
(conformational and topol. requirements of cell-permeable peptide function)

RN 131089-11-7 CAPLUS
CN L-Leucine, L-asparaginyl-L-tyrosyl-L-lysyl-L-lysyl-L-prolyl-L-lysyl- (9CI) (CA INDEX NAME)

SEQ 1 NYKKPKL

L17 ANSWER 16 OF 26 CAPLUS COPYRIGHT 2003 ACS on STN
ACCESSION NUMBER: 1998:708467 CAPLUS
DOCUMENT NUMBER: 130:47576
TITLE: Strong suppression of feeding by a **peptide** containing both the nuclear localization sequence of fibroblast growth factor-1 and a cell **membrane -permeable** sequence
AUTHOR(S): Li, Ai-Jun; Tsuboyama, Hiroyuki; Komi, Akiko; Ikekita, Masahiko; Imamura, Toru
CORPORATE SOURCE: Biosignaling Department, National Institute of Bioscience and Human Technology, Tsukuba, 305-8566, Japan
SOURCE: Neuroscience Letters (1998), 255(1), 41-44
CODEN: NELED5; ISSN: 0304-3940
PUBLISHER: Elsevier Science Ireland Ltd.
DOCUMENT TYPE: Journal
LANGUAGE: English

AB Earlier studies have shown that fibroblast growth factor (FGF)-1 in the brain regulates feeding behavior. In the present study, food intake in rats was strongly suppressed by an infusion into the lateral cerebroventricle of a synthetic peptide (26 amino acids) which contains both the N-terminal nuclear localization sequence (NLS) of FGF-1 and a recently identified **membrane-permeable** sequence. When the NLS motif in the peptide was destroyed by mutations of two lysine residues, the mutant peptide failed to affect eating. The results suggest that the NLS of FGF-1 plays an important role in FGF-1-induced feeding suppression and they introduce a novel compd. for feeding regulation.

IT **131089-11-7**
RL: BAC (Biological activity or effector, except adverse); BSU (Biological study, unclassified); PRP (Properties); BIOL (Biological study)
(FGF-1 peptide contg. nuclear localization sequence and a cell **membrane-permeable** sequence suppresses food intake in rats)
RN 131089-11-7 CAPLUS
CN L-Leucine, L-asparaginyl-L-tyrosyl-L-lysyl-L-lysyl-L-prolyl-L-lysyl- (9CI) (CA INDEX NAME)

SEQ 1 NYKKPKL

L17 ANSWER 25 OF 26 CAPLUS COPYRIGHT 2003 ACS on STN
ACCESSION NUMBER: 1990:402125 CAPLUS
DOCUMENT NUMBER: 113:2125
TITLE: Induction of non-bilayer lipid structures by functional signal **peptides**
AUTHOR(S): Killian, J. A.; De Jong, A. M. P.; Bijvelt, J.; Verkleij, A. J.; De Kruijff, B.
CORPORATE SOURCE: Inst. Mol. Biol. Med. Biotechnol., Univ. Utrecht, Utrecht, 3584 CH, Neth.
SOURCE: EMBO Journal (1990), 9(3), 815-19
CODEN: EMJODG; ISSN: 0261-4189
DOCUMENT TYPE: Journal
LANGUAGE: English

AB Using 31P NMR and freeze-fracture electron microscopy the effect of several synthetic signal peptides on lipid structure in model membranes mimicking the lipid compn. of the Escherichia coli inner membrane was studied. It is demonstrated that the signal peptide of the E. coli outer membrane protein PhoE, as well as that of the M13 phage coat protein, strongly promote the formation of nonbilayer lipid structures. This effect appears to be correlated to in vivo translocation efficiency, since a less functional analog of the PhoE signal peptide was found to be less active in destabilizing the bilayer. It is proposed that signal sequences can induce local changes in lipid structure that are involved in protein **translocation** across the **membrane**.

IT **114460-44-5**
RL: BIOL (Biological study)
(glycerolipid membrane interaction with, nonbilayer structure induction in, as signal peptide model)

RN 114460-44-5 CAPLUS
CN L-Alanine, N-[N-[N-[N-[N2-(N2-L-methionyl-L-lysyl)-L-lysyl]-L-seryl]-L-threonyl]-L-leucyl]- (9CI) (CA INDEX NAME)

SEQ 1 MKKSTLA

L12 ANSWER 23 OF 27 CAPLUS COPYRIGHT 2003 ACS on STN
ACCESSION NUMBER: 1997:218431 CAPLUS
DOCUMENT NUMBER: 126:212413
TITLE: Synthesis of a Novel Esterase-Sensitive Cyclic Prodrug of a Hexapeptide Using an (Acyloxy)alkoxy Promoiety
AUTHOR(S): Gangwar, Sanjeev; Pauletti, Giovanni M.; Siahaan, Teruna J.; Stella, Valentino J.; Borchardt, Ronald T.
CORPORATE SOURCE: Department of Pharmaceutical Chemistry, University of Kansas, Lawrence, KS, 66047, USA
SOURCE: Journal of Organic Chemistry (1997), 62(5), 1356-1362
CODEN: JOCEAH; ISSN: 0022-3263
PUBLISHER: American Chemical Society
DOCUMENT TYPE: Journal
LANGUAGE: English

AB Synthetic methodol. for prepg. novel esterase-sensitive cyclic prodrugs of peptides with increased protease stability and cell **membrane permeability** compared to linear **peptides** is described. Cyclic prodrug cyclo(Ala-OCH2O2C-Trp-Ala-Gly-Gly-Asp) (I) of the hexapeptide H-Trp-Ala-Gly-Gly-Asp-Ala-OH linked by the N-terminal amino group to the C-terminal carboxyl group via an (acyloxy)alkoxy promoiety was synthesized. A convergent synthetic approach involving Boc-Ala-OCH2O2C-Trp-OH (Boc = Me3CO2C), with the promoiety inserted between the Ala and the Trp residues, and H-Ala-Gly-Gly-Asp(OCH2Ph)-OCH2CCl3 (II) was used. Fragment II was synthesized by a soln.-phase approach using std. Boc amino acid chem. These fragments were coupled to produce the protected linear hexapeptide, which after deprotection was cyclized using std. high-diln. techniques to yield cyclic prodrug I. In pH 7.4 buffer (HBSS) at 37.degree., cyclic prodrug I was shown to degrade quant. to the hexapeptide (t1/2 = 206 .+-. 11 min). The rate of hydrolysis of cyclic prodrug I was significantly faster in human blood (t1/2 = 132 .+-. 4 min) than in HBSS. Paraoxon, a known inhibitor of esterases, slowed this hydrolysis of cyclic prodrug I to a value (t1/2 = 198 .+-. 9 min) comparable to the chem. stability. In human blood, cyclic prodrug I was 25-fold more stable than the linear hexapeptide.

IT **185348-61-2P**
RL: BAC (Biological activity or effector, except adverse); BSU (Biological study, unclassified); PRP (Properties); SPN (Synthetic preparation); THU (Therapeutic use); BIOL (Biological study); PREP (Preparation); USES (Uses)
(prepn. of novel esterase-sensitive (acyloxyalkoxy)hexapeptide cyclic prodrug)

RN 185348-61-2 CAPLUS
CN 1-6-Delta sleep-inducing peptide (rabbit), N-[(hydroxymethoxy)carbonyl]-, (6.fwdarw.1)-lactone (9CI) (CA INDEX NAME)

L12 ANSWER 20 OF 27 CAPLUS COPYRIGHT 2003 ACS on STN
ACCESSION NUMBER: 1998:72644 CAPLUS
DOCUMENT NUMBER: 128:141012
TITLE: Rational design of **peptides** with enhanced **membrane permeability**
AUTHOR(S): Borchardt, Ronald T.
CORPORATE SOURCE: Department of Pharmaceutical Chemistry, The University of Kansas, Lawrence, KS, 66045, USA
SOURCE: Medicinal Chemistry: Today and Tomorrow, Proceedings of the AFMC International Medicinal Chemistry Symposium, Tokyo, Sept. 3-8, 1995 (1997), Meeting Date 1995, 191-196. Editor(s): Yamazaki, Mikio. Blackwell: Oxford, UK.
CODEN: 65ONAG
DOCUMENT TYPE: Conference
LANGUAGE: English

AB Through rational drug design and combinatorial library strategies, medicinal chemists are capable of synthesizing very potent and very specific drug candidates. These drug candidates are developed with mol. characteristics that permit optimal interaction with the specific macromols. (e.g., receptors, enzymes) that mediate their pharmacol. effects. However, these drug design strategies, as currently practiced in many pharmaceutical companies, do not necessarily insure optimal delivery of the drug to its site of action. This manuscript describes ongoing research the authors have designed to elucidate the general structural features of peptides and peptide mimetics that afford optimal permeation of these types of mols. through the intestinal mucosa. In addn., a novel prodrug methodol. used to prep. cyclic derivs., which increases their ability to permeate membranes and stabilizes them to metab. peptidases, is described.

IT **185348-61-2 187978-53-6**
RL: BUU (Biological use, unclassified); PRP (Properties); BIOL (Biological study); USES (Uses)
(rational design of **peptides** with enhanced **membrane permeability**)

RN 185348-61-2 CAPLUS
CN 1-6-Delta sleep-inducing peptide (rabbit), N-[(hydroxymethoxy)carbonyl]-, (6.fwdarw.1)-lactone (9CI) (CA INDEX NAME)

NTE cyclic

SEQ 1 AGGDAXW

L15 ANSWER 749 OF 749 CAPLUS COPYRIGHT 2003 ACS on STN
ACCESSION NUMBER: 1931:689 CAPLUS
DOCUMENT NUMBER: 25:689
ORIGINAL REFERENCE NO.: 25:77i,78a-d
TITLE: The behavior of N sodium hydroxide, erepsin and trypsin-kinase toward poly-**peptides** built up from glycine
AUTHOR(S): Abderhalden, Emil; Heumann, Jolan
SOURCE: Fermentforschung (**1930**), 12, 42-54
CODEN: FEFOAG; ISSN: 0367-2034
DOCUMENT TYPE: Journal
LANGUAGE: Unavailable

AB A study of the hydrolysis of glycine peptides, from the dipeptide to the hexapeptide inclusive, has already been reported (C. A. 22, 426, 1572). The series has now been extended from there on to the decapeptide. The usual method of coupling the next lower peptide with ClCH2COCl and aminating the product was unsuccessful beyond the heptapeptide because of insoly. of the substance in dil. alkali. The difficulty was overcome by dispersing the peptide in 50% LiBr, then adding NaOH, dilg. with H2O and finally adding the ClCH2COCl. The ClCH2CO deriv. thus obtained was best aminated by mech. shaking of its suspension in liquid NH3. New derivs. described are chloroacetylpentaglycylglycine (74% yield), sinters and becomes yellow at 225.degree., .fwdarw. hexaglycylglycine (84% yield), sinters above 230.degree., .fwdarw. chloroacetylhexaglycylglycine (79% yield), decomps. above 225.degree., .fwdarw. heptaglycylglycine (70% yield), .fwdarw. chloroacetylheptaglycylglycine (74% yield) .fwdarw. octaglycylglycine (85% yield) .fwdarw. chloroacetyloctaglycylglycine (79% yield) .fwdarw. nonaglycylglycine (70% amination, but the product could not be completely purified). .beta.-Naphthalenesulfonylhexaglycylglycine was obtained in 50% yield from the heptapeptide and .beta.-C10H7SO2Cl in the usual manner. None of these higher peptides were attacked by erepsin at pH 7.8, but the hexapeptide was partially hydrolyzed at pH 8.4. All of the ClCH2CO derivs. were hydrolyzed to some extent by trypsin-kinase at pH 7.8, but to a less extent, if at all, at pH 8.4. The polypeptides were all resistant to trypsin-kinase. When dispersed in LiBr and brought to N by NaOH the rate of hydrolysis at 37.degree. increased with increasing length of the peptide chain. The .beta.-C10H7SO2 deriv. was more resistant to alkali than the unsubstituted hexapeptide.

IT **18861-82-0**, Glycine, (glycylglycylglycylglycylglycylglycylglycyl)- (prepn. of)
RN 18861-82-0 CAPLUS
CN Glycine, glycylglycylglycylglycylglycylglycylglycyl- (9CI) (CA INDEX NAME)

SEQ 1 GGGGGGG

L20 ANSWER 24 OF 24 CAPLUS COPYRIGHT 2003 ACS on STN
ACCESSION NUMBER: 1985:107223 CAPLUS
DOCUMENT NUMBER: 102:107223
TITLE: A short amino acid sequence able to specify nuclear location
AUTHOR(S): Kalderon, Daniel; Roberts, Bruce L.; Richardson, William D.; Smith, Alan E.
CORPORATE SOURCE: Biochem. Div., Natl. Inst. Med. Res., London, NW7 1AA, UK
SOURCE: Cell (Cambridge, MA, United States) (**1984**), 39(3, Pt. 2), 499-509
CODEN: CELLB5; ISSN: 0092-8674
DOCUMENT TYPE: Journal
LANGUAGE: English
AB A short sequence of amino acids including Lys-128 is required for the normal nuclear accumulation of wild-type and deleted forms of SV40 virus large T antigen. A cytoplasmic large T mutant that lacks sequences from around Lys-128 localizes to the nucleus if the missing sequence is attached to its amino terminus. The implication that the sequence element around Lys-128 acts as an autonomous signal capable of specifying nuclear location was tested directly by transferring it to the amino terminal of .beta.-galactosidase and of pyruvate kinase [9001-59-6], normally a cytoplasmic protein. Sequences that included the putative signal induced each of the fusion proteins to accumulate completely in the nucleus but had no discernible effect when Lys-128 was replaced by Thr. By reducing the size of the transposed sequence, it was concluded that Pro-Lys-Lys-Lys-Arg-Lys-Val [**95088-49-6**] can act as a nuclear location signal. The sequence may represent a prototype of similar sequences in other nuclear proteins.

L17 ANSWER 8 OF 26 CAPLUS COPYRIGHT 2003 ACS on STN
ACCESSION NUMBER: 2001:166563 CAPLUS
DOCUMENT NUMBER: 134:337296
TITLE: Arginine-rich **peptides**: an abundant source of **membrane-permeable** **peptides** having potential as carriers for intracellular protein delivery
AUTHOR(S): Futaki, Shiroh; Suzuki, Tomoki; Ohashi, Wakana; Yagami, Takeshi; Tanaka, Seigo; Ueda, Kunihiro; Sugiura, Yukio
CORPORATE SOURCE: Institute for Chemical Research, Kyoto University, Kyoto, 611-0011, Japan
SOURCE: Journal of Biological Chemistry (2001), 276(8), 5836-5840
CODEN: JBCHA3; ISSN: 0021-9258
PUBLISHER: American Society for Biochemistry and Molecular Biology
DOCUMENT TYPE: Journal
LANGUAGE: English

AB A basic peptide derived from human immunodeficiency virus (HIV)-1 Tat protein (positions 48-60) has been reported to have the ability to translocate through the cell membranes and accumulate in the nucleus, the characteristics of which are utilized for the delivery of exogenous proteins into cells. Based on the fluorescence microscopic observations of mouse macrophage RAW264.7 cells, we found that various arginine-rich peptides have a translocation activity very similar to Tat-(48-60). These included such peptides as the D-amino acid- and arginine-substituted Tat-(48-60), the RNA-binding peptides derived from virus proteins, such as HIV-1 Rev, and flock house virus coat proteins, and the DNA binding segments of leucine zipper proteins, such as cancer-related proteins c-Fos and c-Jan, and the yeast transcription factor GCN4. These segments have no specific primary and secondary structures in common except that they have several arginine residues in the sequences. Moreover, these peptides were internalized even at 4.degree.. These results strongly suggested the possible existence of a common internalization mechanism ubiquitous to arginine-rich peptides, which is not explained by a typical endocytosis. Using (Arg)n (n = 4-16) peptides, we also demonstrated that there would be an optimal no. of arginine residues (n .apprx. 8) for the efficient translocation.

IT **337516-16-2**
RL: BPR (Biological process); BSU (Biological study, unclassified); BIOL (Biological study); PROC (Process)
(SV40-NLS; arginine-rich peptides as potential carriers for intracellular protein delivery)

RN 337516-16-2 CAPLUS
CN L-Valinamide, L-prolyl-L-lysyl-L-lysyl-L-lysyl-L-arginyl-L-lysyl- (9CI) (CA INDEX NAME)

NTE modified

SEQ 1 PKKKRKV

L17 ANSWER 22 OF 26 CAPLUS COPYRIGHT 2003 ACS on STN
ACCESSION NUMBER: 1997:640245 CAPLUS
DOCUMENT NUMBER: 127:293643
TITLE: Preparation of cyclic prodrugs of **peptides** and **peptide** nucleic acids having improved metabolic stability and cell **membrane permeability**
INVENTOR(S): Borchardt, Ronald T.; Siahaan, Teruna; Gangwar, Sanjeev; Stella, Valentino J.; Wang, Binghe
PATENT ASSIGNEE(S): University of Kansas, USA
SOURCE: U.S., 53 pp.
CODEN: USXXAM
DOCUMENT TYPE: Patent
LANGUAGE: English
FAMILY ACC. NUM. COUNT: 1
PATENT INFORMATION:

PATENT NO.	KIND	DATE	APPLICATION NO.	DATE
US 5672584	A	19970930	US 1995-429732	19950425
CA 2219151	AA	19971023	CA 1996-2219151	19960408
WO 9739024	A1	19971023	WO 1996-US4180	19960408
W: AL, AM, AT, AU, AZ, BB, BG, BR, BY, CA, CH, CN, CZ, DE, DK, EE, ES, FI, GB, GE, HU, IS, JP, KE, KG, KP, KR, KZ, LK, LR, LS, LT, LU, LV, MD, MG, MK, MN, MW, MX, NO, NZ, PL, PT, RO, RU, SD, SE, SG, SI, SK, TJ, TM, TR, TT, UA, UG, UZ, VN, AM, AZ, BY, KG, KZ, MD, RU, TJ, TM				
RW: KE, LS, MW, SD, SZ, UG, AT, BE, CH, DE, DK, ES, FI, FR, GB, GR, IE, IT, LU, MC, NL, PT, SE, BF, BJ, CF, CG, CI, CM, GA, GN, ML, MR, NE, SN, TD, TG				
AU 9654330	A1	19971107	AU 1996-54330	19960408
AU 702993	B2	19990311		
EP 830372	A1	19980325	EP 1996-911444	19960408
EP 830372	B1	20011010		
R: AT, BE, CH, DE, DK, ES, FR, GB, GR, IT, LI, LU, NL, SE, MC, PT, IE, FI				
JP 11508275	T2	19990721	JP 1996-534725	19960408
AT 206716	E	20011015	AT 1996-911444	19960408
ES 2165492	T3	20020316	ES 1996-911444	19960408

PRIORITY APPLN. INFO.: US 1995-429732 A 19950425
WO 1996-US4180 W 19960408
OTHER SOURCE(S): MARPAT 127:293643
GI

L17 ANSWER 19 OF 26 CAPLUS COPYRIGHT 2003 ACS on STN
ACCESSION NUMBER: 1998:338134 CAPLUS
DOCUMENT NUMBER: 129:32298
TITLE: Polyphosphoinositide binding **peptides** for intracellular drug delivery
INVENTOR(S): Janmey, Paul A.; Cunningham, C. Casey; Hartwig, John H.; Stossel, Thomas P.; Vegner, Roland
PATENT ASSIGNEE(S): Brigham and Women's Hospital, Inc., USA
SOURCE: PCT Int. Appl., 71 pp.
CODEN: PIXXD2
DOCUMENT TYPE: Patent
LANGUAGE: English
FAMILY ACC. NUM. COUNT: 1
PATENT INFORMATION:

PATENT NO.	KIND	DATE	APPLICATION NO.	DATE
WO 9820887	A1	19980522	WO 1996-US18453	19961114
W: AU, CA, JP				
RW: AT, BE, CH, DE, DK, ES, FI, FR, GB, GR, IE, IT, LU, MC, NL, PT, SE				
AU 9677371	A1	19980603	AU 1996-77371	19961114

PRIORITY APPLN. INFO.: WO 1996-US18453 19961114

AB Methods and compns. for facilitating the transport of a membrane-impermeable extracellular agent having an intracellular activity across the membrane of a cell are provided. The methods involve covalently coupling an amino terminal blocking group to a transport-mediating peptide to form a carrier mol. The carrier mol. is covalently coupled to the extracellular agent to form a **membrane -permeable** prodrug. The transport-mediating peptides are highly basic and bind to polyphosphoinositides.

IT **207972-57-4D**, conjugates **207972-62-1D**, conjugates **207972-79-0D**, conjugates **207972-84-7D**, conjugates
RL: BPR (Biological process); BSU (Biological study, unclassified); PEP (Physical, engineering or chemical process); PRP (Properties); BIOL (Biological study); PROC (Process)
(polyphosphoinositide binding peptides for intracellular drug delivery)

RN 207972-57-4 CAPLUS
CN L-Lysine, L-serylglycyl-L-leucyl-L-lysyl-L-tyrosyl-L-lysyl- (9CI) (CA INDEX NAME)

SEQ 1 SGLKYKK

L12 ANSWER 22 OF 27 CAPLUS COPYRIGHT 2003 ACS on STN
ACCESSION NUMBER: 1997:218432 CAPLUS
DOCUMENT NUMBER: 126:212414
TITLE: Synthesis of a Novel Esterase-Sensitive Cyclic Prodrug System for Peptides That Utilizes a "Trimethyl Lock"-Facilitated Lactonization Reaction
AUTHOR(S): Wang, Binghe; Gangwar, Sanjeev; Pauletti, Giovanni M.; Siahaan, Teruna J.; Borchardt, Ronald T.
CORPORATE SOURCE: Department of Pharmaceutical Chemistry, University of Kansas, Lawrence, KS, 66047, USA
SOURCE: Journal of Organic Chemistry (1997), 62(5), 1363-1367
CODEN: JOCEAH; ISSN: 0022-3263
PUBLISHER: American Chemical Society
DOCUMENT TYPE: Journal
LANGUAGE: English
OTHER SOURCE(S): CASREACT 126:212414
GI

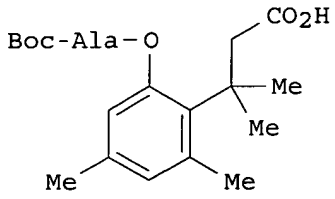

I

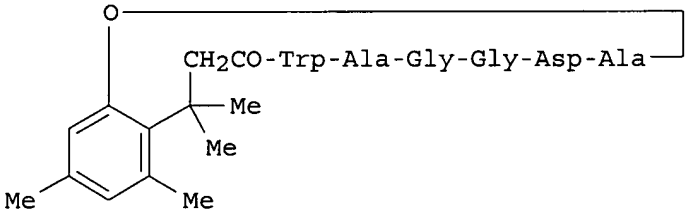

II

AB A unique strategy for prepg. cyclic prodrugs of peptides that have increased metabolic stability and increased cell **membrane permeability** when compared to the linear **peptides** is described. By taking advantage of a unique "trimethyl lock"-facilitated lactonization system, an esterase-sensitive cyclic prodrug of a model hexapeptide H-Trp-Ala-Gly-Gly-Asp-Ala-OH was synthesized by linking the N-terminal amino group to the C-terminal carboxyl group. The key intermediate for both approaches was I (Boc = Me3CO2C) with Boc-Ala attached to the phenol hydroxyl group of the "trimethyl lock" linker through an ester bond, which can then be incorporated into the peptide using a normal coupling reagent for peptide synthesis. The synthesis of the linear peptides was accomplished using both soln.-phase and solid-phase approaches with the soln.-phase approach having the advantage of using the key intermediate I most efficiently. Cyclization using std. high-diln. techniques provided cyclic prodrug II. In 90% human plasma, prodrug II released the original peptide, as designed, through an apparent esterase-catalyzed hydrolysis of the phenol ester bond.

IT **187978-53-6P**
RL: BAC (Biological activity or effector, except adverse); BSU (Biological study, unclassified); PRP (Properties); SPN (Synthetic preparation); THU (Therapeutic use); BIOL (Biological study); PREP (Preparation); USES (Uses)
(prepn. of novel esterase-sensitive cyclopeptide prodrug incorporating

a tri-Me lock-facilitated lactonization)

RN 187978-53-6 CAPLUS

CN L-Alanine, N-[3-(2-hydroxy-4,6-dimethylphenyl)-3-methyl-1-oxobutyl]-L-tryptophyl-L-alanylglycylglycyl-L-.alpha.-aspartyl-, (6.fwdarw.1)-lactone (9CI) (CA INDEX NAME)

L17 ANSWER 18 OF 26 CAPLUS COPYRIGHT 2003 ACS on STN
ACCESSION NUMBER: 1998:479557 CAPLUS
DOCUMENT NUMBER: 129:91439
TITLE: **Peptide** antagonists of DP transcription factors
INVENTOR(S): La Thangue, Nicholas Barrie; Bandara, Lasantha Ranasinghe
PATENT ASSIGNEE(S): Prolifix Ltd., UK
SOURCE: PCT Int. Appl., 55 pp.
CODEN: PIXXD2
DOCUMENT TYPE: Patent
LANGUAGE: English
FAMILY ACC. NUM. COUNT: 1
PATENT INFORMATION:

PATENT NO.	KIND	DATE	APPLICATION NO.	DATE
WO 9828334	A1	19980702	WO 1997-GB3506	19971222
W: AL, AM, AT, AU, AZ, BA, BB, BG, BR, BY, CA, CH, CN, CU, CZ, DE, DK, EE, ES, FI, GB, GE, GH, GM, GW, HU, ID, IL, IS, JP, KE, KG, KP, KR, KZ, LC, LK, LR, LS, LT, LU, LV, MD, MG, MK, MN, MW, MX, NO, NZ, PL, PT, RO, RU, SD, SE, SG, SI, SK, SL, TJ, TM, TR, TT, UA, UG, US, UZ, VN, YU, ZW, AM, AZ, BY, KG, KZ, MD, RU, TJ, TM				
RW: GH, GM, KE, LS, MW, SD, SZ, UG, ZW, AT, BE, CH, DE, DK, ES, FI, FR, GB, GR, IE, IT, LU, MC, NL, PT, SE, BF, BJ, CF, CG, CI, CM, GA, GN, ML, MR, NE, SN, TD, TG				
AU 9853304	A1	19980717	AU 1998-53304	19971222
AU 735032	B2	20010628		
EP 956299	A1	19991117	EP 1997-950295	19971222
R: AT, BE, CH, DE, DK, ES, FR, GB, GR, IT, LI, LU, NL, SE, MC, PT, IE, FI				
NZ 336530	A	20001124	NZ 1997-336530	19971222
JP 2001506863	T2	20010529	JP 1998-528541	19971222
US 6268334	B1	20010731	US 1999-308935	19990527
US 2002103121	A1	20020801	US 2001-900147	20010709

PRIORITY APPLN. INFO.:
GB 1996-26589 A 19961220
WO 1997-GB3506 W 19971222
US 1999-308935 A1 19990527

AB The invention provides a polypeptide consisting essentially of a sequence corresponding to residues 163-199 of DP-1 transcription factor, and fragments and variants thereof capable of antagonizing the heterodimerization of a DP protein with an E2F protein. Such peptides may be used to induce apoptosis in a cell by introducing into the cell an effective amt. of said peptide. Such cells include cardiovascular cells, and the peptide may be delivered in a stent to treat or prevent restinosis.

IT **209599-55-3**
RL: BAC (Biological activity or effector, except adverse); BSU (Biological study, unclassified); THU (Therapeutic use); BIOL (Biological study); USES (Uses)
(peptide antagonists of DP transcription factors)

RN 209599-55-3 CAPLUS
CN L-Alanine, L-alanyl-L-leucyl-L-asparaginyl-L-valyl-L-leucyl-L-methionyl- (9CI) (CA INDEX NAME)

SEQ 1 ALNVLMA

L12 ANSWER 17 OF 27 CAPLUS COPYRIGHT 2003 ACS on STN
ACCESSION NUMBER: 1999:753254 CAPLUS
DOCUMENT NUMBER: 132:8996
TITLE: Antimicrobial cationic peptide derivatives of bactenecin
INVENTOR(S): Hancock, Robert E. W.; Wu, Manhong
PATENT ASSIGNEE(S): University of British Columbia, Can.
SOURCE: PCT Int. Appl., 52 pp.
CODEN: PIXXD2
DOCUMENT TYPE: Patent
LANGUAGE: English
FAMILY ACC. NUM. COUNT: 1
PATENT INFORMATION:

PATENT NO.	KIND	DATE	APPLICATION NO.	DATE
WO 9960016	A2	19991125	WO 1999-CA414	19990520
WO 9960016	A3	20000713		

W: AE, AL, AM, AT, AU, AZ, BA, BB, BG, BR, BY, CA, CH, CN, CU, CZ, DE, DK, EE, ES, FI, GB, GD, GE, GH, GM, HR, HU, ID, IL, IN, IS, JP, KE, KG, KP, KR, KZ, LC, LK, LR, LS, LT, LU, LV, MD, MG, MK, MN, MW, MX, NO, NZ, PL, PT, RO, RU, SD, SE, SG, SI, SK, SL, TJ, TM, TR, TT, UA, UG, UZ, VN, YU, ZA, ZW, AM, AZ, BY, KG, KZ, MD, RU, TJ, TM

RW: GH, GM, KE, LS, MW, SD, SL, SZ, UG, ZW, AT, BE, CH, CY, DE, DK, ES, FI, FR, GB, GR, IE, IT, LU, MC, NL, PT, SE, BF, BJ, CF, CG, CI, CM, GA, GN, GW, ML, MR, NE, SN, TD, TG

US 6172185	B1	20010109	US 1998-82420	19980520
AU 9938048	A1	19991206	AU 1999-38048	19990520

PRIORITY APPLN. INFO.: US 1998-82420 A 19980520
WO 1999-CA414 W 19990520

AB A class of cationic peptides having antimicrobial activity is provided. Exemplary peptides of the invention include RLARIVVIRVAR and RLSRIVVIRVCR. Also provided are methods for inhibiting the growth of bacteria using the peptides of the invention. Methods for inhibiting the growth of eukaryotic cells, e.g. tumor cells, with the peptides of the invention are also disclosed.

IT **1404-90-6**, Vancomycin
RL: BAC (Biological activity or effector, except adverse); BSU (Biological study, unclassified); THU (Therapeutic use); BIOL (Biological study); USES (Uses)
(antimicrobial and cytotoxic cationic peptide derivs. of bactenecin, and therapeutic use, alone or with other agents)

RN 1404-90-6 CAPLUS
CN Vancomycin (8CI, 9CI) (CA INDEX NAME)

NTE modified (modifications unspecified)

SEQ 1 LYNXXYX

L12 ANSWER 15 OF 27 CAPLUS COPYRIGHT 2003 ACS on STN
ACCESSION NUMBER: 2000:283998 CAPLUS
DOCUMENT NUMBER: 132:318008
TITLE: Antimicrobial cationic peptides
INVENTOR(S): Hancock, Robert E. W.; Karunaratne, Nedra
PATENT ASSIGNEE(S): University of British Columbia, Can.
SOURCE: U.S., 42 pp., Cont.-in-part of U.S. Ser. No. 658,857.
CODEN: USXXAM
DOCUMENT TYPE: Patent
LANGUAGE: English
FAMILY ACC. NUM. COUNT: 4
PATENT INFORMATION:

PATENT NO.	KIND	DATE	APPLICATION NO.	DATE
US 6057291	A	20000502	US 1996-763226	19961210
US 5877274	A	19990302	US 1995-460464	19950602
US 6040435	A	20000321	US 1996-658857	19960531
WO 9825953	A1	19980618	WO 1997-CA954	19971210
W: AL, AM, AT, AU, AZ, BA, BB, BG, BR, BY, CA, CH, CN, CU, CZ, DE, DK, EE, ES, FI, GB, GE, GH, GM, HU, ID, IL, IS, JP, KE, KG, KP, KR, KZ, LC, LK, LR, LS, LT, LU, LV, MD, MG, MK, MN, MW, MX, NO, NZ, PL, PT, RO, RU, SD, SE, SG, SI, SK, SL, TJ, TM, TR, TT, UA, UG, UZ, VN, YU, ZW, AM, AZ, BY, KG, KZ, MD, RU, TJ, TM				
RW: GH, GM, KE, LS, MW, SD, SZ, UG, ZW, AT, BE, CH, DE, DK, ES, FI, FR, GB, GR, IE, IT, LU, MC, NL, PT, SE, BF, BJ, CF, CG, CI, CM, GA, GN, ML, MR, NE, SN, TD, TG				
AU 9852206	A1	19980703	AU 1998-52206	19971210
US 6297215	B1	20011002	US 1999-307200	19990507
US 6465429	B1	20021015	US 2000-593321	20000613
US 2003176337	A1	20030918	US 2002-272248	20021015

PRIORITY APPLN. INFO.:

US 1995-460464	A2	19950602
US 1996-658857	A2	19960531
US 1996-763226	A	19961210
WO 1997-CA954	W	19971210
US 1999-307200	A3	19990507
US 2000-593321	A1	20000613

OTHER SOURCE(S): MARPAT 132:318008

AB A novel class of cationic peptides having antimicrobial activity is provided. Examples of such peptides include H2N-KWKSFIKKLTTAVKKVLTTGLPALIS-COOH and H2N-KWKSFIKKLTSAAKKVVTTAKPLISS-COOH. Also provided are methods for inhibiting the growth of bacteria using the peptides of the invention. The peptides are particularly useful for inhibiting endotoxemia in a subject.

IT **1404-90-6**, Vancomycin
RL: BAC (Biological activity or effector, except adverse); BSU (Biological study, unclassified); THU (Therapeutic use); BIOL (Biological study); USES (Uses)
(antimicrobial cationic peptides, and combinations with antibiotics)

RN 1404-90-6 CAPLUS
CN Vancomycin (8CI, 9CI) (CA INDEX NAME)

Absolute stereochemistry.

L17 ANSWER 12 OF 26 CAPLUS COPYRIGHT 2003 ACS on STN
ACCESSION NUMBER: 2000:3821 CAPLUS
DOCUMENT NUMBER: 132:148941
TITLE: Use of the cell wall precursor lipid II by a pore-forming **peptide** antibiotic
AUTHOR(S): Breukink, E.; Wiedemann, I.; Van Kraaij, C.; Kuipers, O. P.; Sahl, H.-G.; De Kruijff, B.
CORPORATE SOURCE: Center of Biomembranes and lipid Enzymology, Department of Biochemistry of Membranes, Institute for Biomembranes, Utrecht University, Utrecht, 3584, Neth.
SOURCE: Science (Washington, D. C.) (1999), 286(5448), 2361-2364
CODEN: SCIEAS; ISSN: 0036-8075
PUBLISHER: American Association for the Advancement of Science
DOCUMENT TYPE: Journal
LANGUAGE: English
AB Resistance to antibiotics is increasing in some groups of clin. important pathogens. For instance, high vancomycin resistance has emerged in enterococci. Promising alternative antibiotics are the peptide antibiotics, abundant in host defense systems, which kill their targets by **permeabilizing** the plasma **membrane**. These peptides generally do not act via specific receptors and are active in the micromolar range. Here it is shown that vancomycin and the antibacterial peptide nisin Z use the same target: the membrane-anchored cell wall precursor lipid II. Nisin combines high affinity for lipid II with its pore-forming ability, thus causing the peptide to be highly active (in the nanomolar range).
IT **1404-90-6**, Vancomycin
RL: BAC (Biological activity or effector, except adverse); BSU (Biological study, unclassified); BIOL (Biological study)
(bacterial cell wall precursor lipid II as target for antibiotics)
RN 1404-90-6 CAPLUS
CN Vancomycin (8CI, 9CI) (CA INDEX NAME)

NTE modified (modifications unspecified)

SEQ 1 LYNXXYX